EFFECTS OF HYDRODYNAMIC CULTURE ON EMBRYONIC STEM CELL DIFFERENTIATION: CARDIOGENIC MODULATION

A Dissertation
Presented to
The Academic Faculty

by

Carolyn Yeago Sargent

In Partial Fulfillment
of the Requirements for the Degree
Doctor of Philosophy in Biomedical Engineering in the
Wallace H. Coulter Department of Biomedical Engineering at Georgia Tech and Emory University

Georgia Institute of Technology
August 2010

EFFECTS OF HYDRODYNAMIC CULTURE ON EMBRYONIC STEM CELL DIFFERENTIATION: CARDIOGENIC MODULATION

Approved by:

Dr. Todd C. McDevitt, Advisor
Department of Biomedical Engineering
Georgia Institute of Technology

Dr. Ajit Yoganathan
Department of Biomedical Engineering
Georgia Institute of Technology

Dr. Gilda Barabino
Department of Biomedical Engineering
Georgia Institute of Technology

Dr. Leonard Anderson
Cardiovascular Research Institute
Morehouse School of Medicine

Dr. Hanjoong Jo
Department of Biomedical Engineering
Georgia Institute of Technology and Emory Univeristy

Date Approved: June 25th, 2010

This work is dedicated to my parents, John and Polly, my brother, Will Yeago, and to my loving husband, Matt Sargent, in appreciation for all of their encouragement and support.

ACKNOWLEDGEMENTS

I have grown an immense amount, scientifically and personally, during my time in the Biomedical Engineering program at Georgia Tech and Emory. There are numerous people who have contributed to my growth and who have supported me throughout this grueling process, and to them, I owe many thanks.

To my committee, Dr. Todd McDevitt (my advisor), Dr. Leonard Anderson, Dr. Gilda Barabino, Dr. Hanjoong Jo, and Dr. Ajit Yoganathan, I thank them for their instruction and input which have served to improve the quality and impact for my work. With his thoughts on cell-cell contacts and interactions, Dr. Leonard Anderson played an early and important role in the direction of my project. Dr. Gilda Barabino not only challenged me mentally as a scientist but also as person looking for larger meaning and purpose; she has been an important role-model for me since my proposal back in December 2007. Dr. Hanjoong Jo always offered stimulating thoughts about the biological and clinical relevance of my work, forcing me to think beyond the bench-top. As a very fluid dynamically oriented engineer, Dr. Ajit Yoganathan helped me to see my work from a different perspective of velocity profiles and turbulent mixing, and although my project ended being less "engineered" environments, his inputs on the mathematical side of my system were invaluable.

I owe the most thanks to my advisor, Todd. When I came to Georgia Tech, what seems now so long ago, I knew I did not want to join a new lab. I had worked in start-up lab as an undergraduate at North Carolina State University, and I was looking for more senior students, post-docs, and established lab practices in the graduate lab I would be

joining. However, as it can now be seen, that intention did not hold, and I was excited to join Todd's lab after my first year of classes and lab rotations. Over these years, Todd has pushed me, and supported me, somehow always knowing when to give that extra nudge and when to give some extra space. I feel he is unsurpassed in this dedication to his students as well as his joy in watching our successes. Over the past six year, Todd's lab has grown, and he's great successes due to his immeasurable talent and dedicated work ethic, but he has always made time for his students. He has offered me scientific advice with regards to my project, but more importantly he has offered wisdom regarding what is to become a scientist. He been a model of a true mentor and leader, and I cannot express my full gratitude for all the opportunity he has afforded me. And what would Todd without his better half, Meg? I may owe her more thanks than I know for keeping Todd in-line and always reprimanding him if he called too late at night or over a weekend to discuss research, grants, or conference talks (and also for providing us with amazing food and plenty of vino!) Meg is such a strong and independent woman but also a loving and supportive wife, so thank you Meg for being that role model for me.

I owe innumerable thanks to all of my lab mates, but especially to the first, Rich Carpenedo, Ima Ebong, and Rekha Nair. I was only lucky enough to actually have a cell culture hood to work in and supplied to use when I did my lab rotation because the three of them had ordered and set-up all of equipment. Ima always knew how to have a good time, and I always smiled when I could hear her singing with her ipod at her desk or in the tissue culture room. Poor Rich was the only guy in the lab for quite a while, and he started off pretty quiet. My goal was to get him to talk, but all that really takes is a couple drinks. I'm sure over the years he's really come to look forward to my

complaining, and as I've told others, you only need to worry that Rich doesn't like you if he's not giving you a hard time. Rekha was in my BME class, so we "struggled" through PBL projects and Emory tests together, but she's been more to me than I could ever truly say. She's been the one who understands exactly everything I'm feeling when work or life's not going right. She's always had an ear to lend, and you couldn't ask for a more genuine person. And Rekha's work ethic is unsurpassed; she's super productive and goes about all her work with a smile (most times). Thank you Rekha for inspiring me to just generally be better.

Alyssa Ngangan was the next to join our group, going from 4 to 5, followed by Andrés Bratt-Leal, and shortly after Ken Sutha and Barbara Nsiah. Alyssa has been a great work-out partner, and biking buddy. She and Ken trained with me a triathlon about a year or so ago. They both add light-heartedness and a food-focus to the lab. (Although, the lab is strangely food and fitness focused in general…) I always appreciate Alyssa for her willing attitude and her awesome laugh! I'm pretty sure Rich was happy to have another male around when Andrés joined on; until that point there had been a couple male undergrads, but that was about it in the testosterone department. Andrés added a new level of… well of everything when he added to our ranks. There was just no line he wouldn't cross. I truly admire Barbara for her directness and complete disregard of peer-pressure. She's definitely fun around the lab, and a great shopping partner as well. Melissa Kinney is latest and greatest Ph.D. student to join, and I owe her several thanks because she's the one who's done some follow-up to my project. She's the one who was "queen of the rotaries" with me for while (that is until Jesse came along and was saddled with the unruly rotaries). Melissa has been a great help with experiments, and I have had

the best time "mentoring" her, helping with experimental design and reading conference abstracts. I know she will contribute a lot to the lab. Kirsten Kepple is the first Master's student Todd has hired, and so far she's adding a lot to the projects she's working on. I'm sure her contributions will be many over the next year as she completes her Master's Degree. And so to all of the students in the lab, I owe more than just thanks for good times; thanks also for your thoughts and questions about my work and science in general.

It's not just the students in the lab who have been ever so important to me over the years, but also research technicians and post-docs. First Beth Krauth helped get the lab organized as our first lab manager. I thank her for her help with staining protocols and ordering reagents, and she always seemed to know the latest departmental gossip. After Beth moved on, Marissa Cooke joined us, and she is an incredible researcher. She brought new expertise in proteomics, as well as some more food focus! I have enjoyed getting to know Marissa over the past year, and I know she will continue to do great work while raising a soon to be new family! (Congrats again Marissa). Jesse McClellon is the newest research technician, and I owe him at least one more bottle of wine for all the help he's been with running my last round of PCR, as well as taking over the maintenance of the blasted rotaries. Thank you, thank you Jesse.

Priya Baraniak was the first post-doc to join the McDevitt lab, and although I'm pretty sure she didn't know what she was signing up for at the time, I think she's come to appreciate the lab for what it is (very different from where she was). Priya added a whole new level of scientific knowledge. I appreciate her suggestions and concerns about my work, and I think her comments have improved my research. I also admire Priya for her candor and quick-wit; she's always hilarious to be around, and I know she has so much to

look forward to with her career, but more importantly her young family. Ankur Singh was the second post-doc to come around, and he's a recent addition. Although I don't know him well, I'm impressed by his decision to take on two post-doc advisors with strong opinions about things. I can already tell though that Ankur adds a new perspective and his comments are always welcomed.

I also owe a few extra important undergrads a very big thank you. First, thank you to Geoffrey Berguig who started going down this path of variable rotary speeds, or maybe not such a big thank you for that (just kidding). Geoffrey's inquisitive nature and dedication helped me get through hard times and retain some excitement about my work. He was truly a special undergrad, and is now doing great work in Pat Stayton's lab the University of Washington. Gayathri Balasubramanian and Virginia Chu were two undergrads who also contributed to progression of my research. I thank them for their many hours sectioning and IHC staining. And there a few undergrads that did not work directly with me, but were an instrumental party of the lab: Ross Marklein, Shreya Shukla, and Scot Seaman. Also, Katy Hammersmith is becoming a true McDevitt lab member and is working hard under Andrés' instruction.

I feel my success as a graduate student is in large part due to the overall success of the McDevitt lab. The dynamic between all of the researchers and Todd is special and unique. Without every single one of my lab mates, I wouldn't be the scientist or the person I am today.

Besides my fellow lab people, several friends who started the BME program with me deserve my thanks and gratitude. Brock Wester, Abbey Wojtowicz, Victoria Stahl, Priya Santhanam, and Swathi Ravi have all been super supportive, especially during

those first couple of years of classes. Victoria got me hooked on endurance racing, by helping me train for my first ½ marathon, which we accomplished with several other BME students. But most of all, I have to thank Amanda Walls Bridges, who started as Amanda Walls when I first met in back in undergrad at NC State. I can't thank her enough for all of her support and encouragement over the years, in addition to the many glasses of wine and shopping trips.

I thank my parents John and Polly Yeago, for their support. Even though they may not have understood what I was talking about, they would always patiently listen to me talk about school projects and my research work. I thank them for instilling in me a sense of self and an appreciation of hard work and hard play. My brother has always been there to remind me to have fun, and I thank him for that. And to my husband Matt Sargent, thank you for everything. That's really all I can say, I know it should be more, but words just aren't enough. Thank you. Thank you.

TABLE OF CONTENTS

LIST OF TABLES

LIST OF FIGURES

LIST OF SYMBOLS AND ABBREVIATIONS

ABC	Active β-catenin
AFP	α-fetoprotein
α-MHC	α-myosin heavy chain
APC	adenomatous poliposis coli
AVE	anterior visceral endoderm
BMP	bone morphogenetic protein
B-T	brachyury T
C7	clone 7
C21	clone 21
CFD	computational fluid dynamics
Dkk	dickkopf
EB	embryoid body
EC	endothelial cell
EPC	endothelial progenitor cell
ESC	embryonic stem cell
GAPDH	glyceraldhyde-3-phosphate-dehydrogenase
GSK3β	glycogen synthase kinase 3β
HARV	high aspect ratio vessel
HD	hanging drop
hEB	human embryoid body
hESC	human embryonic stem cell
IGF	insulin growth factor
IHC	immunohistochemistry

iPS cell	induced pluripotent stem cell
IR	infra red
Isl-1	islet-1
LIF	leukemia inhibitory factor
LRP	low-density lipoprotein receptor-related protein
MEF	mouse embryonic fibroblast
Mef-2c	myosin enhancer factor 2c
mESC	mouse embryonic stem cell
mEB	mouse embryoid body
Mesp-1	mesoderm posterior protein 1
MLC-2v	myosin light chain 2 ventricle
MOI	multiplicity of infection
Myf-5	myogenic factor 5
qPCR	quantitative polymerase chain reaction
RLU	relative light unit
SDS	sodium dodecyl sulfate
SEM	scanning electron microscopy
Sfrp s	secreted frizzled-related protein
STLV	slow turning lateral vessel
TCF/LEF	T-cell factor/lymphocyte enhancer factor
TGFβ	transforming growth factor β
TRE	transcriptional response element

SUMMARY

Embryonic stem cells (ESCs), pluripotent cells derived from the inner cell mass of blastocysts, have the unique potential to differentiate into all somatic cell types, making ESCs not only a model for the study of early mammalian development but also a potential therapeutic cell source for degenerative diseases, including heart disease. However, to effectively use ESCs for regenerative cell-based therapies, both efficient directed differentiation and scalable culture techniques are needed. Although bioreactors are beginning to be utilized for large-scale ESC culture and differentiation, little is known about the response of ESCs to hydrodynamic conditions and the mechanisms regulating differentiation that may be affected. This project examined the response of ESCs to various hydrodynamic conditions generated via rotary orbital suspension culture, in particular investigating the formation and maintenance of cell aggregates, the differentiation of cells within these aggregates, and the modulation of the β-catenin signaling pathway implicated in regulating differentiation.

Mouse ESC differentiation is commonly initiated via spontaneous aggregation of single-cell suspensions into clusters of cells termed embryoid bodies (EBs). EBs recapitulate many cellular morphogenic events similar to those of post-implantation stage embryos, leading to formation of the three germ lineages (ectoderm, endoderm, and mesoderm) and further differentiate into specialized cell types, such as cardiomyocytes. Rotary orbital suspension culture more efficiently generates large yields of uniform embryoid bodies compared to both static suspension and hanging drop suspension culture. EBs were formed under various rotary orbital speeds and formation kinetics,

morphology, and differentiation were examined to further assess the effects of rotary orbital suspension culture.

Embryoid bodies can be formed at many rotary orbital speeds with a lower limit of 20 rpm and an upper limit of 60 rpm. EB size was inversely regulated by rotary speed, with slower rotary speeds generating larger EBs than faster rotary speeds, while EB yield was directly regulated by rotary speed. In addition to controlling the overall size of EBs, rotary orbital speed also altered the kinetics of EB formation, with slower rotary speeds generating distinct, primitive EBs within 6 hours of inoculation and faster speeds requiring as much as 24 hours to attain primitive EB formation. Shear stresses within rotary orbital culture were relatively uniform and mild ($\leq$ 2.5 dyn/cm^2) as determined by computational fluid dynamics; however the three speeds examined (25, 40, and 55 rpm) did result in unique shear stress profiles under which the EBs were formed and cultured. The differences observed in EB formation kinetics and size were accompanied by alterations in the global gene expression patterns between static and rotary culture conditions as well as between rotary orbital speeds. Global differences in signaling genes (*Notch*, *Frat*, *Fzd*, *Wnt*, etc) were observed between static and rotary culture conditions, as well as differences in the expression of genes indicative of germ lineage differentiation, suggesting that the different hydrodynamic conditions imparted by rotary orbital speed could modulate EB differentiation.

Rotary orbital culture was compared static suspension and hanging drop culture to further assess the effects of hydrodynamic conditions on EB differentiation. EBs formed under rotary orbital culture at 40 rpm were found to enhance mesoderm differentiation, particularly cardiomycoyte differentiation, compared to static culture, exhibiting

increased levels cardiogenic-related genes (*Nkx2.5*, *MLC-2v*, and *α-MHC*) and protein (α-sarcomeric actin) expression as well as increased contractile frequency. The differences of rotary orbital culture compared to static and hanging drop culture demonstrated the ability of hydrodynamic conditions to affect cardiomyocyte differentiation and led to the investigation of how rotary speed may also alter cardiomyocyte differentiation.

Rotary orbital speed modulated the temporal pattern of mesoderm and endoderm related genes (*Nkx2.5*, *Gata-4*, and *AFP*) with slower speeds exhibiting earlier increases in expression levels. Similarly, cardiogenic-related genes (*MLC-2v* and *α-MHC*) were increased earlier within slower rotary speed culture conditions, and increased contractile frequency was also observed within EBs from slower rotary speeds. These differences in gene expression, specifically related to cardiogenic differentiation, due to rotary orbital culture conditions suggested the regulation of EB formation and size by rotary orbital speeds may modulate signaling pathways that govern mesoderm and cardiogenic differentiation.

Beta-catenin signaling is an important signaling pathway active in early embryonic development, aiding in the regulation of embryonic patterning, axis formation, primitive streak formation, and mesoderm development. In differentiating ESCs, β-catenin signaling is required for initial mesoderm differentiation, and temporal regulation of β-catenin signaling is necessary for cardiomyocyte development from ESCs (early activation leads to cardiomyocyte progenitor development, followed by later inhibition, resulting in mature cardiomyocyte differentiation). Two pools of β-catenin are present within cells, 1- phosphorylated β-catenin sequestered within cell adherens junctions, specifically with E-cadherin at the cell membrane, and 2 – desphosphorylated β-catenin

located within the nucleus, specifically associated with TCF/LEF to mediate transcription.

The effects of hydrodynamic conditions from rotary orbital culture on β-catenin expression and cardiogenic gene transcription were examined by assessing TCF/LEF luciferase reporter expression, immuno-staining and immune-blotting for dephosphorylated β-catenin, and gene expression analysis of genes known to be directly and indirectly affected by β-catenin-regulated transcription. Rotary orbital speed modulated both spatiotemporal location of β-catenin and the phosphorylation state of β-catenin with slower rotary speeds resulting in earlier nuclear dephosphorylated β-catenin expression. Hydrodynamic culture in general appeared to increase β-catenin-regulated transcription (*Mesp-1, Mef-2c*) and cardiogenic gene expression (*Nkx2.5, MLC-2v*) compared to static culture conditions. These results led to a proposed model of hydrodynamic regulation of cardiomyocyte differentiation, suggesting that enhanced EB formation resulted in increased β-catenin availability from E-cadherin for transcriptional regulation upon activation. The increased nuclear β-catenin increased transcription of *Mef-2c*, which in turn inhibits the β-catenin signaling pathway, allowing for mature cardiomyocyte differentiation.

Overall, this project illustrates how hydrodynamic conditions can modulate a developmentally relevant signaling pathway and result in differential regulation of downstream differentiation.

CHAPTER 1

INTRODUCTION

Stem and progenitor cells have emerged over the past 30 years as an attractive cell source for the *in vitro* study of differentiation and development due to their potential to differentiate into multiple cell types and provide large cell yields. Embryonic stem cells (ESCs) have garnered much attention recently because of their unique ability to differentiate into all somatic cell types (derivatives of all three germ layers, mesoderm, endoderm, and ectoderm) as well as germ cells, a property known as pluripotency. ESCs are derived from the inner cell mass of blastocyst stage embryos and were initially derived from mouse embryos [1-3], followed by the establishment of ESC lines from primates [4] and ultimately human sources [5-6]. ESCs have been of particular interest in the study of embryonic development, as direct examination of human embryos is not possible [7-9]. Recently, investigators have demonstrated the ability to produce pluripotent cells via retroviral transduction of transcription factors into mammalian somatic cells [10-11]. These induced pluripotent stem (iPS) cells appear to exhibit characteristic differentiation and self-renewal similar to ESCs. In addition to their utility as a developmental model, ESCs and iPS cells also have the promising potential to serve as a cell source for clinical therapies for a variety of degenerative diseases, such as cardiovascular disease, diabetes, Alzheimer's, and Parkinson's, as well as for traumatic injuries, including brain and spinal cord damage. Because of their pluripotent character and ability to produce large yields of differentiating cells, ESCs have been investigated for regenerative therapy applications [12-16], which endeavor to restore cellular function

at the site of damaged tissue. Thus far, however, clinical applications have been relatively limited due to inefficient differentiation into desired cell types with sufficient yields necessary for adequate tissue repair and regeneration.

Differentiation of embryonic stem cells is commonly initiated by allowing ESCs in suspension to spontaneously aggregate into cell clusters termed embryoid bodies (EBs), which mimic the early cell signaling and fate decisions of pre-implantation embryos [1, 17-21]. The ability to spontaneously aggregate in suspension makes ESCs amenable to large-scale culture techniques for the production of EB [22-31]; translational approaches are increasingly moving toward larger scale culture systems, in which mixing becomes necessary to reduce nutrient gradients and promote enhanced gas exchange within the culture volume [32]. Mixing is accomplished either via external agitation of the entire vessel, as in rotating wall vessels (RWVs), such as the slow turning lateral vessel (STLV) and high aspect rotating vessel (HARV), or by internal agitation of an impeller, as in stirred flasks and pitched-blade bioreactors [33-34]. Mixing within reactors introduces hydrodynamic conditions to the cell culture, which may affect aspects of ESC differentiation, including EB formation, morphology, and subsequent differentiation. In contrast to large volume systems (0.5L – 2L), rotary orbital suspension culture is an externally agitated lab-scale (10mL) system in which many hydrodynamic conditions and additional variables can be screened in parallel [35-37]. Rotary orbital suspension culture has been shown to increase EB formation efficiency, increase EB and cell yield, increase EB homogeneity, and support differentiation of all three germ lineages [35].

Current trends in directing ESC differentiation focus on providing exogenous factors as signaling cues; however, progression towards controlling environmental conditions including both biochemical and mechanical stimuli may result in increased control over differentiation. For example, hemodynamic forces are important for the regulation of cardiac morphogenesis in developing embryos, where altered flow patterns result in cardiac defects [38-41]. High wall shear stresses have been measured within developing cardiac structures *in vivo* [41], and can be correlated to specific patterns of gene regulation in endocardial tissue [42]. Additionally, mesenchymal stem cells (MSCs) can be induced to differentiate along the endothelial lineage in response to fluid flow *in vitro* within a parallel plate system [43]. More recently, embryonic stem cells cultured in the presence of fluid shear stress in monolayer exhibited increased expression of hematopoetic markers, which is dependent upon nitric oxide mediated mechanotransduction [44-45]. The evidence for hydrodynamic modulation of stem cell phenotype and function in adherent monolayer format motivates the investigation of the response of three-dimensional stem cell culture to hydrodynamic environments (spheroid aggregation, morphology, and phenotype).

Efficient cardiomyocyte differentiation from ESCs is of great interest because of the possibility of regenerative therapies after an ischemic event, which is typically followed by deleterious muscle remodeling and permanent loss of contractile cell function [46-49]. Initial cardiomyocyte development within the embryo depends heavily on tightly regulated spatial and temporal endogenous signaling profiles and proper germ layer differentiation [50-55]. Most attempts to direct differentiation of ESCs to cardiomyocytes focus on the administration and screening of individual biochemical

factors [56-57], and although some progress has been made in identifying key factors for cardiomyocyte differentiation, little work has been conducted to define mechanical stimuli capable of initiating and supporting cardiomyogenesis *in vitro*. Examining the potential to regulate ESC endogenous cardiomyocyte differentiation by applying hydrodynamic culture conditions may provide a more effective differentiation method, resulting in a scalable technique for generating cardiomyocytes. Therefore, the *overall objective* of this project was to employ hydrodynamic conditions from rotary orbital suspension culture to control EB formation and modulate cardiomyogenic differentiation of ESCs. The *central hypothesis* of this project was that the hydrodynamic environment created by rotary orbital culture during the initial stages of ESC differentiation is able to regulate endogenous signaling pathways implicated in cardiomyocyte differentiation. The objective was accomplished and the hypothesis tested by completing the following specific aims:

Specific Aim 1: Examine the effects applied rotary orbital motion has on EB formation, morphology, and general differentiation.

The working hypothesis of this aim was that rotary orbital motion applied during EB formation regulates EB size and morphology, potentially modulating differentiation. The hypothesis was tested by forming EBs under static and rotary orbital conditions at various rotation speeds. The resulting formation kinetics, size and internal organization were compared across culture conditions by analyzing phase images, histological staining, and scanning electron microscopy images. The shear stress environment that the EBs were exposed to was defined by computational fluid dynamic modeling of the rotary orbital

system with different rotational speeds. Global differentiation was assessed by a qPCR array examining the expression levels of 84 genes.

Specific Aim 2: Evaluate the cardiomyogenic differentiation of ESCs cultured under rotary orbital suspension.

The working hypothesis of this aim was that rotary orbital speed affects EB differentiation and modulates cardiomyogenesis. The hypothesis was first tested by comparing the cardiogenic potential of hydrodynamic culture (one rotary orbital speed) to static suspension culture methods (hanging drop and bulk static suspension). Various rotary orbital speeds were then applied to further modulate differentiation and were compared to bulk static suspension. Contractile frequency, immunohistochemical staining (α-sarcomeric actin), qPCR analysis (early mesoderm and cardiac markers), and immunocytometry were analyzed to assess EB differentiation and cardiomyocyte development.

Specific Aim 3: Assess the effects of rotary orbital speed on β-catenin expression and signaling within differentiating EBs.

The working hypothesis of this aim was that rotary orbital suspension culture regulates EB formation, modulating direct cell-cell contacts and signaling pathways. A stably transduced ESC line was generated with a luciferase TCF/LEF reporter construct to quantitatively assay β-catenin-regulated transcription within EBs under different hydrodynamic conditions over a time course of differentiation. Non-transduced EBs were formed at a range of rotary speeds as well as static conditions and β-catenin

immune-staining with confocal imaging was assessed to determine the localization of β-catenin expression. Immuno-blots of cytoplasmic and nuclear protein fractions were also analyzed to assess the phosphorylation state and location of β-catenin. Additionally, qPCR of β-catenin-related gene expression was performed.

The work presented here employs a novel, laboratory-scale hydrodynamic culture model to systematically interrogate the effects of ESC culture hydrodynamics on cardiomyocyte differentiation through the modulation of a developmentally-relevant signaling pathway. The dynamic fluid environment in which ESCs differentiate is not typically thought of as a significant modulator of differentiation; however, hydrodynamic environments are being increasingly applied to scale-up ESC and EB production and differentiation. Little is currently known about how the mechanical environment influences early ESC differentiation and subsequent terminal differentiation, such as cardiomyogenesis. This work is significant because it illustrates that simple mixing conditions can modulate common signaling pathways active in ESC differentiation, and it lays the foundation for the potential regulation of differentiation via bioprocessing parameters and bioreactor design.

References

1. Doetschman, T.C., H. Eistetter, M. Katz, W. Schmidt, and R. Kemler, *The in vitro development of blastocyst-derived embryonic stem cell lines: Formation of visceral yolk sac, blood islands and myocardium.* J Embryol Exp Morphol, 1985. 87: p. 27-45.

2. Evans, M.J. and M.H. Kaufman, *Establishment in culture of pluripotential cells from mouse embryos.* Nature, 1981. 292(5819): p. 154-6.

3. Martin, G.R., *Isolation of a pluripotent cell line from early mouse embryos cultured in medium conditioned by teratocarcinoma stem cells.* Proc Natl Acad Sci U S A, 1981. 78(12): p. 7634-8.

4. Thomson, J.A., J. Kalishman, T.G. Golos, M. Durning, C.P. Harris, R.A. Becker, and J.P. Hearn, *Isolation of a primate embryonic stem cell line.* Proc Natl Acad Sci U S A, 1995. 92(17): p. 7844-8.

5. Reubinoff, B.E., M.F. Pera, C.Y. Fong, A. Trounson, and A. Bongso, *Embryonic stem cell lines from human blastocysts: Somatic differentiation in vitro.* Nat Biotechnol, 2000. 18(4): p. 399-404.

6. Thomson, J.A., J. Itskovitz-Eldor, S.S. Shapiro, M.A. Waknitz, J.J. Swiergiel, V.S. Marshall, and J.M. Jones, *Embryonic stem cell lines derived from human blastocysts.* Science, 1998. 282(5391): p. 1145-7.

7. Desbaillets, I., U. Ziegler, P. Groscurth, and M. Gassmann, *Embryoid bodies: An in vitro model of mouse embryogenesis.* Exp Physiol, 2000. 85(6): p. 645-51.

8. Prelle, K., N. Zink, and E. Wolf, *Pluripotent stem cells--model of embryonic development, tool for gene targeting, and basis of cell therapy.* Anat Histol Embryol, 2002. 31(3): p. 169-86.

9. Wobus, A.M. and K.R. Boheler, *Embryonic stem cells: Prospects for developmental biology and cell therapy.* Physiol Rev, 2005. 85(2): p. 635-78.

10. Takahashi, K., K. Tanabe, M. Ohnuki, M. Narita, T. Ichisaka, K. Tomoda, and S. Yamanaka, *Induction of pluripotent stem cells from adult human fibroblasts by defined factors.* Cell, 2007. 131(5): p. 861-72.

11. Takahashi, K. and S. Yamanaka, *Induction of pluripotent stem cells from mouse embryonic and adult fibroblast cultures by defined factors.* Cell, 2006. 126(4): p. 663-76.

12. Hodgson, D.M., A. Behfar, L.V. Zingman, G.C. Kane, C. Perez-Terzic, A.E. Alekseev, M. Puceat, and A. Terzic, *Stable benefit of embryonic stem cell therapy*

in myocardial infarction. Am J Physiol Heart Circ Physiol, 2004. 287(2): p. H471-9.

13. Klug, M.G., M.H. Soonpaa, G.Y. Koh, and L.J. Field, *Genetically selected cardiomyocytes from differentiating embronic stem cells form stable intracardiac grafts.* J Clin Invest, 1996. 98(1): p. 216-24.

14. Kofidis, T., J.L. de Bruin, G. Hoyt, Y. Ho, M. Tanaka, T. Yamane, D.R. Lebl, R.J. Swijnenburg, C.P. Chang, T. Quertermous, and R.C. Robbins, *Myocardial restoration with embryonic stem cell bioartificial tissue transplantation.* J Heart Lung Transplant, 2005. 24(6): p. 737-44.

15. Menard, C., A.A. Hagege, O. Agbulut, M. Barro, M.C. Morichetti, C. Brasselet, A. Bel, E. Messas, A. Bissery, P. Bruneval, M. Desnos, M. Puceat, and P. Menasche, *Transplantation of cardiac-committed mouse embryonic stem cells to infarcted sheep myocardium: A preclinical study.* Lancet, 2005. 366(9490): p. 1005-12.

16. Singla, D.K., T.A. Hacker, L. Ma, P.S. Douglas, R. Sullivan, G.E. Lyons, and T.J. Kamp, *Transplantation of embryonic stem cells into the infarcted mouse heart: Formation of multiple cell types.* J Mol Cell Cardiol, 2006. 40(1): p. 195-200.

17. Coucouvanis, E. and G.R. Martin, *Signals for death and survival: A two-step mechanism for cavitation in the vertebrate embryo.* Cell, 1995. 83(2): p. 279-87.

18. Doevendans, P.A., S.W. Kubalak, R.H. An, D.K. Becker, K.R. Chien, and R.S. Kass, *Differentiation of cardiomyocytes in floating embryoid bodies is comparable to fetal cardiomyocytes.* J Mol Cell Cardiol, 2000. 32(5): p. 839-51.

19. Hopfl, G., M. Gassmann, and I. Desbaillets, *Differentiating embryonic stem cells into embryoid bodies.* Methods Mol Biol, 2004. 254: p. 79-98.

20. Itskovitz-Eldor, J., M. Schuldiner, D. Karsenti, A. Eden, O. Yanuka, M. Amit, H. Soreq, and N. Benvenisty, *Differentiation of human embryonic stem cells into embryoid bodies compromising the three embryonic germ layers.* Mol Med, 2000. 6(2): p. 88-95.

21. Keller, G.M., *In vitro differentiation of embryonic stem cells.* Curr Opin Cell Biol, 1995. 7(6): p. 862-9.

22. Bauwens, C., T. Yin, S. Dang, R. Peerani, and P.W. Zandstra, *Development of a perfusion fed bioreactor for embryonic stem cell-derived cardiomyocyte generation: Oxygen-mediated enhancement of cardiomyocyte output.* Biotechnol Bioeng, 2005. 90(4): p. 452-61.

23. Cameron, C.M., W.S. Hu, and D.S. Kaufman, *Improved development of human embryonic stem cell-derived embryoid bodies by stirred vessel cultivation.* Biotechnol Bioeng, 2006. 94(5): p. 938-48.

24. Dang, S.M., S. Gerecht-Nir, J. Chen, J. Itskovitz-Eldor, and P.W. Zandstra, *Controlled, scalable embryonic stem cell differentiation culture.* Stem Cells, 2004. 22(3): p. 275-82.

25. Dang, S.M., M. Kyba, R. Perlingeiro, G.Q. Daley, and P.W. Zandstra, *Efficiency of embryoid body formation and hematopoietic development from embryonic stem cells in different culture systems.* Biotechnol Bioeng, 2002. 78(4): p. 442-53.

26. Gerecht-Nir, S., S. Cohen, and J. Itskovitz-Eldor, *Bioreactor cultivation enhances the efficiency of human embryoid body (heb) formation and differentiation.* Biotechnol Bioeng, 2004. 86(5): p. 493-502.

27. Kurosawa, H., *Methods for inducing embryoid body formation: In vitro differentiation system of embryonic stem cells.* J Biosci Bioeng, 2007. 103(5): p. 389-98.

28. Niebruegge, S., A. Nehring, H. Bar, M. Schroeder, R. Zweigerdt, and J. Lehmann, *Cardiomyocyte production in mass suspension culture: Embryonic stem cells as a source for great amounts of functional cardiomyocytes.* Tissue Eng Part A, 2008.

29. Schroeder, M., S. Niebruegge, A. Werner, E. Willbold, M. Burg, M. Ruediger, L.J. Field, J. Lehmann, and R. Zweigerdt, *Differentiation and lineage selection of mouse embryonic stem cells in a stirred bench scale bioreactor with automated process control.* Biotechnol Bioeng, 2005. 92(7): p. 920-33.

30. Wang, X., G. Wei, W. Yu, Y. Zhao, X. Yu, and X. Ma, *Scalable producing embryoid bodies by rotary cell culture system and constructing engineered cardiac tissue with es-derived cardiomyocytes in vitro.* Biotechnol Prog, 2006. 22(3): p. 811-8.

31. Zandstra, P.W., C. Bauwens, T. Yin, Q. Liu, H. Schiller, R. Zweigerdt, K.B. Pasumarthi, and L.J. Field, *Scalable production of embryonic stem cell-derived cardiomyocytes.* Tissue Eng, 2003. 9(4): p. 767-78.

32. Bueno, E.M., B. Bilgen, R.L. Carrier, and G.A. Barabino, *Increased rate of chondrocyte aggregation in a wavy-walled bioreactor.* Biotechnology and Bioengineering, 2004. 88(6): p. 767-77.

33. Prewett, T., T. Goodwin, and G. Spaulding, *Three-dimensional modeling of t-24 human bladder carcinoma cell line: A new simulated microgravity culture vessel.* Methods in Cell Science, 1993. 15(1): p. 29-36.

34. Schwarz, R.P., T.J. Goodwin, and D.A. Wolf, *Cell culture for three-dimensional modeling in rotating-wall vessels: An application of simulated microgravity.* J Tissue Cult Methods, 1992. 14(2): p. 51-7.

35. Carpenedo, R.L., C.Y. Sargent, and T.C. McDevitt, *Rotary suspension culture enhances the efficiency, yield, and homogeneity of embryoid body differentiation.* Stem Cells, 2007. 25(9): p. 2224-34.

36. Sargent, C.Y., G.Y. Berguig, M.A. Kinney, L.A. Hiatt, R.L. Carpenedo, R.E. Berson, and T.C. McDevitt, *Hydrodynamic modulation of embryonic stem cell differentiation by rotary orbital suspension culture.* Biotechnol Bioeng, 2010. 105(3): p. 611-26.

37. Sargent, C.Y., G.Y. Berguig, and T.C. McDevitt, *Cardiomyogenic differentiation of embryoid bodies is promoted by rotary orbital suspension culture.* Tissue Eng Part A, 2009. 15(2): p. 331-342.

38. Hogers, B., M.C. DeRuiter, A.M. Baasten, A.C. Gittenberger-de Groot, and R.E. Poelmann, *Intracardiac blood flow patterns related to the yolk sac circulation of the chick embryo.* Circ Res, 1995. 76(5): p. 871-7.

39. Hogers, B., M.C. DeRuiter, A.C. Gittenberger-de Groot, and R.E. Poelmann, *Unilateral vitelline vein ligation alters intracardiac blood flow patterns and morphogenesis in the chick embryo.* Circ Res, 1997. 80(4): p. 473-81.

40. Hove, J.R., *In vivo biofluid dynamic imaging in the developing zebrafish.* Birth Defects Res C Embryo Today, 2004. 72(3): p. 277-89.

41. Hove, J.R., R.W. Koster, A.S. Forouhar, G. Acevedo-Bolton, S.E. Fraser, and M. Gharib, *Intracardiac fluid forces are an essential epigenetic factor for embryonic cardiogenesis.* Nature, 2003. 421(6919): p. 172-7.

42. Groenendijk, B.C.W., B.P. Hierck, J. Vrolijk, M. Baiker, M.J.B.M. Pourquie, A.C. Gittenberger-de Groot, and R.E. Poelmann, *Changes in shear stress-related gene expression after experimentally altered venous return in the chicken embryo.* Circulation Research, 2005. 96(12): p. 1291-8.

43. Wang, H., G.M. Riha, S. Yan, M. Li, H. Chai, H. Yang, Q. Yao, and C. Chen, *Shear stress induces endothelial differentiation from a murine embryonic mesenchymal progenitor cell line.* Arterioscler Thromb Vasc Biol, 2005. 25(9): p. 1817-23.

44. Adamo, L., O. Naveiras, P.L. Wenzel, S. McKinney-Freeman, P.J. Mack, J. Gracia-Sancho, A. Suchy-Dicey, M. Yoshimoto, M.W. Lensch, M.C. Yoder, G. Garcia-Cardena, and G.Q. Daley, *Biomechanical forces promote embryonic haematopoiesis.* Nature, 2009. 459(7250): p. 1131-5.

45. Yamamoto, K., T. Sokabe, T. Watabe, K. Miyazono, J.K. Yamashita, S. Obi, N. Ohura, A. Matsushita, A. Kamiya, and J. Ando, *Fluid shear stress induces differentiation of flk-1-positive embryonic stem cells into vascular endothelial cells in vitro.* Am J Physiol Heart Circ Physiol, 2005. 288(4): p. H1915-24.

46. Lutgens, E., M.J. Daemen, E.D. de Muinck, J. Debets, P. Leenders, and J.F. Smits, *Chronic myocardial infarction in the mouse: Cardiac structural and functional changes.* Cardiovasc Res, 1999. 41(3): p. 586-93.

47. Pfeffer, J.M., M.A. Pfeffer, P.J. Fletcher, and E. Braunwald, *Progressive ventricular remodeling in rat with myocardial infarction.* Am J Physiol, 1991. 260(5 Pt 2): p. H1406-14.

48. Pfeffer, M.A. and E. Braunwald, *Ventricular remodeling after myocardial infarction. Experimental observations and clinical implications.* Circulation, 1990. 81(4): p. 1161-72.

49. Weisman, H.F. and B. Healy, *Myocardial infarct expansion, infarct extension, and reinfarction: Pathophysiologic concepts.* Prog Cardiovasc Dis, 1987. 30(2): p. 73-110.

50. Foley, A. and M. Mercola, *Heart induction: Embryology to cardiomyocyte regeneration.* Trends Cardiovasc Med, 2004. 14(3): p. 121-5.

51. Chen, J.N. and M.C. Fishman, *Genetics of heart development.* Trends Genet, 2000. 16(9): p. 383-8.

52. Klaus, A. and W. Birchmeier, *Developmental signaling in myocardial progenitor cells: A comprehensive view of bmp- and wnt/beta-catenin signaling.* Pediatr Cardiol, 2009. 30(5): p. 609-16.

53. Naito, A.T., I. Shiojima, H. Akazawa, K. Hidaka, T. Morisaki, A. Kikuchi, and I. Komuro, *Developmental stage-specific biphasic roles of wnt/beta-catenin signaling in cardiomyogenesis and hematopoiesis.* Proc Natl Acad Sci U S A, 2006. 103(52): p. 19812-7.

54. van de Schans, V.A., J.F. Smits, and W.M. Blankesteijn, *The wnt/frizzled pathway in cardiovascular development and disease: Friend or foe?* Eur J Pharmacol, 2008. 585(2-3): p. 338-45.

55. Zaffran, S. and M. Frasch, *Early signals in cardiac development.* Circ Res, 2002. 91(6): p. 457-69.

56. Kawai, T., T. Takahashi, M. Esaki, H. Ushikoshi, S. Nagano, H. Fujiwara, and K. Kosai, *Efficient cardiomyogenic differentiation of embryonic stem cell by*

fibroblast growth factor 2 and bone morphogenetic protein 2. Circ J, 2004. 68(7): p. 691-702.

57. Yoon, B.S., S.J. Yoo, J.E. Lee, S. You, H.T. Lee, and H.S. Yoon, *Enhanced differentiation of human embryonic stem cells into cardiomyocytes by combining hanging drop culture and 5-azacytidine treatment.* Differentiation, 2006. 74(4): p. 149-59.

CHAPTER 2

BACKGROUND

Embryonic Stem Cells and Differentiation

Embryonic stem cells (ESCs) are pluripotent cells derived from the inner cell mass of blastocysts stage embryos capable of differentiating into all somatic cell types. ESCs are defined by their ability to both self-renew indefinitely in an undifferentiated state and differentiate into cells comprising the three germ lineages (mesoderm, endoderm, and ectoderm), as well as germ cells [1-3]. ESCs were derived first from mouse embryos [1-2, 4], followed by non-human primates [5-6], and finally human ESCs were obtained [3, 7]. Mouse and human ESCs share several of the same transcriptional programs, but they can respond differently to exogenous factors, such as leukemia inhibitory factor (LIF), required to maintain the undifferentiated state of mESCs. Additionally, hESCs require slightly different culture techniques, as hESCs are either co-cultured with mouse embryonic fibroblasts (MEFs) or cultured on Matrigel™ [8-9]. The ability of ESCs to differentiate into many desirable cell types that are not easily isolated and expanded from primary sources, such as pancreatic β-cells [10-12], neurons [13-16], endothelial cells [17-19], and cardiomyocytes [20-23], has led many scientists to focus on the use of ESCs for potential therapies of degenerative diseases where native tissues and cells have lost function. In fact, ESC-derived cardiomyocytes are unique in their ability to functionally couple with host cardiac tissue [24]. Recently, investigators have demonstrated the ability to produce pluripotent cells via retroviral transduction of transcription factors (typically Oct3/4, Sox2, Klf4, and c-Myc) into mammalian somatic

cells [25-26]. These induced pluripotent stem (iPS) cells exhibit characteristic differentiation and self-renewal similar to ESCs, and may offer several advantages compared to ESCs including the ability to derive autologous cells for regenerative medicine or derive stem cell lines from specific diseases to study *in vitro* cellular responses to potential therapies. Additionally, iPS cells can be cultured and induced to differentiate using similar methods applied to ESCs, including the spontaneous formation of cellular aggregates in suspension. Differentiation into hematopoietic and cardiomyogenic lineages and the response to Wnt and Bmp signaling are similar in iPS cells and ESCs [27-31]. However, continued examination is necessary to directly compare the properties of iPS cells to ESCs since several lines of iPS cells have been derived from numerous cell types as well as with varying transcription factors, and several studies have illustrated discrepancies in the differentiation potential between iPS cell lines and ESCs, including induction to oligodendrocytes, hematopoietic cells, neuronal cells [32-34]. Additionally, the reprogramming transcription factors are currently delivered via viral transduction, which may increase the occurrence of tumor formation; therefore, continued work is necessary to derive iPS cells that remain comparable to ESCs and without immune-response or tumorgenesis.

Several methods exist to induce ESC differentiation, most simply in the mouse system by maintaining monolayer culture in the absence of LIF. However, differentiation is most commonly initiated via spontaneous aggregation of single-cell suspensions into clusters of cells mediated by cell-cell adhesion molecule, E-cadherin [35] because the yield of differentiating cells is increased compared to monolayer culture and three-dimensional is believed to be biologically preferred to two-dimensional culture allowing

for native cell-cell contacts and signaling. These cell spheroids are termed embryoid bodies (EBs) and recapitulate many of the cellular morphogenic events similar to those of pre-implantation stage embryos, eventually leading to formation of cell types comprising the three germ lineages (ectoderm, endoderm and mesoderm) [4, 36-40]. Several different techniques have been developed to promote the necessary aggregation of ESCs to facilitate EB formation and differentiation, including methods that physically separate individual EBs to yield homogenous populations and batch methods that result in increased yields of EBs but with increased heterogeneity. Hanging drop cultures are initiated by suspending small volumes of culture media (10-20 μL) containing a defined number of cells (200-1000 cells) from the lid of a Petri dish. For experimental studies, hanging drop cultures are typically employed to study mesoderm differentiation because of the high frequency with which cardiogenic differentiation can be readily observed [41-42]; however, mechanisms behind this observation of increased cardiogenic differentiation remain largely unknown. Additionally, hanging drops yield uniformly-sized EBs, but the need to physically separate individual drops limits the number of EBs formed per dish (~100 per 10 cm plate); thus, hanging drops are not readily amenable to scale-up methods [22, 42-43]. Centrifugation of a defined number of ESCs in individual wells of 96-well round bottom dishes also yields uniform EBs, but it does not overcome the scalability issue [44]. Recently, ultra-high throughput microwells have been utilized in conjunction with forced aggregation via centrifugation to produce high yields of EBs, but maintaining the EBs in the individual microwells can be difficult for longer duration differentiation studies [45]. Thus, physically separating EBs during formation and culture results in homogeneous populations of EB, but these methods either do not

produce high enough yields for large comparative studies or clinically relevant cell numbers or are difficult to maintain; therefore, EB culture techniques that produce homogeneous EB with high yields are necessary for stem cell field and tissue engineering to ultimately be successful.

In contrast to physically separated EB culture methods, suspension cultures are typically initiated by simply inoculating 10^{4-6} cells/mL under non-adherent culture conditions. In static suspension, ESCs form a population of EBs heterogeneous in size and shape that tend to readily agglomerate, thereby further increasing the heterogeneity of differentiation among EBs and reducing the overall efficiency of cell differentiation [46]. However, static suspension culture does offer the advantage of relatively easy manipulation, larger EB yields per dish, and screening of several variables in parallel, including the addition of exogenous soluble factors and exposure to hypoxic conditions, implicated in regulating EB differentiation. Hanging drop and suspension culture methods can be combined by initiating EBs in hanging drop before transferring to suspension [42, 47]; however, this combined approach still limits the overall yield of EBs since EBs are still originally formed in individual drops, requiring 10-20 plates to produce 1,000 – 2,000 EBs and may only temporarily inhibit agglomeration of the EBs in suspension. Combining ultra-high throughput technology with static suspension culture may address the limited yield of EBs, but although static culture techniques are adequate for the purpose of small-scale experimentation (~25 x 10^6 cells per 10mL dish after 7 days of differentiation initiated with 4 x 10^6 cells [48]), such methods are not efficient means of producing large populations of EBs and differentiated cells as upwards of two billion cells are estimated to be required for some final clinical applications [49].

Hydrodynamic Culture

Bioreactor Systems

The application of larger-volume bioreactors (10^{2-4} mL) for EB culture is a promising approach to scale the production of differentiated ESC and iPS cell populations because larger yields of EB can be obtained from similar inoculation densities to smaller volume, static cultures. However, compared to conventional static EB culture techniques, mixed or stirred bioreactors introduce added complexities, including the hydrodynamic properties of shear stress and convective transport which could impact EB formation, maintenance, and subsequent differentiation. It has been shown that stem cells respond to a variety of cues *in vitro* to either maintain pluripotency or regulate differentiation; these cues include biochemical factors (both exogenous and endogenous), cell-cell interactions, cell-matrix interactions, and mechanical stimuli. All of these factors are largely interconnected within the context of stem cell biology, and several of these parameters are modulated within hydrodynamic systems. For example, spheroid formation and size regulated by cell-cell adhesion are modulated hydrodynamic mixing speeds, but spheroid size can also lead to diffusion limitations (biomolecule concentrations) in addition to the inherent transport characteristics of the mixing speed utilized, therefore, stem cell fate is likely a result of synergy between direct and indirect responses of cells to the hydrodynamic environment. Therefore, stem cell maintenance and differentiation within fluid dynamic systems are beginning to be investigated [35, 47, 50-57]. The ability to maintain the pluripotent state of stem cells while achieving large expansion within bioreactors is imperative to the continued study and possible clinical application of stem cells. Both mESCs adherent to microcarriers in spinner flaks

and mESC aggregates without substrates in bioreactors maintain expression of pluripotent markers and retain the ability to differentiate [55-56]. Similarly, hESCs maintain pluripotency when hydrodynamically cultured on microcarriers or in aggregates and can be subsequently differentiated after expansion [58-59]. Utilizing microcarriers within bioreactors is a relatively straight-forward first step in the scale-up of ESC culture, moving from a static adhesive surface in a culture dish to a mobile adhesive surface increasing the available surface area for cell growth in a hydrodynamic environment without greatly altering exposure to media nutrients or waste removal. The three-dimensional culture of cells, however, is thought to more accurately recapitulate cellular adhesions and signaling exhibited by native tissue, particularly in the absence of exogenous adherent scaffolding [60-61], and culturing cell spheroids within hydrodynamic conditions introduces additional variables such as aggregation kinetics, fluidic forces, and perfusion through the spheroid. Encapsulation methods have also been utilized to culture EBs in mixed hydrodynamic bioreactors to allow for three-dimensional culture without agglomeration. However, although encapsulation of ESCs within non-adherent hydrodgels prevented agglomeration initially, as EBs grew in size they emerged from agarose or alginate beads and still underwent occasional agglomeration events [35, 62]. Encapsulation techniques also result in additional diffusional barriers which must be accounted for to ensure adequate nutrient exchange and also the potential delivery of soluble morphogens. Taken together, stem cells can be cultured in a variety of formats within bioreactors, including on adherent microcarriers, encapsulated within hydrogels, and as cellular aggregates free of exogenous substrates and to maintain more native cell-cell contacts and potentially generate endogenous adhesive matrices.

In addition to varying the format of ESC culture in hydrodynamic systems, a variety of existing bioreactor systems have been examined as initial means of scaling up differentiating EB cultures. Spinner flasks can produce EBs from single cell suspensions, but the EBs agglomerate into large masses of cells, ultimately increasing the heterogeneity of the resulting population and decreasing the effective cell yield [46]. The use of other bioreactor systems, such as slow turning lateral vessel (STLV), and improvements in stirred vessels by changing the geometry of the impellor blade have resulted in controlled environments capable of forming and maintaining EBs with little agglomeration [54, 63-65]. The fact that simple modification of a pitched blade impellor to a bulb-shaped impellor within spinner flasks resulted in efficient and homogeneous EB formation suggests that even a slight change in the hydrodynamic profile may affect EB properties that might alter differentiation. In addition, the vessel type can alter cellular aggregation dynamics, as indicated by modulation of spheroid formation rate within different mixed cultures under similar agitation speeds [63, 66]. Although these bioreactor systems have been in used in attempts to increase differentiating cell yields from EBs, few have systematically examined how the hydrodynamic mixing conditions affect ESC differentiation. It has been established that many bioreactor systems do not inhibit the ability of stem cells to differentiate [48, 52, 63-64]; however, studies indicate changes in global gene expression profiles within differentiating mEBs from hydrodynamic culture conditions compared to static conditions [57]. There are discrepancies in the endogenous ability of dynamically cultured EBs to differentiate towards particular lineages. Fok and colleagues observed no statistical difference in cardiac or hematopoietic differentiation between mEBs cultured in spinner flasks (60 and

100 rpm) and statically differentiated mEBs [52], and there was no difference in cardiomyocyte differentiation between static mEBs and those cultured within STLVs [54]. However, others have reported enhanced cardiomyocyte differentiation within mEBs cultured in spinner flasks compared to static conditions [51, 65]. The discrepancies in differentiation observed between different large-scale bioreactor systems suggest that hydrodynamic conditions may affect ESC differentiation.

Attempts have been made to quantify the resulting hydrodynamic forces within bioreactors, specifically within spinner flask systems, using combinations of computational fluid dynamic (CFD) simulations and experimental particle-image velocimetry (PIV) [67-68]. These analyses help to define hydrodynamic properties including shear stress and velocity profiles as well as frequency characteristics of the mixing system. Sliding-mesh and multiple reference frame methods are typically used for CFD analysis of bioreactor systems, which only models the fluid dynamics within the reactor and does not account for the air-fluid interface [69]. This limitation of CFD modeling is acceptable within large bioreactor systems because the fluid-air interface is relatively small area compared to the fluid volume; however, approaches to account for the effects of the fluid-air interface would be required to simulate smaller-volume hydrodynamic systems. Altogether, continued examination of hydrodynamic systems and their effects on stem cell culture and differentiation along with the determination of system characteristics responsible for the cellular responses observed is needed to progress stem cell technologies towards therapeutics and clinical applications.

Bench-Scale Hydrodynamic Culture

To fully interrogate the large experimental space of the various hydrodynamic states which could influence EBs, smaller-scale systems that impart hydrodynamic conditions on differentiating ESC spheroids are necessary. Direct scaling-down of traditional bioreactor systems faces several challenges. Typically the volumes and dimensions of reactors do not directly scale in relation to their resultant shear forces and transport properties; therefore, the hydrodynamic environment of a smaller reactor may be significantly different to that of its larger counter-part. Since the resulting hydrodynamics within smaller-scaled bioreactors are not equal to those within larger-scale bioreactors, it makes sense to first examine the effects of hydrodynamics on stem cell culture in a simpler system, more similar to traditional Petri-dish EB culture to determine general responses of aggregate formation and differentiation and what variables might be most important to regulate within mixed cultures. In contrast to large volume systems (0.5L – 2L), the simple application of gentle external rocking or shaking can be used to impart hydrodynamic mixing directly to commonly used laboratory culture dishes. Rotary orbital suspension culture is an externally agitated lab-scale (10mL) system where mixing is initiated by placing Petri dishes on rotary orbital shakers, and therefore, many hydrodynamic conditions and additional variables can be screened in parallel [48, 54, 70]. Rotary orbital culture has been shown to increase EB yield and homogeneity as defined by shape and size of EBs compared to equivalent inoculation densities within static suspension cultures [48, 54, 70]. Our laboratory has compared the effects of rotary orbital suspension culture (40 rpm) on EB formation and differentiation to hanging drop and static suspension [48]. The application of constant orbital shaking

during EB suspension culture enhanced the formation efficiency of EBs from a single inoculation density of ESC-cell suspension and yielded significantly greater numbers of individual EBs and EB-derived cells after 7 days of culture, compared to static suspension [48]. Additional studies directly comparing various ESC densities should be conducted to determine if EB formation efficiency and yield are impacted by starting cell density. Compared to static culture, rotary orbital culture produced more homogeneous populations of EBs and EBs were still able to differentiate into derivatives of all three germ lineages [48], and an initial study by Zweigerdt *et al.* suggested that cardiogenic differentiation was potentially enhanced by rotary culture [70]. Preliminary evidence suggested that rotary orbital speed could regulate EBs size, and endoderm associated differentiation was significantly increased in rotary EBs compared to static; however, detailed effects of rotary orbital suspension culture on EB differentiation towards germ lineages and specific cell types still need to be determined. Utilizing this simple bench-scale system of rotary orbital culture to examine the effects of hydrodynamic conditions on stem cell formation, morphology, and differentiation would allow for the determination of the governing hydrodynamic parameters, such as shear stress ranges, that regulate cell responses; these parameters could then be engineered into the design of larger-scale bioreactors.

Early Development and Differentiation

EB formation is the most commonly applied method for the differentiation of ESCs because the progression of cellular differentiation within the ESC aggregates closely mimics patterns of gene expression and phenotypic differentiation of developing embryos [4]. In development, the pluripotent inner cell mass (which ESCs are derived

from) rapidly differentiates into the primitive ectoderm, and upon implantation, these cells undergo apoptosis forming a cavity surrounded by a pseudostratified columnar layer of cells [39]. This structure is termed the epiblast [71-73], and from this point the embryo undergoes axis patterning to determine the posterior side of the embryo, where a transient structure referred to as the primitive streak is formed, and the anterior side of the embryo, where the anterior visceral endoderm (AVE) secretes signals antagonist to those from the primitive streak. While the primitive streak is associated with expression of transforming growth factor β (TGFβ) family members (eg. *Nodal and Lefty1)* and Wnt family ligands (secreted glycoproteins) [74], the AVE is characterized by expression of Nodal and Wnt repressors (*Dkk-1, Sfrp1 and Sfrp5)* [75-76]. As epiblast cells migrate through the primitive streak, they undergo an epithelial to mesenchymal transition (EMT), are marked by transient expression of the mesoderm marker *brachyury T*, and eventually continue to form the mesoderm and definitive endoderm [77-78]. Cells which do not transverse the primitive streak give rise to the ectoderm. Migration events and EMT are regulated in part by cell-cell adhesions, primarily through the expression of cell adhesion molecule E-cadherin, a Ca^{2+} dependent homophilic adhesion molecule [79-81]. E-cadherin is expressed during morula compaction and implantation of mouse embryos [82-83], and disruption of E-cadherin binding during development allows for cell migration and may be accomplished by receptor tyrosine kinase phosphorylation of the E-cadherin complex resulting in the endocytosis and reduction of E-cadherin [81, 84-86]. Additionally, E-cadherin is present on the surface of ESCs that is responsible for cell-cell adhesion in undifferentiated ESC colonies as well as initial EB formation [35]. These events *in vivo* require tightly controlled spatiotemporal regulation of several signaling

molecules, and although EBs lack the organization to directly mimic the regulation of these events, they maintain the ability to respond to the same molecular instructions [77].

β-catenin Signaling

Beta-catenin signaling is an important signaling pathway active in early embryonic development, aiding in the regulation of embryonic patterning, axis formation, primitive streak formation, and mesoderm differentiation [74, 87]. Similarly, in ESCs, β-catenin signaling is required both for maintenance of pluripotency [88], as well as self-organization, axis formation, and initial mesoderm differentiation [89-90]. Two pools of β-catenin are present within cells: 1- β-catenin sequestered within cell adherens junctions, specifically with E-cadherin at the cell membrane [91-93], and 2 – stabilized cytoplasmic β-catenin that can translocate to the nucleus, and associate with T-cell factor/Leukemia enhancer factor (TCF/LEF) to mediate transcription [94-97]. Thus, β-catenin can serve dual roles within cells, regulating cytoskeletal arrangement and modulating transcription, and the availability of β-catenin for transcriptional regulation may be in part regulated by the stability of the E-cadherin complex.

The canonical Wnt/β-catenin signaling pathway is the best understood method for initiating β-catenin-regulated transcription (Figure 2.1). When Wnt ligands are not present, non-bound cytomplasmic β-catenin phosphorylated by the glycogen synthase kinase 3β (GSK3β)/adenomatous poliposis coli (APC)/Axin complex at serine-threonine residues of the aminoterminus and is targeted for ubiquitination [98-99]. Upon Wnt binding to members of seven-transmembrane Frizzled receptor family, the Frizzled receptor heterodimerizers with low-density lipoprotein receptor-related protein 5 and/or 6 (LRP5/6), which in turn cause the disruption of the GSK3β/APC/Axin complex, resulting

in the accumulation of stabilized cytoplasmic β-catenin. This desphosphorylated form of β-catenin at Ser/Thr residues can translocate to the nucleus where it binds with TCF/LEF to regulate the transcription of target genes [99-103]. Whether there is convergence or cross-talk between the two pools of β-catenin is still under debate. Some evidence indicates that not only is the phosphorylation state important activation of signaling β-catenin, but also there are distinct molecular confirmations that determine whether β-catenin can complex with TCF/LEF or with cadherins [92]. However, much empirical evidence exists to support that the equilibrium between cadherin/β-catenin, β-catenin/APC, and β-catenin/TCF is dependent on cadherin engagement and Wnt activation, suggesting that availability of β-catenin for transcriptional regulation can be regulated by cadherin expression [104]. Additionally, a recent study by Kam and Quaranta illustrated that cadherin-bound β- catenin could be made available for signaling upon E-cadherin endocytosis and subsequent Wnt activation [105]. What is known for certain is that β-catenin is a central component in both cell-cell interactions and gene transcription, both of which are highly important in regulating embryonic development and ESC differentiation.

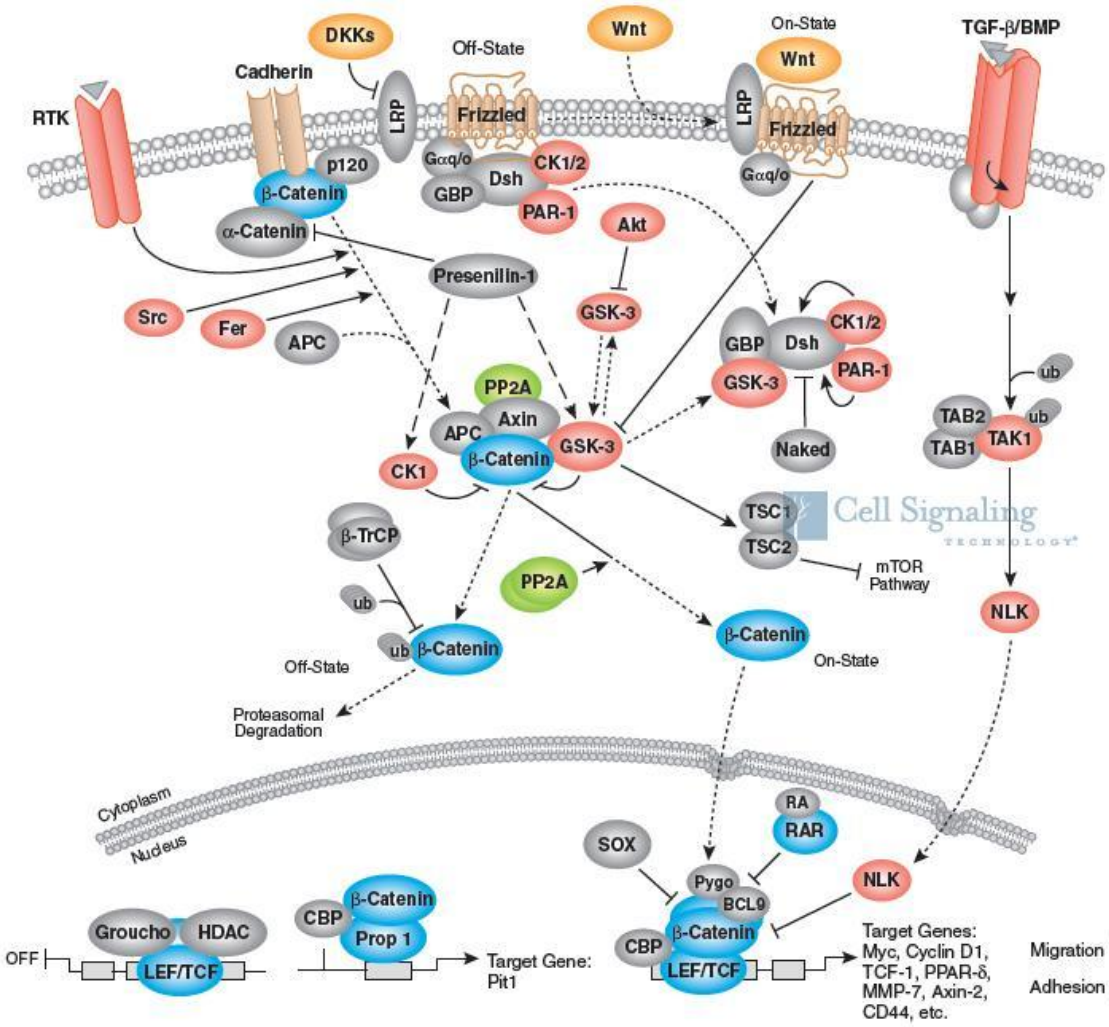

Figure 2.1: β-catenin signaling pathway. β-catenin may be associated with E-cadherin and the cell membrane, or it can translocate to the nucleus where it binds to TCF/LEF and regulates transcription. In the presence of Wnt binding to frizzled, β-catenin Scr/Thr phosphorylation by the GSK3β complex is prevented, and the stabilized β-catenin accumulates in the cytomplasm and can move to the nucleus. In the absence of Wnt, cytoplasmic β-catenin is phosphorylated by the GSK3β complex and degraded. Modified from http://www.cellsignal.com/pathways/wnt-hedgehog.jsp (Cell Signaling Technology)

Cardiogenic Differentiation

The heart is the first organ to form in the developing mammal. Proper heart development relies on an exact interplay of cell-cell and tissue signaling events that are spatially and temporally controlled [106]. In the early embryo, the heart derives from the

anterior mesoderm, from which two separate progenitor are formed, the first heart field and the second heart field [107-108]. Both inductive and repressive signals from the surrounding tissue, including the endoderm, direct cardiac maturation. Cells within the first heart field form the cardiac crescent migrate with cells from the second heart field to the midline where they form a linear tube and later contribute to the left ventricle. Cells within the second heart field do not differentiation until they migrate to the midline, where they join the first heart field to induce rightward looping of the linear heart tube and finally contribute to the right ventricle and inflow and outflow tracts [109-113]. Not only are these proliferation, migration, and differentiation events induced by signaling from cell-cell and paracrine pathways, but the physical environment including fluid flow also plays an essential role in proper heart formation [114-116]. For example, hemodynamic forces are important for the regulation of cardiac morphogenesis in developing embryos, where altered flow patterns result in cardiac defects [114-115, 117-118]. High wall shear stresses have been measured within developing cardiac structures *in vivo* [115], and can be correlated to specific patterns of gene regulation in endocardial tissue [119]. The interplay between cell signaling and the physical environment may aid in regulating the necessary spatial and temporal patterns required for final heart development, and thus, both components may be necessary for *in vitro* cardiomyocyte differentiation.

One important signaling pathway in cardiac development is the canonical Wnt/β-catenin pathway, which is highly conserved across most species in developmental regulation, but appears to act in different ways when controlling heart formation in different species. In *Drosophila*, Wingless, a homeolog to Wnt in vertebrates, is required

for cardiac development [120-121]; however, in frog and chick embryos, over-activation of β-catenin by Wnt suppresses cardiac lineage determination, reducing cardiomyocyte differentiation [2, 122]. Recent studies in genetically modified mice and mouse ESCs have illustrated that activation of the Wnt/β-catenin pathway can play both an inductive and repressive role in cardiomyogenesis depending on the temporal aspect of stimulation. Wnt/β-catenin activation during early EB differentiation (between days 2 and 5 of differentiation) increases cardiomyocyte differentiation, while late-stage activation prevents early cardiac committed cells from terminally differentiating into cardiomyocytes [123-124]. The converse is also true; early inhibition of Wnt/β-catenin suppresses cardiac differentiation, while later inhibition increases cardiomyogenesis. It is currently thought that early activation of β-catenin signaling serves to increase the proliferation of Isl1+ cardiomyocyte progenitors [125-128], but to proceed to more definitive cardiomyocyte differentiation, inhibition of β-catenin signaling is required. Inhibition may be a feedback-loop programmed into early cardiomyocyte differentiation, whereupon increased transcription of early mesoderm and cardiac genes *Mesp1* and *Nkx2.5* serves to inhibit future β-catenin through either the increased transcription of *Dkk1* (a Wnt inhibitor) [129] or direct downregulation β-catenin transcription [130]. Recent studies conducted in *Mesp1-cre* and $BmpR1a^{lox/lox}$ mutant mice indicate that cross-talk between the Wnt/β-catenin pathway and BMP signaling is required for cardiogenesis [111], such cross-talk may assist in regulating the spatial, temporal control of Wnt/β-catenin required for cardiac development by first allowing β-catenin transcription of *Mesp1*, and then, in conjunction with BMP activation of SMAD1/5 to increase *Nkx2.5* expression, inhibiting β-catenin transcription. Taken together, the *in vitro* regulation of

Wnt/β-catenin signaling potentially through the modulation of β-catenin availability via E-cadherin regulation and in possible combination with paracrine and autocrine BMP signaling may enhance cardiomyogenesis. Components of this tightly regulated signaling cascade may be altered due EB formation methods, including hydrodynamic conditions, specifically affecting E-cadherin binding and cell-cell aggregation kinetics and thus potentially modulating the cardiomyogenic potential of the EB population. Therefore, further investigation of the cardiogenic response of ESCs to hydrodynamic conditions via β-catenin signaling is highly warranted.

References

1. Evans, M.J. and M.H. Kaufman, *Establishment in culture of pluripotential cells from mouse embryos.* Nature, 1981. 292(5819): p. 154-6.

2. Martin, G.R., *Isolation of a pluripotent cell line from early mouse embryos cultured in medium conditioned by teratocarcinoma stem cells.* Proc Natl Acad Sci U S A, 1981. 78(12): p. 7634-8.

3. Thomson, J.A., J. Itskovitz-Eldor, S.S. Shapiro, M.A. Waknitz, J.J. Swiergiel, V.S. Marshall, and J.M. Jones, *Embryonic stem cell lines derived from human blastocysts.* Science, 1998. 282(5391): p. 1145-7.

4. Doetschman, T.C., H. Eistetter, M. Katz, W. Schmidt, and R. Kemler, *The in vitro development of blastocyst-derived embryonic stem cell lines: Formation of visceral yolk sac, blood islands and myocardium.* J Embryol Exp Morphol, 1985. 87: p. 27-45.

5. Thomson, J.A., J. Kalishman, T.G. Golos, M. Durning, C.P. Harris, R.A. Becker, and J.P. Hearn, *Isolation of a primate embryonic stem cell line.* Proc Natl Acad Sci U S A, 1995. 92(17): p. 7844-8.

6. Thomson, J.A., J. Kalishman, T.G. Golos, M. Durning, C.P. Harris, and J.P. Hearn, *Pluripotent cell lines derived from common marmoset (callithrix jacchus) blastocysts.* Biol Reprod, 1996. 55(2): p. 254-9.

7. Reubinoff, B.E., M.F. Pera, C.Y. Fong, A. Trounson, and A. Bongso, *Embryonic stem cell lines from human blastocysts: Somatic differentiation in vitro.* Nat Biotechnol, 2000. 18(4): p. 399-404.

8. Ginis, I., Y. Luo, T. Miura, S. Thies, R. Brandenberger, S. Gerecht-Nir, M. Amit, A. Hoke, M.K. Carpenter, J. Itskovitz-Eldor, and M.S. Rao, *Differences between human and mouse embryonic stem cells.* Dev Biol, 2004. 269(2): p. 360-80.

9. Sato, N., I.M. Sanjuan, M. Heke, M. Uchida, F. Naef, and A.H. Brivanlou, *Molecular signature of human embryonic stem cells and its comparison with the mouse.* Dev Biol, 2003. 260(2): p. 404-13.

10. Champeris Tsaniras, S. and P.M. Jones, *Generating pancreatic {beta}-cells from embryonic stem cells by manipulating signaling pathways.* J Endocrinol, 2010.

11. Bernardo, A.S., C.H. Cho, S. Mason, H.M. Docherty, R.A. Pedersen, L. Vallier, and K. Docherty, *Biphasic induction of pdx1 in mouse and human embryonic stem cells can mimic development of pancreatic beta-cells.* Stem Cells, 2009. 27(2): p. 341-51.

12. Shi, Y., L. Hou, F. Tang, W. Jiang, P. Wang, M. Ding, and H. Deng, *Inducing embryonic stem cells to differentiate into pancreatic beta cells by a novel three-step approach with activin a and all-trans retinoic acid.* Stem Cells, 2005. 23(5): p. 656-62.

13. Nakayama, T. and N. Inoue, *Neural stem sphere method: Induction of neural stem cells and neurons by astrocyte-derived factors in embryonic stem cells in vitro.* Methods Mol Biol, 2006. 330: p. 1-13.

14. Sasai, Y., *Generation of dopaminergic neurons from embryonic stem cells.* J Neurol, 2002. 249 Suppl 2: p. II41-4.

15. Strubing, C., G. Ahnert-Hilger, J. Shan, B. Wiedenmann, J. Hescheler, and A.M. Wobus, *Differentiation of pluripotent embryonic stem cells into the neuronal lineage in vitro gives rise to mature inhibitory and excitatory neurons.* Mech Dev, 1995. 53(2): p. 275-87.

16. Fraichard, A., O. Chassande, G. Bilbaut, C. Dehay, P. Savatier, and J. Samarut, *In vitro differentiation of embryonic stem cells into glial cells and functional neurons.* J Cell Sci, 1995. 108 (Pt 10): p. 3181-8.

17. Watabe, T., A. Nishihara, K. Mishima, J. Yamashita, K. Shimizu, K. Miyazawa, S. Nishikawa, and K. Miyazono, *Tgf-beta receptor kinase inhibitor enhances growth and integrity of embryonic stem cell-derived endothelial cells.* J Cell Biol, 2003. 163(6): p. 1303-11.

18. Fraser, S.T., M. Ogawa, and S. Nishikawa, *Embryonic stem cell differentiation as a model to study hematopoietic and endothelial cell development.* Methods Mol Biol, 2002. 185: p. 71-81.

19. Balconi, G., R. Spagnuolo, and E. Dejana, *Development of endothelial cell lines from embryonic stem cells: A tool for studying genetically manipulated endothelial cells in vitro.* Arterioscler Thromb Vasc Biol, 2000. 20(6): p. 1443-51.

20. Boheler, K.R., J. Czyz, D. Tweedie, H.T. Yang, S.V. Anisimov, and A.M. Wobus, *Differentiation of pluripotent embryonic stem cells into cardiomyocytes.* Circ Res, 2002. 91(3): p. 189-201.

21. Fijnvandraat, A.C., A.C. van Ginneken, C.A. Schumacher, K.R. Boheler, R.H. Lekanne Deprez, V.M. Christoffels, and A.F. Moorman, *Cardiomyocytes purified from differentiated embryonic stem cells exhibit characteristics of early chamber myocardium.* J Mol Cell Cardiol, 2003. 35(12): p. 1461-72.

22. Maltsev, V.A., A.M. Wobus, J. Rohwedel, M. Bader, and J. Hescheler, *Cardiomyocytes differentiated in vitro from embryonic stem cells developmentally*

express cardiac-specific genes and ionic currents. Circ Res, 1994. 75(2): p. 233-44.

23. Wobus, A.M., G. Wallukat, and J. Hescheler, *Pluripotent mouse embryonic stem cells are able to differentiate into cardiomyocytes expressing chronotropic responses to adrenergic and cholinergic agents and ca2+ channel blockers.* Differentiation, 1991. 48(3): p. 173-82.

24. Kehat, I., L. Khimovich, O. Caspi, A. Gepstein, R. Shofti, G. Arbel, I. Huber, J. Satin, J. Itskovitz-Eldor, and L. Gepstein, *Electromechanical integration of cardiomyocytes derived from human embryonic stem cells.* Nat Biotechnol, 2004. 22(10): p. 1282-9.

25. Takahashi, K., K. Okita, M. Nakagawa, and S. Yamanaka, *Induction of pluripotent stem cells from fibroblast cultures.* Nat Protoc, 2007. 2(12): p. 3081-9.

26. Takahashi, K. and S. Yamanaka, *Induction of pluripotent stem cells from mouse embryonic and adult fibroblast cultures by defined factors.* Cell, 2006. 126(4): p. 663-76.

27. Kaichi, S., K. Hasegawa, T. Takaya, N. Yokoo, T. Mima, T. Kawamura, T. Morimoto, K. Ono, S. Baba, H. Doi, S. Yamanaka, T. Nakahata, and T. Heike, *Cell line-dependent differentiation of induced pluripotent stem cells into cardiomyocytes in mice.* Cardiovasc Res, 2010.

28. Wang, Y., K. Umeda, and N. Nakayama, *Collaboration between wnt and bmp signaling promotes hemoangiogenic cell development from human fibroblast-derived ips cells.* Stem Cell Res, 2010. 4(3): p. 223-31.

29. Narazaki, G., H. Uosaki, M. Teranishi, K. Okita, B. Kim, S. Matsuoka, S. Yamanaka, and J.K. Yamashita, *Directed and systematic differentiation of cardiovascular cells from mouse induced pluripotent stem cells.* Circulation, 2008. 118(5): p. 498-506.

30. Schenke-Layland, K., K.E. Rhodes, E. Angelis, Y. Butylkova, S. Heydarkhan-Hagvall, C. Gekas, R. Zhang, J.I. Goldhaber, H.K. Mikkola, K. Plath, and W.R. MacLellan, *Reprogrammed mouse fibroblasts differentiate into cells of the cardiovascular and hematopoietic lineages.* Stem Cells, 2008. 26(6): p. 1537-46.

31. Zhang, J., G.F. Wilson, A.G. Soerens, C.H. Koonce, J. Yu, S.P. Palecek, J.A. Thomson, and T.J. Kamp, *Functional cardiomyocytes derived from human induced pluripotent stem cells.* Circ Res, 2009. 104(4): p. e30-41.

32. Kulkeaw, K., Y. Horio, C. Mizuochi, M. Ogawa, and D. Sugiyama, *Variation in hematopoietic potential of induced pluripotent stem cell lines.* Stem Cell Rev, 2010.

33. Tokumoto, Y., S. Ogawa, T. Nagamune, and J. Miyake, *Comparison of efficiency of terminal differentiation of oligodendrocytes from induced pluripotent stem cells versus embryonic stem cells in vitro.* J Biosci Bioeng, 2010. 109(6): p. 622-8.

34. Hu, B.Y., J.P. Weick, J. Yu, L.X. Ma, X.Q. Zhang, J.A. Thomson, and S.C. Zhang, *Neural differentiation of human induced pluripotent stem cells follows developmental principles but with variable potency.* Proc Natl Acad Sci U S A, 2010. 107(9): p. 4335-40.

35. Dang, S.M., S. Gerecht-Nir, J. Chen, J. Itskovitz-Eldor, and P.W. Zandstra, *Controlled, scalable embryonic stem cell differentiation culture.* Stem Cells, 2004. 22(3): p. 275-82.

36. Doevendans, P.A., S.W. Kubalak, R.H. An, D.K. Becker, K.R. Chien, and R.S. Kass, *Differentiation of cardiomyocytes in floating embryoid bodies is comparable to fetal cardiomyocytes.* J Mol Cell Cardiol, 2000. 32(5): p. 839-51.

37. Hopfl, G., M. Gassmann, and I. Desbaillets, *Differentiating embryonic stem cells into embryoid bodies.* Methods Mol Biol, 2004. 254: p. 79-98.

38. Itskovitz-Eldor, J., M. Schuldiner, D. Karsenti, A. Eden, O. Yanuka, M. Amit, H. Soreq, and N. Benvenisty, *Differentiation of human embryonic stem cells into embryoid bodies compromising the three embryonic germ layers.* Mol Med, 2000. 6(2): p. 88-95.

39. Coucouvanis, E. and G.R. Martin, *Signals for death and survival: A two-step mechanism for cavitation in the vertebrate embryo.* Cell, 1995. 83(2): p. 279-87.

40. Keller, G.M., *In vitro differentiation of embryonic stem cells.* Curr Opin Cell Biol, 1995. 7(6): p. 862-9.

41. Kurosawa, H., *Methods for inducing embryoid body formation: In vitro differentiation system of embryonic stem cells.* J Biosci Bioeng, 2007. 103(5): p. 389-98.

42. Yoon, B.S., S.J. Yoo, J.E. Lee, S. You, H.T. Lee, and H.S. Yoon, *Enhanced differentiation of human embryonic stem cells into cardiomyocytes by combining hanging drop culture and 5-azacytidine treatment.* Differentiation, 2006. 74(4): p. 149-59.

43. Wiese, C., G. Kania, A. Rolletschek, P. Blyszczuk, and A.M. Wobus, *Pluripotency: Capacity for in vitro differentiation of undifferentiated embryonic stem cells.* Methods Mol Biol, 2006. 325: p. 181-205.

44. Ng, E.S., R.P. Davis, L. Azzola, E.G. Stanley, and A.G. Elefanty, *Forced aggregation of defined numbers of human embryonic stem cells into embryoid bodies fosters robust, reproducible hematopoietic differentiation.* Blood, 2005. 106(5): p. 1601-3.

45. Ungrin, M.D., C. Joshi, A. Nica, C. Bauwens, and P.W. Zandstra, *Reproducible, ultra high-throughput formation of multicellular organization from single cell suspension-derived human embryonic stem cell aggregates.* PLoS One, 2008. 3(2): p. e1565.

46. Dang, S.M., M. Kyba, R. Perlingeiro, G.Q. Daley, and P.W. Zandstra, *Efficiency of embryoid body formation and hematopoietic development from embryonic stem cells in different culture systems.* Biotechnol Bioeng, 2002. 78(4): p. 442-53.

47. Zandstra, P.W., C. Bauwens, T. Yin, Q. Liu, H. Schiller, R. Zweigerdt, K.B. Pasumarthi, and L.J. Field, *Scalable production of embryonic stem cell-derived cardiomyocytes.* Tissue Eng, 2003. 9(4): p. 767-78.

48. Carpenedo, R.L., C.Y. Sargent, and T.C. McDevitt, *Rotary suspension culture enhances the efficiency, yield, and homogeneity of embryoid body differentiation.* Stem Cells, 2007. 25(9): p. 2224-34.

49. Murry, C.E., H. Reinecke, and L.M. Pabon, *Regeneration gaps: Observations on stem cells and cardiac repair.* J Am Coll Cardiol, 2006. 47(9): p. 1777-85.

50. zur Nieden, N.I., J.T. Cormier, D.E. Rancourt, and M.S. Kallos, *Embryonic stem cells remain highly pluripotent following long term expansion as aggregates in suspension bioreactors.* J Biotechnol, 2007. 129(3): p. 421-32.

51. Bauwens, C., T. Yin, S. Dang, R. Peerani, and P.W. Zandstra, *Development of a perfusion fed bioreactor for embryonic stem cell-derived cardiomyocyte generation: Oxygen-mediated enhancement of cardiomyocyte output.* Biotechnol Bioeng, 2005. 90(4): p. 452-61.

52. Fok, E.Y. and P.W. Zandstra, *Shear-controlled single-step mouse embryonic stem cell expansion and embryoid body-based differentiation.* Stem Cells, 2005. 23(9): p. 1333-42.

53. Niebruegge, S., A. Nehring, H. Bar, M. Schroeder, R. Zweigerdt, and J. Lehmann, *Cardiomyocyte production in mass suspension culture: Embryonic stem cells as a source for great amounts of functional cardiomyocytes.* Tissue Eng Part A, 2008.

54. Wang, X., G. Wei, W. Yu, Y. Zhao, X. Yu, and X. Ma, *Scalable producing embryoid bodies by rotary cell culture system and constructing engineered cardiac tissue with es-derived cardiomyocytes in vitro.* Biotechnol Prog, 2006. 22(3): p. 811-8.

55. Fernandes, A.M., T.G. Fernandes, M.M. Diogo, C.L. da Silva, D. Henrique, and J.M. Cabral, *Mouse embryonic stem cell expansion in a microcarrier-based stirred culture system.* J Biotechnol, 2007. 132(2): p. 227-36.

56. Cormier, J.T., N.I. zur Nieden, D.E. Rancourt, and M.S. Kallos, *Expansion of undifferentiated murine embryonic stem cells as aggregates in suspension culture bioreactors.* Tissue Eng, 2006. 12(11): p. 3233-45.

57. Liu, H., J. Lin, and K. Roy, *Effect of 3d scaffold and dynamic culture condition on the global gene expression profile of mouse embryonic stem cells.* Biomaterials, 2006. 27(36): p. 5978-89.

58. Krawetz, R., J.T. Taiani, S. Liu, G. Meng, X. Li, M.S. Kallos, and D. Rancourt, *Large-scale expansion of pluripotent human embryonic stem cells in stirred suspension bioreactors.* Tissue Eng Part C Methods, 2009.

59. Lock, L.T. and E.S. Tzanakakis, *Expansion and differentiation of human embryonic stem cells to endoderm progeny in a microcarrier stirred-suspension culture.* Tissue Eng Part A, 2009. 15(8): p. 2051-63.

60. Akins, R.E., D. Rockwood, K.G. Robinson, D. Sandusky, J. Rabolt, and C. Pizarro, *Three-dimensional culture alters primary cardiac cell phenotype.* Tissue engineering Part A, 2009.

61. Chang, T.T. and M. Hughes-Fulford, *Monolayer and spheroid culture of human liver hepatocellular carcinoma cell line cells demonstrate distinct global gene expression patterns and functional phenotypes.* Tissue engineering Part A, 2009. 15(3): p. 559-67.

62. Dang, S.M. and P.W. Zandstra, *Scalable production of embryonic stem cell-derived cells.* Methods Mol Biol, 2005. 290: p. 353-64.

63. Cameron, C.M., W.S. Hu, and D.S. Kaufman, *Improved development of human embryonic stem cell-derived embryoid bodies by stirred vessel cultivation.* Biotechnol Bioeng, 2006. 94(5): p. 938-48.

64. Gerecht-Nir, S., S. Cohen, and J. Itskovitz-Eldor, *Bioreactor cultivation enhances the efficiency of human embryoid body (heb) formation and differentiation.* Biotechnol Bioeng, 2004. 86(5): p. 493-502.

65. Schroeder, M., S. Niebruegge, A. Werner, E. Willbold, M. Burg, M. Ruediger, L.J. Field, J. Lehmann, and R. Zweigerdt, *Differentiation and lineage selection of mouse embryonic stem cells in a stirred bench scale bioreactor with automated process control.* Biotechnol Bioeng, 2005. 92(7): p. 920-33.

66. Gerecht-Nir, S., S. Cohen, and J. Itskovitz-Eldor, *Bioreactor cultivation enhances the efficiency of human embryoid body (heb) formation and differentiation.* Biotechnology and Bioengineering, 2004. 86(5): p. 493-502.

67. Bilgen, B., I.M. Chang-Mateu, and G.A. Barabino, *Characterization of mixing in a novel wavy-walled bioreactor for tissue engineering.* Biotechnol Bioeng, 2005. 92(7): p. 907-19.

68. Unger, D.R., F.J. Muzzio, J.G. Aunins, and R. Singhvi, *Computational and experimental investigation of flow and fluid mixing in the roller bottle bioreactor.* Biotechnol Bioeng, 2000. 70(2): p. 117-30.

69. Reuss, M., S. Schmalzriedt, and M. Jenne, *Application of computational fluid dynamics (cfd) to modeling stirred tank bioreactors. In:*. Bioreaction engineering modeling and control., ed. K. Schugerl and K.H. Bellgardt. 2000, Berlin; New York: Springer.

70. Zweigerdt, R., M. Burg, E. Willbold, H. Abts, and M. Ruediger, *Generation of confluent cardiomyocyte monolayers derived from embryonic stem cells in suspension: A cell source for new therapies and screening strategies.* Cytotherapy, 2003. 5(5): p. 399-413.

71. Haub, O. and M. Goldfarb, *Expression of the fibroblast growth factor-5 gene in the mouse embryo.* Development, 1991. 112(2): p. 397-406.

72. Hebert, J.M., M. Boyle, and G.R. Martin, *Mrna localization studies suggest that murine fgf-5 plays a role in gastrulation.* Development, 1991. 112(2): p. 407-15.

73. Rogers, M.B., B.A. Hosler, and L.J. Gudas, *Specific expression of a retinoic acid-regulated, zinc-finger gene, rex-1, in preimplantation embryos, trophoblast and spermatocytes.* Development, 1991. 113(3): p. 815-24.

74. Rivera-Perez, J.A. and T. Magnuson, *Primitive streak formation in mice is preceded by localized activation of brachyury and wnt3.* Dev Biol, 2005. 288(2): p. 363-71.

75. Finley, K.R., J. Tennessen, and W. Shawlot, *The mouse secreted frizzled-related protein 5 gene is expressed in the anterior visceral endoderm and foregut endoderm during early post-implantation development.* Gene Expr Patterns, 2003. 3(5): p. 681-4.

76. Kemp, C., E. Willems, S. Abdo, L. Lambiv, and L. Leyns, *Expression of all wnt genes and their secreted antagonists during mouse blastocyst and postimplantation development.* Dev Dyn, 2005. 233(3): p. 1064-75.

77. Keller, G., *Embryonic stem cell differentiation: Emergence of a new era in biology and medicine.* Genes Dev, 2005. 19(10): p. 1129-55.

78. Tam, P.P. and R.R. Behringer, *Mouse gastrulation: The formation of a mammalian body plan.* Mech Dev, 1997. 68(1-2): p. 3-25.

79. Halbleib, J.M. and W.J. Nelson, *Cadherins in development: Cell adhesion, sorting, and tissue morphogenesis.* Genes Dev, 2006. 20(23): p. 3199-214.

80. Johnson, M.H., *From mouse egg to mouse embryo: Polarities, axes, and tissues.* Annu Rev Cell Dev Biol, 2009. 25: p. 483-512.

81. Miller, J.R. and D.R. McClay, *Characterization of the role of cadherin in regulating cell adhesion during sea urchin development.* Dev Biol, 1997. 192(2): p. 323-39.

82. Peyrieras, N., F. Hyafil, D. Louvard, H.L. Ploegh, and F. Jacob, *Uvomorulin: A nonintegral membrane protein of early mouse embryo.* Proc Natl Acad Sci U S A, 1983. 80(20): p. 6274-7.

83. Yoshida, C. and M. Takeichi, *Teratocarcinoma cell adhesion: Identification of a cell-surface protein involved in calcium-dependent cell aggregation.* Cell, 1982. 28(2): p. 217-24.

84. Daniel, J.M. and A.B. Reynolds, *Tyrosine phosphorylation and cadherin/catenin function.* Bioessays, 1997. 19(10): p. 883-91.

85. Fujita, Y., G. Krause, M. Scheffner, D. Zechner, H.E. Leddy, J. Behrens, T. Sommer, and W. Birchmeier, *Hakai, a c-cbl-like protein, ubiquitinates and induces endocytosis of the e-cadherin complex.* Nat Cell Biol, 2002. 4(3): p. 222-31.

86. Lu, Z., S. Ghosh, Z. Wang, and T. Hunter, *Downregulation of caveolin-1 function by egf leads to the loss of e-cadherin, increased transcriptional activity of beta-catenin, and enhanced tumor cell invasion.* Cancer Cell, 2003. 4(6): p. 499-515.

87. Nakaya, M.A., K. Biris, T. Tsukiyama, S. Jaime, J.A. Rawls, and T.P. Yamaguchi, *Wnt3a links left-right determination with segmentation and anteroposterior axis elongation.* Development, 2005. 132(24): p. 5425-36.

88. Anton, R., H.A. Kestler, and M. Kuhl, *Beta-catenin signaling contributes to stemness and regulates early differentiation in murine embryonic stem cells.* FEBS Lett, 2007. 581(27): p. 5247-54.

89. Lindsley, R.C., J.G. Gill, M. Kyba, T.L. Murphy, and K.M. Murphy, *Canonical wnt signaling is required for development of embryonic stem cell-derived mesoderm.* Development, 2006. 133(19): p. 3787-96.

90. ten Berge, D., W. Koole, C. Fuerer, M. Fish, E. Eroglu, and R. Nusse, *Wnt signaling mediates self-organization and axis formation in embryoid bodies.* Cell Stem Cell, 2008. 3(5): p. 508-18.

91. Gavard, J. and R.M. Mege, *Once upon a time there was beta-catenin in cadherin-mediated signalling.* Biol Cell, 2005. 97(12): p. 921-6.

92. Gottardi, C.J. and B.M. Gumbiner, *Distinct molecular forms of beta-catenin are targeted to adhesive or transcriptional complexes.* J Cell Biol, 2004. 167(2): p. 339-49.

93. Jamora, C. and E. Fuchs, *Intercellular adhesion, signalling and the cytoskeleton.* Nat Cell Biol, 2002. 4(4): p. E101-8.

94. Cadigan, K.M. and R. Nusse, *Wnt signaling: A common theme in animal development.* Genes Dev, 1997. 11(24): p. 3286-305.

95. Hecht, A., C.M. Litterst, O. Huber, and R. Kemler, *Functional characterization of multiple transactivating elements in beta-catenin, some of which interact with the tata-binding protein in vitro.* J Biol Chem, 1999. 274(25): p. 18017-25.

96. Hecht, A., K. Vleminckx, M.P. Stemmler, F. van Roy, and R. Kemler, *The p300/cbp acetyltransferases function as transcriptional coactivators of beta-catenin in vertebrates.* EMBO J, 2000. 19(8): p. 1839-50.

97. Barker, N., A. Hurlstone, H. Musisi, A. Miles, M. Bienz, and H. Clevers, *The chromatin remodelling factor brg-1 interacts with beta-catenin to promote target gene activation.* EMBO J, 2001. 20(17): p. 4935-43.

98. Behrens, J., B.A. Jerchow, M. Wurtele, J. Grimm, C. Asbrand, R. Wirtz, M. Kuhl, D. Wedlich, and W. Birchmeier, *Functional interaction of an axin homolog, conductin, with beta-catenin, apc, and gsk3beta.* Science, 1998. 280(5363): p. 596-9.

99. van Noort, M., J. Meeldijk, R. van der Zee, O. Destree, and H. Clevers, *Wnt signaling controls the phosphorylation status of beta-catenin.* J Biol Chem, 2002. 277(20): p. 17901-5.

100. Behrens, J., J.P. von Kries, M. Kuhl, L. Bruhn, D. Wedlich, R. Grosschedl, and W. Birchmeier, *Functional interaction of beta-catenin with the transcription factor lef-1.* Nature, 1996. 382(6592): p. 638-42.

101. Pinson, K.I., J. Brennan, S. Monkley, B.J. Avery, and W.C. Skarnes, *An ldl-receptor-related protein mediates wnt signalling in mice.* Nature, 2000. 407(6803): p. 535-8.

102. Tamai, K., M. Semenov, Y. Kato, R. Spokony, C. Liu, Y. Katsuyama, F. Hess, J.P. Saint-Jeannet, and X. He, *Ldl-receptor-related proteins in wnt signal transduction.* Nature, 2000. 407(6803): p. 530-5.

103. Logan, C.Y. and R. Nusse, *The wnt signaling pathway in development and disease.* Annu Rev Cell Dev Biol, 2004. 20: p. 781-810.

104. Nelson, W.J. and R. Nusse, *Convergence of wnt, beta-catenin, and cadherin pathways.* Science, 2004. 303(5663): p. 1483-7.

105. Kam, Y. and V. Quaranta, *Cadherin-bound beta-catenin feeds into the wnt pathway upon adherens junctions dissociation: Evidence for an intersection between beta-catenin pools.* PLoS One, 2009. 4(2): p. e4580.

106. Zaffran, S. and M. Frasch, *Early signals in cardiac development.* Circ Res, 2002. 91(6): p. 457-69.

107. Buckingham, M., S. Meilhac, and S. Zaffran, *Building the mammalian heart from two sources of myocardial cells.* Nat Rev Genet, 2005. 6(11): p. 826-35.

108. Srivastava, D., *Making or breaking the heart: From lineage determination to morphogenesis.* Cell, 2006. 126(6): p. 1037-48.

109. Cai, C.L., X. Liang, Y. Shi, P.H. Chu, S.L. Pfaff, J. Chen, and S. Evans, *Isl1 identifies a cardiac progenitor population that proliferates prior to differentiation and contributes a majority of cells to the heart.* Dev Cell, 2003. 5(6): p. 877-89.

110. Kelly, R.G., N.A. Brown, and M.E. Buckingham, *The arterial pole of the mouse heart forms from fgf10-expressing cells in pharyngeal mesoderm.* Dev Cell, 2001. 1(3): p. 435-40.

111. Klaus, A., Y. Saga, M.M. Taketo, E. Tzahor, and W. Birchmeier, *Distinct roles of wnt/beta-catenin and bmp signaling during early cardiogenesis.* Proc Natl Acad Sci U S A, 2007. 104(47): p. 18531-6.

112. Tirosh-Finkel, L., H. Elhanany, A. Rinon, and E. Tzahor, *Mesoderm progenitor cells of common origin contribute to the head musculature and the cardiac outflow tract.* Development, 2006. 133(10): p. 1943-53.

113. Waldo, K.L., D.H. Kumiski, K.T. Wallis, H.A. Stadt, M.R. Hutson, D.H. Platt, and M.L. Kirby, *Conotruncal myocardium arises from a secondary heart field.* Development, 2001. 128(16): p. 3179-88.

114. Hogers, B., M.C. DeRuiter, A.C. Gittenberger-de Groot, and R.E. Poelmann, *Unilateral vitelline vein ligation alters intracardiac blood flow patterns and morphogenesis in the chick embryo.* Circ Res, 1997. 80(4): p. 473-81.

115. Hove, J.R., R.W. Koster, A.S. Forouhar, G. Acevedo-Bolton, S.E. Fraser, and M. Gharib, *Intracardiac fluid forces are an essential epigenetic factor for embryonic cardiogenesis.* Nature, 2003. 421(6919): p. 172-7.

116. Reckova, M., C. Rosengarten, A. deAlmeida, C.P. Stanley, A. Wessels, R.G. Gourdie, R.P. Thompson, and D. Sedmera, *Hemodynamics is a key epigenetic factor in development of the cardiac conduction system.* Circ Res, 2003. 93(1): p. 77-85.

117. Hogers, B., M.C. DeRuiter, A.M. Baasten, A.C. Gittenberger-de Groot, and R.E. Poelmann, *Intracardiac blood flow patterns related to the yolk sac circulation of the chick embryo.* Circ Res, 1995. 76(5): p. 871-7.

118. Hove, J.R., *In vivo biofluid dynamic imaging in the developing zebrafish.* Birth Defects Res C Embryo Today, 2004. 72(3): p. 277-89.

119. Groenendijk, B.C.W., B.P. Hierck, J. Vrolijk, M. Baiker, M.J.B.M. Pourquie, A.C. Gittenberger-de Groot, and R.E. Poelmann, *Changes in shear stress-related gene expression after experimentally altered venous return in the chicken embryo.* Circulation Research, 2005. 96(12): p. 1291-8.

120. Park, M., X. Wu, K. Golden, J.D. Axelrod, and R. Bodmer, *The wingless signaling pathway is directly involved in drosophila heart development.* Dev Biol, 1996. 177(1): p. 104-16.

121. Wu, X., K. Golden, and R. Bodmer, *Heart development in drosophila requires the segment polarity gene wingless.* Dev Biol, 1995. 169(2): p. 619-28.

122. Schneider, V.A. and M. Mercola, *Wnt antagonism initiates cardiogenesis in xenopus laevis.* Genes Dev, 2001. 15(3): p. 304-15.

123. Naito, A.T., I. Shiojima, H. Akazawa, K. Hidaka, T. Morisaki, A. Kikuchi, and I. Komuro, *Developmental stage-specific biphasic roles of wnt/beta-catenin signaling in cardiomyogenesis and hematopoiesis.* Proc Natl Acad Sci U S A, 2006. 103(52): p. 19812-7.

124. Ueno, S., G. Weidinger, T. Osugi, A.D. Kohn, J.L. Golob, L. Pabon, H. Reinecke, R.T. Moon, and C.E. Murry, *Biphasic role for wnt/beta-catenin signaling in cardiac specification in zebrafish and embryonic stem cells.* Proc Natl Acad Sci U S A, 2007. 104(23): p. 9685-90.

125. Kwon, C., J. Arnold, E.C. Hsiao, M.M. Taketo, B.R. Conklin, and D. Srivastava, *Canonical wnt signaling is a positive regulator of mammalian cardiac progenitors.* Proc Natl Acad Sci U S A, 2007. 104(26): p. 10894-9.

126. Kwon, C., L. Qian, P. Cheng, V. Nigam, J. Arnold, and D. Srivastava, *A regulatory pathway involving notch1/beta-catenin/isl1 determines cardiac progenitor cell fate.* Nat Cell Biol, 2009. 11(8): p. 951-7.

127. Lin, L., L. Cui, W. Zhou, D. Dufort, X. Zhang, C.L. Cai, L. Bu, L. Yang, J. Martin, R. Kemler, M.G. Rosenfeld, J. Chen, and S.M. Evans, *Beta-catenin directly regulates islet1 expression in cardiovascular progenitors and is required for multiple aspects of cardiogenesis.* Proc Natl Acad Sci U S A, 2007. 104(22): p. 9313-8.

128. Qyang, Y., S. Martin-Puig, M. Chiravuri, S. Chen, H. Xu, L. Bu, X. Jiang, L. Lin, A. Granger, A. Moretti, L. Caron, X. Wu, J. Clarke, M.M. Taketo, K.L. Laugwitz, R.T. Moon, P. Gruber, S.M. Evans, S. Ding, and K.R. Chien, *The renewal and differentiation of isl1+ cardiovascular progenitors are controlled by a wnt/beta-catenin pathway.* Cell Stem Cell, 2007. 1(2): p. 165-79.

129. David, R., C. Brenner, J. Stieber, F. Schwarz, S. Brunner, M. Vollmer, E. Mentele, J. Muller-Hocker, S. Kitajima, H. Lickert, R. Rupp, and W.M. Franz, *Mesp1 drives vertebrate cardiovascular differentiation through dkk-1-mediated blockade of wnt-signalling.* Nat Cell Biol, 2008. 10(3): p. 338-45.

130. Riazi, A.M., J.K. Takeuchi, L.K. Hornberger, S.H. Zaidi, F. Amini, J. Coles, B.G. Bruneau, and G.S. Van Arsdell, *Nkx2-5 regulates the expression of beta-catenin and gata4 in ventricular myocytes.* PLoS One, 2009. 4(5): p. e5698.

CHAPTER 3

ROTARY ORBITAL SPEEDS REGULATE EMBRYOID BODY FORMATION, SIZE, AND YIELD AND CHANGE THE SHEAR STRESS ENVIRONMENT*

Introduction

Pluripotent embryonic stem cells derived from the inner cell mass of blastocysts are capable of differentiating into all somatic cell types, as well as germ cells [1-3]. In addition to their utility for developmental biology studies, ESCs may be useful for novel regenerative cell therapies and *in vitro* diagnostic tools. ESC differentiation may be induced in several manners, but it is most commonly initiated via aggregation under suspension conditions into clusters of cells, referred to as embryoid bodies (EBs) [4-8]. EBs recapitulate many of the cellular morphogenic events of embryos in the post-implantation stage of development, eventually leading to the formation of cell types comprising each of the three germ lineages (ectoderm, endoderm and mesoderm) [8-9]. While some success has been achieved in regulating EB differentiation through soluble delivery of biomolecules, the modulation of EB environments by other biochemical and/or biophysical means remains largely unexplored.

---

*Modified from:

CY Sargent, GY Berguig, MA Kinney, LA Hiatt, RL Carpenedo, RE Berson, TC McDevitt. *Hydrodynamic Modulation of Embryonic Stem Cell Differentiation by Rotary Orbital Culture.* Biotechnology and Bioengineering, 2010, 105(3):611-626.

Various methods have been developed to promote the necessary aggregation of ESCs to facilitate EB formation and differentiation. Hanging drops, initiated by suspending small volumes of culture media (10-20 μL) containing a defined number of cells (200-1000 cells) from the lid of a Petri dish, is a common method to reproducibly control EB formation. Although hanging drops yield uniformly-sized EBs, the need to physically separate individual aggregates within distinct drops limits both the number of EBs formed per dish (~100 per 10 cm plate) and the inherent scalability of the method [10-12]. Centrifugation of a defined number of ESCs in individual wells of 96-well round bottom dishes also yields uniform EBs, but it does not overcome the scalability issue [13]. In contrast, suspension cultures are typically initiated by simply inoculating 10^{4-6} cells/mL under non-adherent culture conditions [4, 6, 8]. In static suspension, ESCs form a population of EBs that readily agglomerate resulting in aggregates of various sizes and shapes, thereby increasing the heterogeneity of differentiation among EBs and reducing the overall efficiency of cell differentiation [14]. In addition, although static suspension and hanging drop culture techniques are adequate for the purpose of small-scale experimentation, such methods are not efficient means of producing large populations of EBs and differentiated cells.

The application of larger-volume bioreactors (10^{2-4} mL) for EB culture is a promising approach to scale the production of differentiated ESC populations. However, compared to conventional static EB culture techniques, mixed or stirred bioreactors introduce added complexities, such as hydrodynamic forces which could impact EB formation and subsequent differentiation. Systematic investigation of the various hydrodynamic states which could influence EBs, however, is a large experimental space

that cannot be easily interrogated by large volume bioreactor systems. The external application of simple controlled rocking or shaking of standard culture dishes (10^1 mL) introduces hydrodynamic conditions to EB culture on a smaller scale, and can therefore be easily employed to methodically examine effects on subsequent ESC differentiation. Recently our laboratory compared the effects of rotary orbital suspension culture (40 rpm) on EB formation and differentiation to hanging drop and static suspension [15-16]. The application of constant orbital shaking during EB suspension culture enhanced the formation efficiency of EBs from single-cell suspensions and yielded significantly greater numbers of individual EBs and EB-derived cells after 7 days of culture, compared to static suspension [15]. Rotary orbital culture also produced more homogeneous populations of EBs that differentiated into derivatives of all three germ lineages [15]. Although preliminary observations from previous studies suggested that varying rotary orbital speeds could modulate the average size of EB populations, characterization of the different hydrodynamic environments resulting from various rotary speeds and their effects on EB formation was not fully defined.

Thus, the objective of the present study was to determine the effects of hydrodynamic forces created by variable rotary orbital speeds on EB formation, size, and global differentiation, as well as define the fluid shear conditions within rotary orbital culture. EBs were formed from a single-cell suspension and maintained at different rotary orbital speeds (between 20-60 rpm) for 7 days of suspension culture. EB formation, morphology, and structure were analyzed as a function of rotary speed over time compared to static suspension cultures. Computational fluid dynamic analysis was performed to characterize the hydrodynamic environments created by rotary orbital

shaking at different speeds. The results of this study indicate that hydrodynamic environments effectively regulate not only the size and yield of EBs in suspension culture, but also influence the organization of differentiating cells within the EBs and modulate the global differentiation patterns. These findings suggest that modulation of hydrodynamic properties of stem cell environments may be used as a novel route to regulate ESC aggregate formation and size, and potentially direct differentiation within suspension culture systems.

Materials and Methods

Embryonic Stem Cell Culture

Murine ESCs (D3 cell line) were cultured on tissue culture-treated dishes (Corning) pre-adsorbed with gelatin (0.1% solution in diH_2O). Culture media consisted of Dulbecco's modified Eagle's medium (DMEM) supplemented with 15% fetal bovine serum (Hyclone), 100 U/mL penicillin, 100 ug/mL streptomycin and 0.25 ug/mL amphotericin (Mediatech), 2mM L-glutamine (Mediatech), 1x MEM nonessential amino acid solution (Mediatech), 0.1 mM 2-mercaptoethanol (Fisher Chemical), and 10^3 U/mL of leukemia inhibitory factor (LIF; ESGRO, Chemicon). Cultures were re-fed with fresh media every other day, and passaged at approximately 70% confluence.

Embryonic Stem Cell Differentiation

A single-cell suspension of ESCs (0.4, 1 or 2 x 10^5 cell/mL) in 10 mL of ESC media without LIF was cultured in 100 mm bacteriological grade polystyrene Petri dishes (Becton Dickenson). For static cultures, the cell suspension was inoculated into agar coated Petri dishes to prevent adherence to the dish. To initiate rotary EB formation,

dishes were placed on rotary orbital shakers (Lab-Line Lab Rotator, Barnstead International) at 20, 25, 30, 35, 40, 45, 50, 55, or 60 rpm. Rotary orbital shakers were calibrated daily to ensure consistency of rotary speeds. EB media was exchanged every 2 days by harvesting EBs via gravity-induced sedimentation in a conical tube, re-suspending the EBs in 10 mL of differentiation media (media with no LIF), and returning them to the Petri dishes and rotary orbital shakers.

Morphometric Analysis

Phase images of rotary EBs were acquired at 6 hours, 12 hours, and 24 hours, and on days 2, 4, and 7 of differentiation using a Nikon TE 2000 inverted microscope (Nikon Inc.) in combination with a SpotFlex camera (Diagnostic Instruments). For morphometric analysis, images of approximately 100 EBs were obtained from each EB culture dish and analyzed using ImageJ (NIH) image analysis software to measure the cross-sectional area. A custom-written computational macro was used to perform several image processing measures prior to quantitative image analysis An iterative threshold function was employed to remove any debris and only consider distinct EBs, an edge filter was applied to delineate clear EB boundaries, and edges were "smoothed" to accurately define EB edges prior to image analysis. The distribution of EB areas was plotted in a histogram format (divided among 30 bins) and each point represents the average frequency occurring within each bin with error bars representing ± the standard deviation (n=3 plates at each rotary orbital speed).

Embryoid Body Yield Analysis

The yield of EBs was assessed at days 2, 4 and 7 of suspension culture. EB samples from each of the different experimental conditions were collected by

sedimentation, as described above. The EBs were re-suspended in 2 mL of media, serially diluted 1:5 in 1 mL volumes until reaching a concentration where 30-50 EBs could be counted in individual wells of a 24-well non-tissue culture treated polystyrene plate. The entire number of EBs per well were counted by visual inspection using an inverted phase microscope (Nikon Eclipse TS100) and the final dilution factor was used to determine the yield of EBs.

Video Capture and Shear Stress Computation

Video footage was acquired by placing EB dishes on a rotary orbital shaker outside of the incubator with a camera mounted to the rotating platform and directly above the dish, and video in phase with rotation was captured for less than 1 minute. Video of EB dishes at 3 rotary speeds (25, 40, and 55 rpm) was acquired intermittently during 12 days of suspension culture using a Sony Cyber-Shot DSC-W1, at a frame capture rate of 16 Hz. Individual frames were extracted throughout one orbit at each speed/time point using Windows Movie Maker (Supplemental Figure 3 A-C). Each image file was converted to a grayscale image with 5 colors representing distinct intensities to clearly separate the EB population from the background using Matlab (Supplemental Figure 3D). From each set of frames, the distance from the EBs' population center (center of the dish) to the furthest point of the EB population was used to define the radius for the respective speed/time point to ensure maximum coverage of the EB area.

The fluid motion inside the orbiting Petri dish was modeled by solving the three-dimensional (3-D) Navier-Stokes equations using Fluent 6.2 (ANSYS, Inc.), a commercial computational fluid dynamics (CFD) software. A 3-D rendering of the dish

was created in the pre-processor, GAMBIT, with dimensions and orbital parameters that mimicked the actual dish and experimental conditions: diameter - 100 mm; initial fluid height - 1.27 mm; orbital radius - 0.19 mm; and three rotation rates, 25, 40, and 55 rpm. A mesh with 336,226 hexahedral computational cells was applied to the volume. The modeling technique, convergence criteria, grid optimization, and time needed to reach steady-state for the transient solution have been described previously [17]. Shear stress was derived from the computed fluid motion at fluid depths (10 μm from the bottom of the dish) and dish radii encompassing regions where the EB's generally reside as seen in the video capture.

Histological Analysis

EB samples from the various experimental conditions were harvested from suspension rotary culture on days 2, 4, and 7, rinsed in PBS and fixed in 4% formaldehyde for 30 minutes at room temperature in suspension, rinsed in PBS (3x) and embedded in Histogel® (Richard Allen Scientific) at 4^{o} C for 2 hours. EB constructs were immersed in 70% ethanol and subjected to a series of alcohol and xylene rinses in order to dehydrate the samples prior to embedding the constructs in paraffin. Paraffin-embedded samples were sectioned at 5 microns using a rotary microtome (Microm HM 355S), deparaffinized and stained with hematoxylin and eosin for histological assessment or with Hoechst for nuclear assessment. Stained sections were imaged using a Nikon Eclipse 80i upright microscope in combination with a SpotFlex camera (Diagnostic Instruments).

Scanning Electron Microscopy

Samples were fixed in 2.5% glutaraldehyde (Electron Microscopy Sciences) diluted in sodium cacodylate buffer (Electron Microscopy Sciences) for 1 h. After rinsing, samples were further treated in 1% osmium tetroxide (Electron Microscopy Sciences) for 1 h. Samples were dehydrated in graded acetone dilutions and critically point dried using a Polaron E3000 critical point dryer (Quorum Technologies Inc., Guelph, ON, Canada). Samples were sputter coated for 120 s at 2.2 kV using a Polaron SC7640 sputter coater and imaged using a Hitachi S-800 scanning electron microscope (Hitachi High Technologies, Pleasanton, CA).

PCR Array Analysis

The RT^2 Profiler™ PCR Array System (SA Biosciences) with the mouse Stem Cell Array (PAMM-405) was used to assay global gene expression from EBs. Complementary DNA was synthesized from 1 µg total RNA using the RT^2 First Strand Kit (SA Biosciences), and real-time PCR was performed on a BioRad iCycler® using the SYBR green technology-based SuperArray RT^2 qPCR Master Mix (SA Biosciences) and the diluted cDNA reaction. The $\Delta\Delta C_t$ method of quantification was used to assess the fold-change of individual genes (normalized to heatshock protein 90 as housekeeping) compared to undifferentiated ESCs. Fold-change values for genes greater than 3-fold were imported into Genesis and normalized using log2 transformations to generate hierarchical clusters. Within Genesis, filtering on $p \leq 0.05$ between groups was performed to produce a heat map with only significantly different expression of genes greater than 3-fold. The above process was repeated to determine the fold-change of rotary EB genes compared to static.

Statistical Analysis

Each experimental condition was examined with a minimum of triplicate samples and each data point is presented as the mean value ± standard deviation. All images are representative of the triplicate samples and independent experiments. Analysis of variance was performed using SYSTAT 12 (SYSTAT Software, Inc.) to determine statistical significance ($p<0.05$) between experimental groups, followed by post-hoc Tukey-Kramer analysis to define statistical differences between specific experimental variables.

Results

Hydrodynamic Modulation of EB Size and Yield

Hydrodynamic conditions modulate embryoid body size and yieldEBs were formed from a single-cell suspension (2.0×10^5 cells/mL) at a range of rotary orbital speeds from 20 to 60 rpm (in 5 rpm increments). At speeds less than 20 rpm, ESCs formed a few (< 10) very large (> 1mm diameter) aggregates within the first day of culture; whereas at rotary speeds > 60 rpm, EBs formed few aggregates larger than 10-20 cells within the first 48-72 hours. However, at rotary orbital speeds between 20-60 rpm, clear differences in EB size and yield were observed after 4 days of suspension culture (Figure 3.1 A). Overall, larger EBs formed at slower rotary orbital speeds ($\leq$ 30 rpm), and EB size decreased as rotary speed increased. There were two ranges of rotary speeds, 25-40 rpm and $\geq$ 55 rpm, over which EB size significantly decreased. The average cross-sectional area of EBs formed at 20-25 rpm was approximately 200,000 μm^2, about 40,000 μm^2 at 40-50 rpm, and roughly 15,000 μm^2 at 55-60 rpm (Figure 1B),

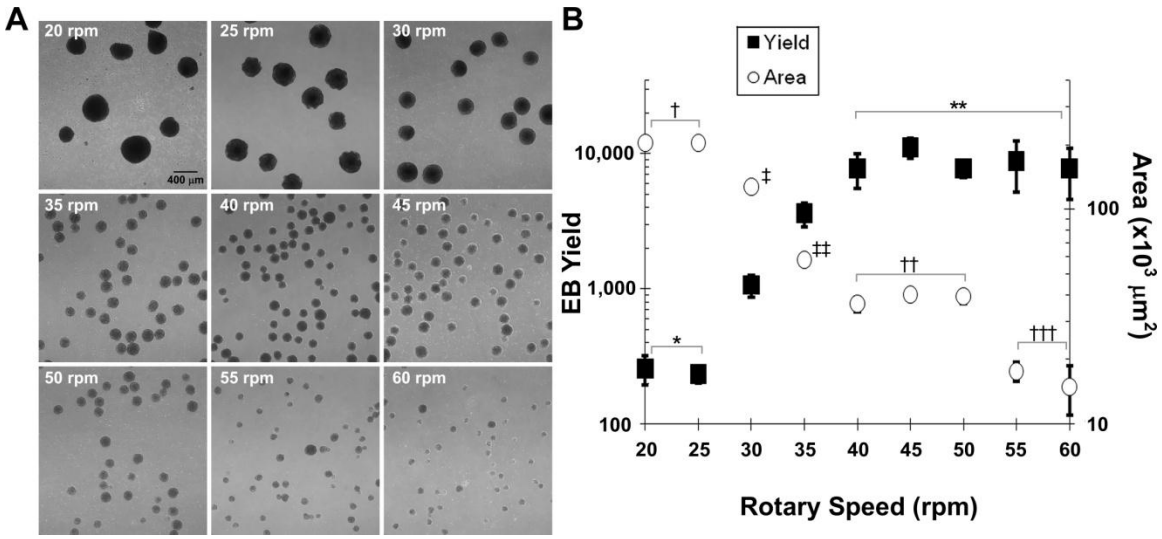

Figure 3.1: **Embryoid body formation at variable rotary orbital speeds.** EBs were formed on rotary orbital shakers at 20, 25, 30, 35, 40, 45, 50, 55, and 60 rpm (2 x 10^5 cells/mL). At day 4 of differentiation, clear differences in EB size were exhibited between rotary speeds (A). Slower speeds generated fewer but larger EBs than faster speeds, which resulted in an increased yield of smaller EBs (B). n = 3. daggers represent EB size $p \leq 0.05$: † compared to 30-60 rpm, ‡ compared to 20, 25, 35-60 rpm, ‡‡ compared to 20-30, 40-60 rpm, †† compared to 20-35, 55-60 rpm, ††† compared to 20-50. asterisks represent EB yield $p \leq 0.05$: * compared to 30-60 rpm, ** compared to 20-35 rpm. Modified from Sargent et al. 2010 [18].

which correlates to EBs with diameters of ~500 µm, ~225 µm, or ~140 µm, respectively. As a corollary to the changes in EB size due to rotary speed, the overall yield of EBs from a constant inoculation density of ESCs increased with increasing rotary speed. Similar to the EB size results, a distinct transition occurred between 25 and 40 rpm, where significant differences in EB yield were observed (Figure 3.1 B). Continuous culture at 25 rpm yielded an average of 233 ± 33 EBs after 4 days of differentiation, whereas 40 rpm yielded 7,778 ± 2,262 EBs. Between 40-60 rpm, the yield of EBs did not vary significantly until efficient EB formation was inhibited at rotary speeds above 60 rpm.

Temporal analysis of EB size and yield over the course of suspension culture focused on 25, 40, or 55 rpm due to the distinct differences initially observed between these populations while systematically modulating rotary orbital speed. After the initial formation period (~2 days), the yield of EBs at each of the rotary speeds did not change significantly with time (Figure 3.2), indicating that continuous rotary EB culture inhibits EB agglomeration, in agreement with previous observations [15].

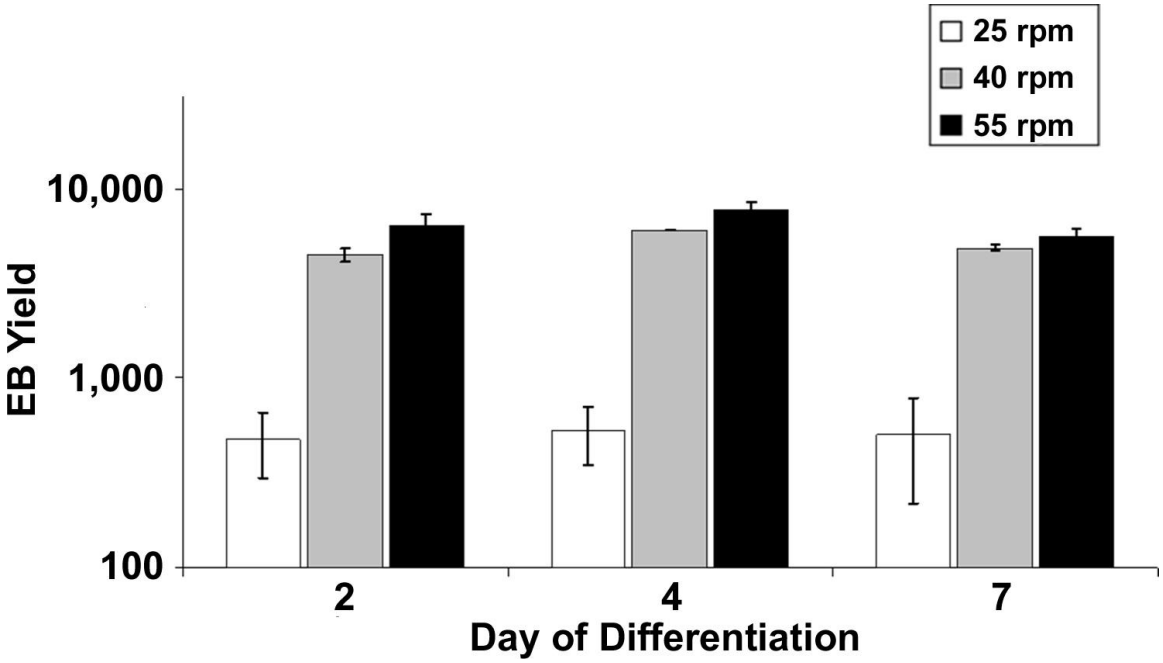

Figure 3.2: Embryoid body yield. EB yields, from an initial inoculation of 2 x 10^5 ESCs/mL, did not change significantly across days 2, 4, and 7 at any speed examined (25, 40, or 55 rpm), suggesting that EB agglomeration was prevented by the constant fluid motion. However, EB yield was directly proportional to formation speed. n = 3. From Sargent et al. 2010 [18].

Based upon the inoculation density and EB yields at day 2 of differentiation, the initial number of cells per EB was calculated to be ~6,100 cells at 25 rpm, ~240 cells at 40 rpm, and ~130 cells at 55 rpm. These values were calculated assuming 100% cell incorporation within EBs and negligible cellular proliferation and death during the first 2 days of formation based on previous incorporation efficiency and BrdU and TUNEL

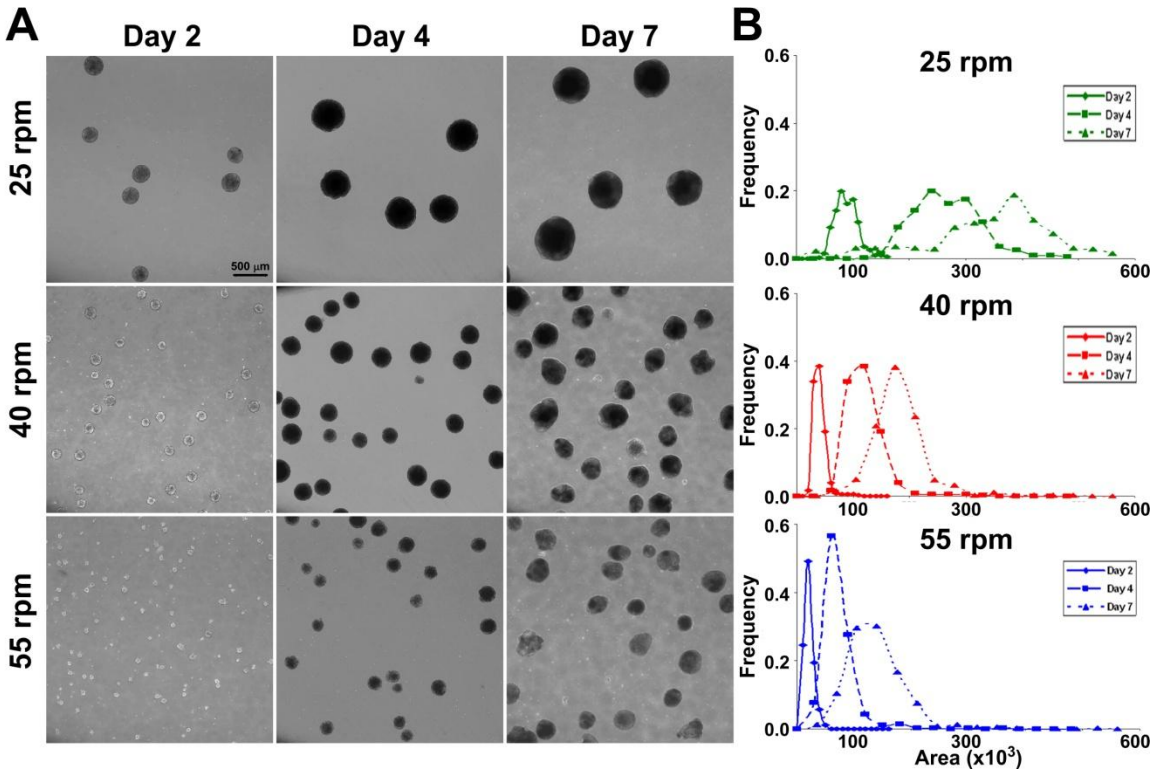

Figure 3.3: Time course of embryoid body sizes at variable rotary orbital speeds. EBs formed with 2 x 10^5 ESCs/mL at 25, 40, and 55 rpm increased in size with time (days 2, 4 and 7), and size was inversely proportional to rotary speed (A) (scale bar = 500 µm). Area distribution plots of EBs indicated that area variation decreased with increased speed and tended to increase with differentiation time (B). n = 3. From Sargent et al. 2010 [18].

staining analysis [15]. The average EB size progressively increased with time at each of the rotary speeds examined (Figure 3.3 A), yet the relative size differences between the rotary EB populations were maintained throughout 7 days of suspension culture (Figure 3.3 B). Potential effects of the initial density of the cell suspension on EB size and yield were also examined, but no significant differences in EB size were found with lower ESC inoculation densities 0.4 and 1.0 x10^5 cells/mL (Figure 3.4). Such results indicate that hydrodynamic conditions impact EB formation more so than the initial density of the cell suspension. Altogether, these results demonstrate that distinct rotary orbital speeds

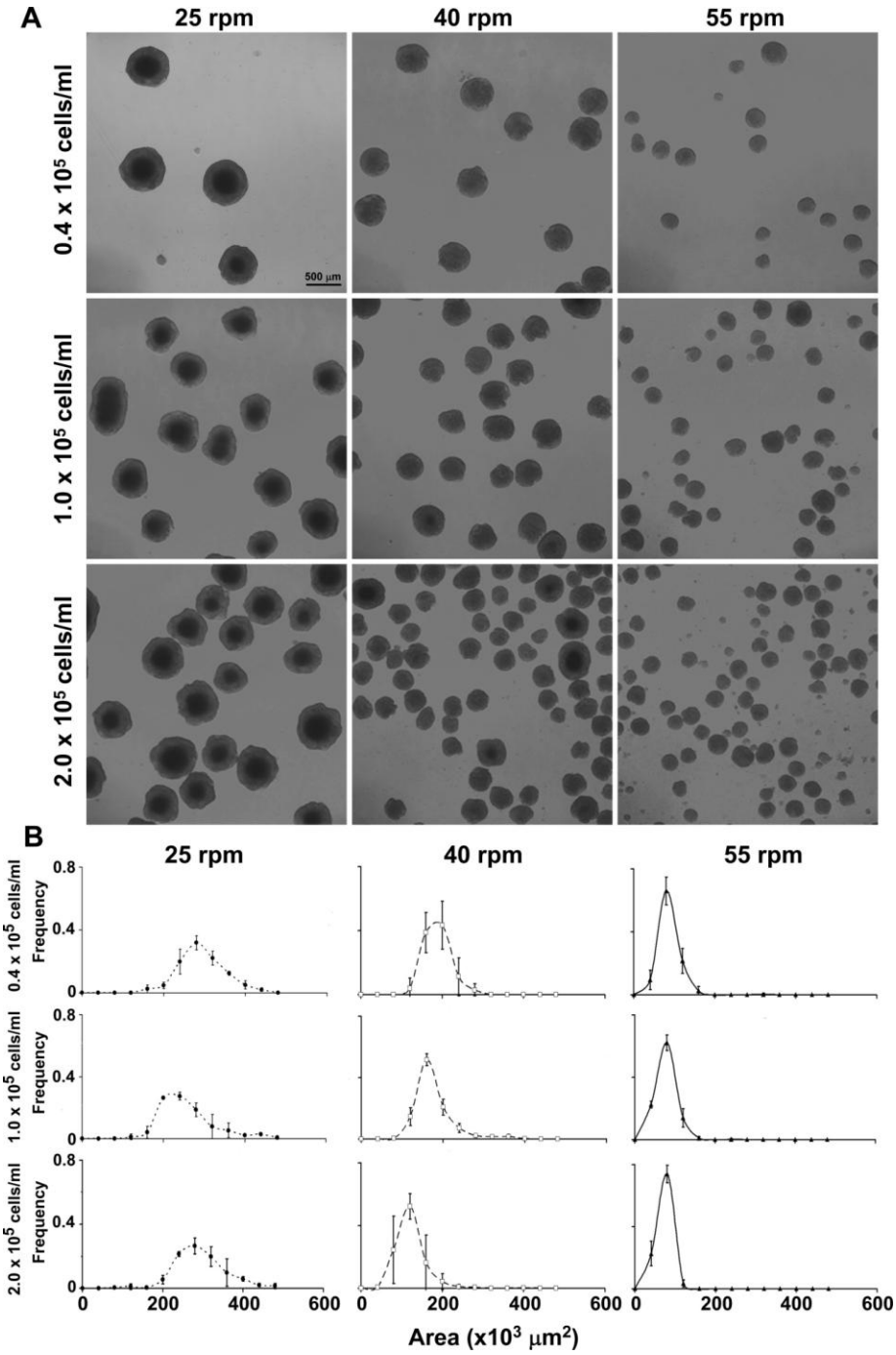

Figure 3.4: Embryoid body size and inoculation density. EBs formed with different inoculation densities (0.4, 1.0 and 2.0 x 10^5 cells/mL) at the same rotary orbital speed obtained similar size at day 4 of differentiation, indicating that EB size is dependent more on rotary speed than inoculation density (A). (Scale bar = 500µm) Histogram plots of EB area displayed essentially the same peak location between densities at fixed speeds (B), but the peak location was distinct between rotary speeds (25, 40. and 55 rpm) at constant density, with size being inversely proportional to speed, in agreement with previous studies. n = 3. Modified from Sargent et al. 2010 [18].

regulate the initial size and resulting yield of EB populations, and therefore serve as a convenient parameter to modulate EB formation in suspension culture.

Embryoid Body Formation is Regulated by the Hydrodynamic Environment

In order to more closely assess the initial formation of EBs, ESC suspensions introduced to rotary orbital conditions at 25, 40, 55 or 0 rpm (static), were examined at 6, 12, 24, and 48 hours after inoculation. ESCs quickly formed noticeable aggregates after 6 hours at 25 rpm (Figure 3.5 A), and by 12 hours many of the initial clusters began to merge to form larger, distinct aggregates (Figure 3.5 B). By 24 hours, the population of putative EBs at 25 rpm was relatively uniform in appearance and size, and very few individual cells appeared to be unincorporated within EBs (Figure 3.5 C). After 48 hours, the EBs at 25 rpm displayed an epithelial-looking exterior cell layer encompassing a mass of cells with a more dense core region (Figure 3.5 D). The initial cell aggregation at rotary speeds of 40 and 55 rpm was delayed compared to 25 rpm (Figure 3.5 A,E,I), as were the kinetics of primitive EB formation, although larger cell aggregates were generated sooner at 40 rpm than at 55 rpm (Figure 3.5 F,G,J,K). By 48 hours, all of the rotary cultures yielded relatively homogeneous populations of cell aggregates with very few single cells remaining in suspension (Figure 3.5 D,H,L). In contrast to the rotary cultures, after 6 hours static EB cultures consisted primarily of single cells and many small cell clusters, but generally lacked distinct cell aggregates (Figure 3.5 M). By 12 hours, cell aggregates were more readily apparent, but the cell clusters were very heterogeneous in appearance and smaller aggregates and single cells persisted throughout the initial 48 hours of suspension culture (Figure 3.5 N-P). Overall, this evidence demonstrates that EB formation kinetics are modulated by hydrodynamic forces imposed

on the individual cells and subsequent aggregates during initial suspension culture.

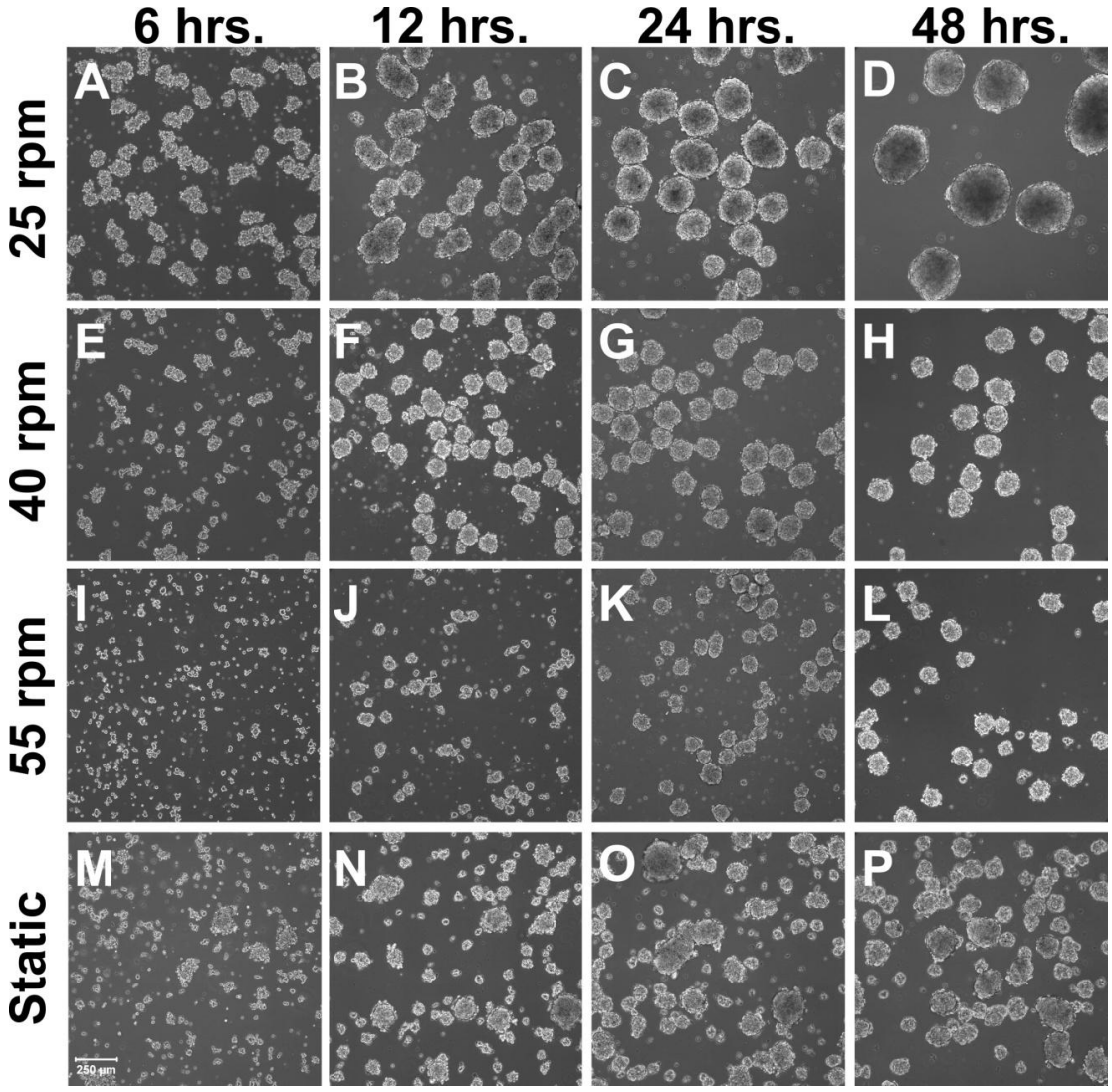

Figure 3.5: Kinetics of initial embryoid body formation. EBs were formed via rotary orbital suspension culture (2 x 10^5 cell/mL) at 25 rpm (A-D), 40 rpm (E-H), 55 rpm (I-L) or static conditions (M-P) and imaged at 6, 12, 24, and 48 hours. Rotary culture at 25 rpm yielded distinct primitive EBs as early as 6 hours after initial single-cell inoculation (A), whereas 40 rpm and 55 rpm conditions required at least 12 hours to form primitive EBs (F&J). Static conditions formed a mixed population of EBs, with a few primitive EBs observable at 6 hours (M), but a population of single cells and small cell clusters remained throughout 24 hours of culture (N-O). After 48 hours of formation, all cultures had distinct, defined EBs but varied in size depending on the conditions (D,H,L,P). (Scale bar = 250 µm.). From Sargent et al. 2010 [18].

Rotary Orbital Culture Generates Relatively Mild and Consistent Shear Stress

After analyzing the differences in EB formation, the hydrodynamic properties created within the orbiting dishes were determined by computational analysis. Video motion capture of orbiting cultures was performed to determine the spatial distributions of EBs within Petri dishes at the different rotary orbital speeds. At rotary speeds below 30-35 rpm, EBs were distributed randomly throughout the entire volume of the dish (i.e. 25 rpm, Figure 3.6 A), whereas EBs populated the center region of the dish at rotary speeds above 30-35 rpm (i.e. 40 and 55 rpm, Figure 3.6 B&C). Interestingly, the aggregation of EBs within the Petri dishes occurred at the same transition range of rotary speeds which modulated EB size most significantly (Figure 3.1 B). The central, circular area occupied by EBs determined via video analysis at 40 (Figure 3.6 D) and 55 rpm remained relatively consistent, but increased slightly over time as individual EBs increased in size. The radius of the EB population at 40 rpm expanded from 17.3 ± 1.4 mm at day 2 to 25.8 ± 1.0 mm at day 12 and from 19.3 ± 1.3 mm at day 2 to 28.5 ± 4.0 mm at day 12 at 55 rpm (Figure 3.6 E).

Following video capture analysis, computational fluid dynamic (CFD) modeling was used to define the hydrodynamic forces imposed on the EBs at different rotation speeds. The shear stresses at different rotary orbital speeds throughout one orbit were calculated for different radii and depths. The EB aggregate areas determined for 40 and 55 rpm rotary orbital speeds were combined with the shear contour plots generated from CFD analysis to define the shear range EBs were exposed to during culture under these conditions (Figure 3.7 C&E, dotted circle). Since 25 rpm EBs did not occupy a centralized area within the dish, the full radius of the dish was used to calculate the range

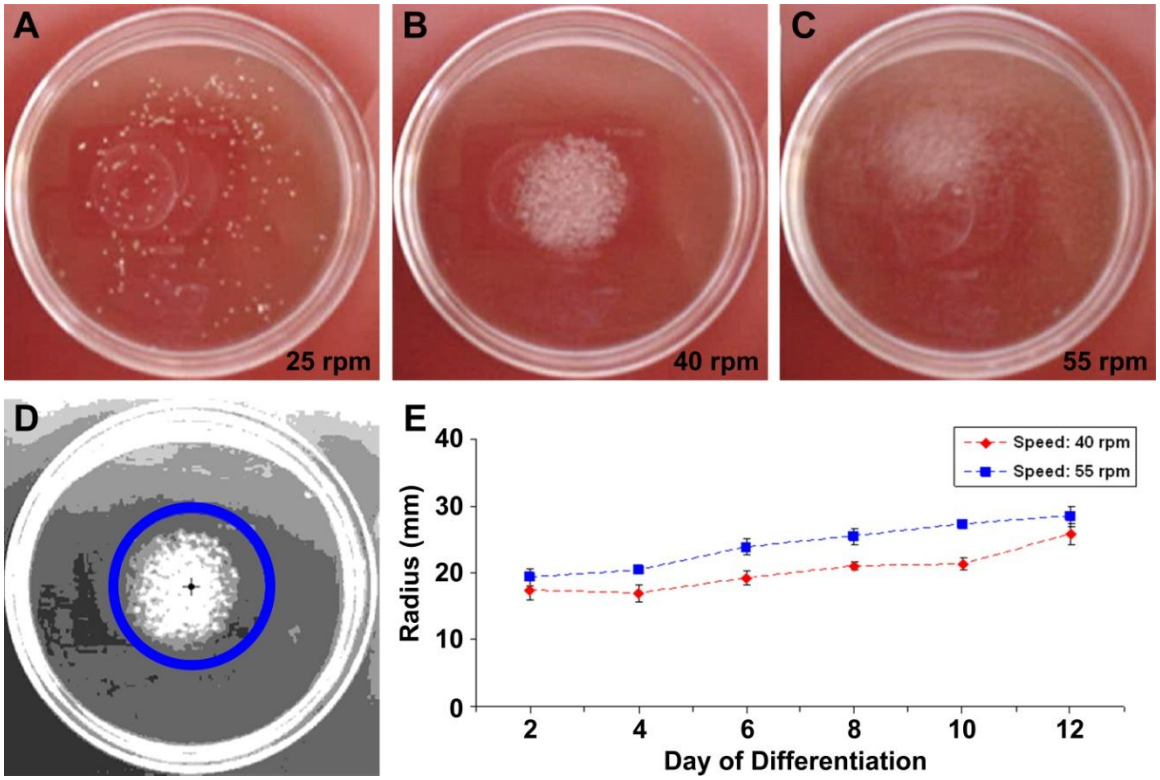

Figure 3.6: Video capture analysis of EB position with rotary orbital culture. Video of rotary orbital dishes with EBs was taken intermittently from days 2 through 12. Video frame shots of day 7, 25 (A), 40 (B), and 55 rpm (C) dishes were representative of all days examined, and revealed 25 rpm EB occupied the entire dish area while 40 and 55 rpm EBs remained localized towards the center of the dish. Image processing of frame shots from 40 rpm resulted in gray-scale representation of the total EB occupied area within the dish (D) (similar to the appearance of 55 rpm processed images). Processed gray-scale images allowed for calculation of the radius of the EB population at 40 and 55 rpm (E). With differentiation time, the radius defining the total EB area changed relatively little. n = 3. From Sargent et al. 2010 [18].

of shear stress experienced by EBs at 25 rpm (Figure 3.7 A, dotted circle). CFD analysis revealed the shear stresses generated during one orbit remained relatively constant within the EB occupied areas at the three speeds examined (Figure 3.7 B,D,F). Interestingly, at all three rotary speeds, the shear stresses varied little within the regions occupied by EBs, indicating that the shear stresses experienced by the population of individual EBs were relatively consistent regardless of specific EB position within the dish (Figure 3.7 B,D,F). The average shear stress experienced by the EBs during one orbit was slightly different at

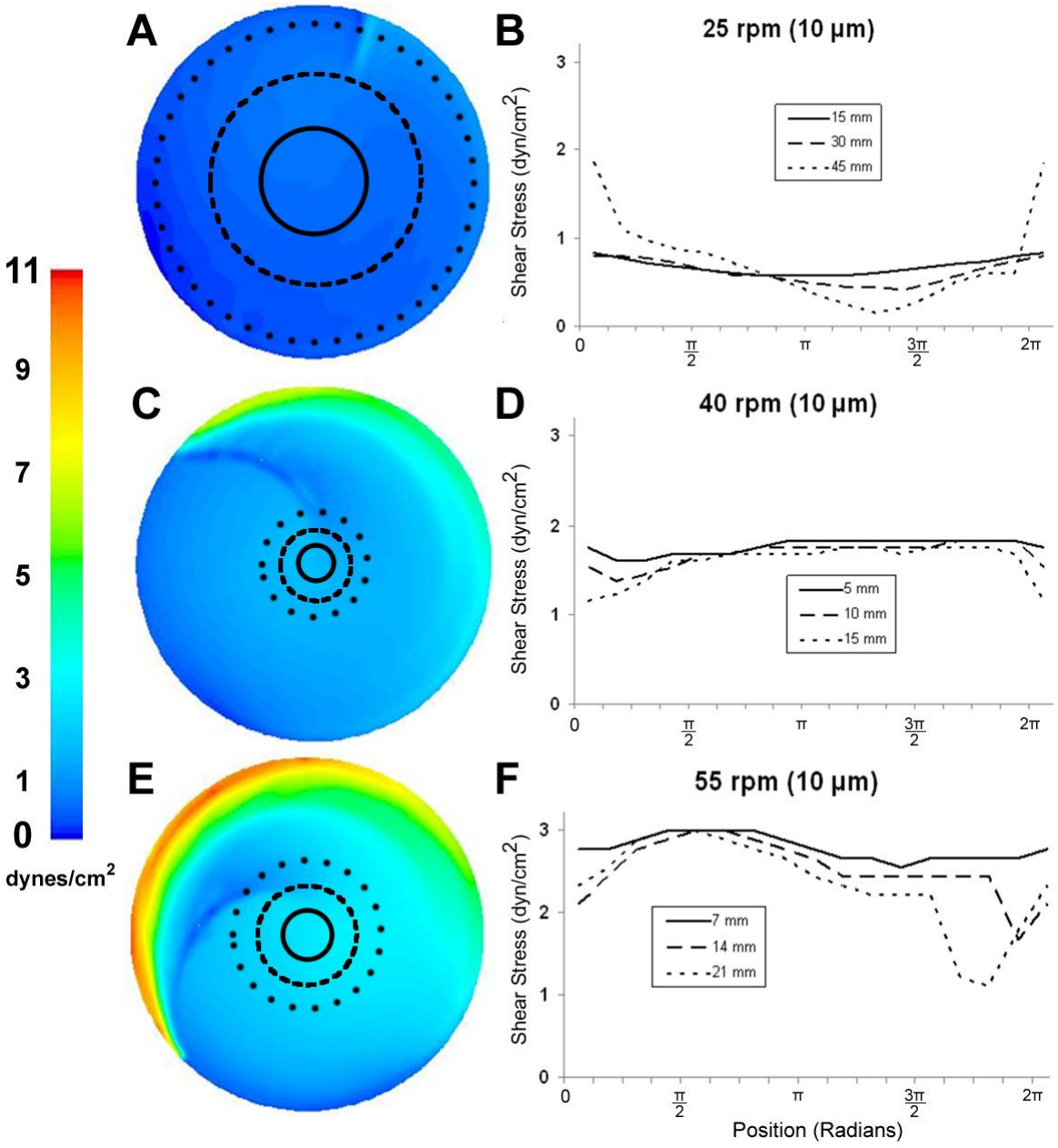

Figure 3.7: Shear stresses generated by rotary orbital culture at various speeds. Shear stress contour plots from CFD analysis were overlaid with circles representing the area occupied by EBs determined by video capture at 25 (A), 40 (C), and 55 rpm (E). (scale = 0 – 11 dyn/cm^2). At 10 µm above the bottom of the dish, the shear stresses throughout an entire orbit vary only slightly at each corresponding radii, but the shear stresses generated at each rotary speed (25, 40, and 55 rpm) remain distinct (B,D,F). From Sargent et al. 2010 [18].

each of the rotary speeds examined: 0.67 ± 0.23 dyn/cm^2 (25 rpm), 1.68 ± 0.14 dyn/cm^2 (40 rpm), and 2.54 ± 0.31 dyn/cm^2 (55 rpm). The CFD results indicate that orbital suspension culture at slow (25-55 rpm) rotational speeds applied in these studies creates relatively low shear stress and uniform hydrodynamic environments, at each of the distinct rotary orbital speeds examined.

Hydrodynamic Conditions Affect Embryoid Body Structure and Morphology

In order to examine the effects of different hydrodynamic conditions on the structural organization of EBs over time, histological analyses were performed. EBs were initially comprised of loosely packed cells at each of the rotary speeds (25, 40, or 55 rpm) and static conditions examined (Figure 3.8 A,D,G,J), and the relative density of the cell organization increased over time (Figure 3.8 C,F,I,L). The outer-most layers of cells within rotary EBs appeared to become more densely packed as rotary speed was increased (Figure 3.8 B,E,H, insets), whereas the cells within static EBs were less compacted (Figure 3.8 K, inset). By day 7 of suspension culture, large 25 rpm EBs exhibited a bi-phasic internal cellular organization, with a necrotic (Figure 3.8 C, black arrows) or hollow core (Figure 3.8 C, asterisk) surrounded by multiple layers of cells and a pyknotic appearance of nuclei towards the interior of the EBs (Figure 3.8 C', asterisk). Additionally, there was a broad distribution of nuclear staining intensity within 25 rpm EBs, suggesting more heterogeneous cell organization than the 40 and 55 rpm EBs, which exhibited less variation in nuclear staining. At day 7 of differentiation, the 40 rpm EBs contained distinct areas of morphologically different cell types (Figure 3.8 F, black arrow heads) and many contained cystic structures, a common feature associated with EB differentiation, while the 55 rpm EBs exhibited fewer cystic areas and a homogeneous

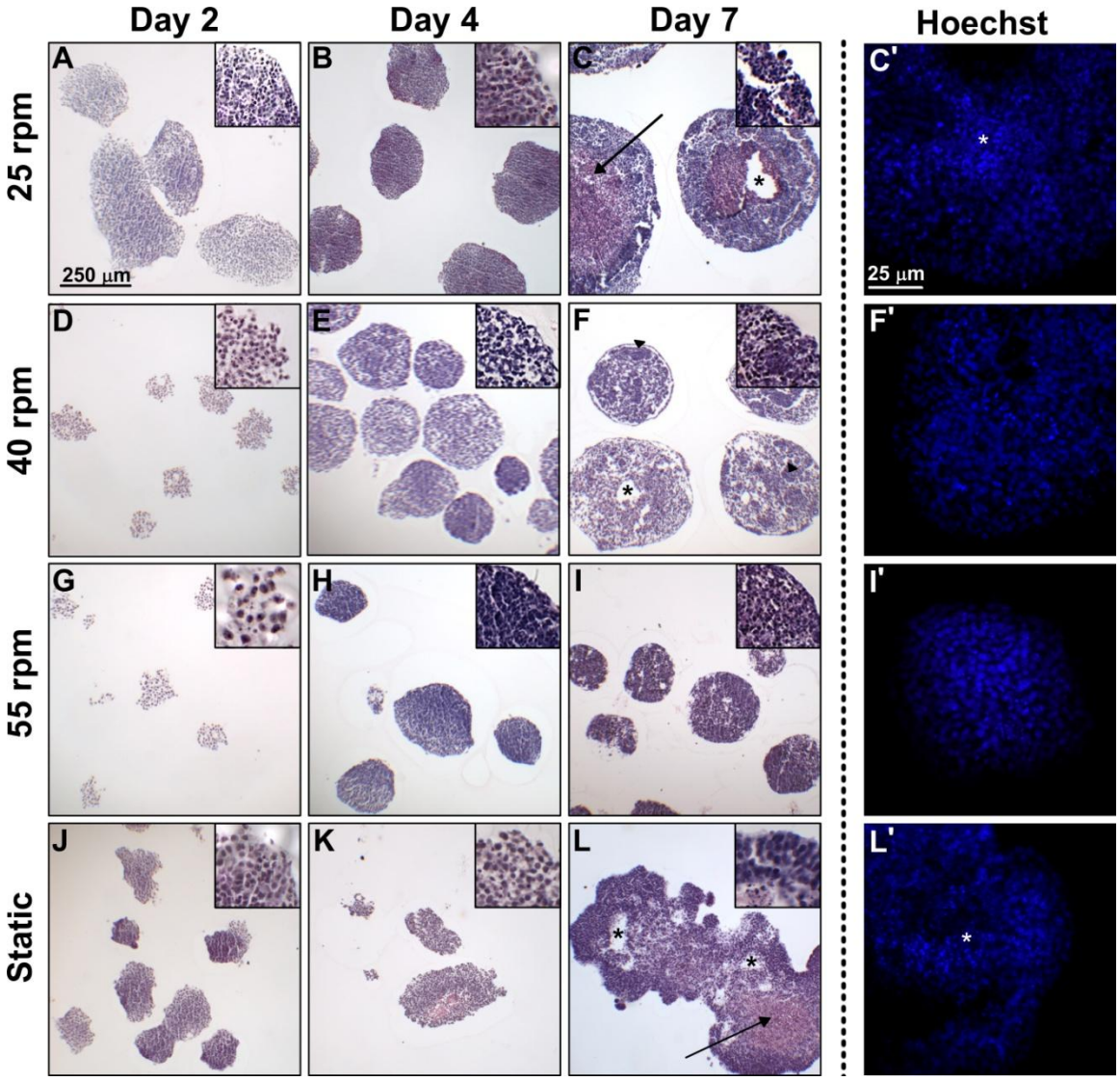

Figure 3.8: Histological embryoid body structure. Hemotoxylin and eosin staining of differentiating EBs at days 2 (A,D,G,J), 4 (B,E,H,K), and 7 (C,F,I,L) of differentiation reveal the cross-sectional EB cellular morphology, and Hoechst staining at day 7 (C',F',I',L') depicts the nuclear appearance. Nuclear density appeared to increase with time in all EBs and increase with rotary speed (figure insets of magnified EB edges). EBs formed at 25 rpm (A-C) had large enucleated centers by day 7 surrounded by layers of differentiating cells, 40 rpm (D-F) EBs had a cystic appearance with distinct areas of cell differentiation, and 55 rpm (G-I) EBs were more uniformly packed with cells throughout the cross-section. Black arrows indicate enucleation, black asterisks indicate cystic formation, black arrow heads indicate areas of cellular differentiation, white asterisks indicate pyknotic nuclei. H&E scale bar = 250 μm. Hoechst scale bar = 25 μm. From Sargent et al. 2010 [18].

cellular distribution throughout the cross-section (Figure 3.8 I). The appearance of pyknotic nuclei within 40 rpm EBs was limited to areas near cyst formation (Figure 3.8 F'), and 55 rpm EBs contained few pyknotic nuclei throughout (Figure 3.8 I'). In contrast to rotary cultures, many large agglomerates formed within static culture at day 7 of differentiation exhibited multiple large necrotic areas and a heterogeneous distribution of pyknotic nuclei (Figure 3.8 K'). Thus, hydrodynamic forces influenced not only EB formation, but also the organization and morphology of cells comprising EBs, potentially indicative of differences in ESC differentiation.

Further EB structure was visualized by SEM imaging. Since EBs exhibited large morphological differences between rotary orbital conditions (25, 40, and 55 rpm) and static conditions at day 7 of differentiation, EBs were also collected an processed for SEM. At low level magnification, little differences in structure were notable between EBs from static or rotary conditions (Figure 3.9 A-D). However, stubble differences are observed upon closer examination of the EB interior (Figure 3.9 E-H). EBs from 25 and 40 rpm rotary conditions appear to slightly less dense center (Figure 3.9 F&G) (similar to H&E staining analysis, Figure 3.8); while, the interior of static and 55 rpm rotary EBs appeared more compacted (Figure 3.9 E&H). Additionally, cells on the exterior of the rotary EBs (particularly 25 rpm) appeared to exhibited cilia, whereas cilia were less apparent on the exterior of static EBs. This morphological divergence again indicates distinct differences between static and hydrodynamic culture conditions, and the emergence of cilia may suggest increased transport across the exterior shell of rotary EBs.

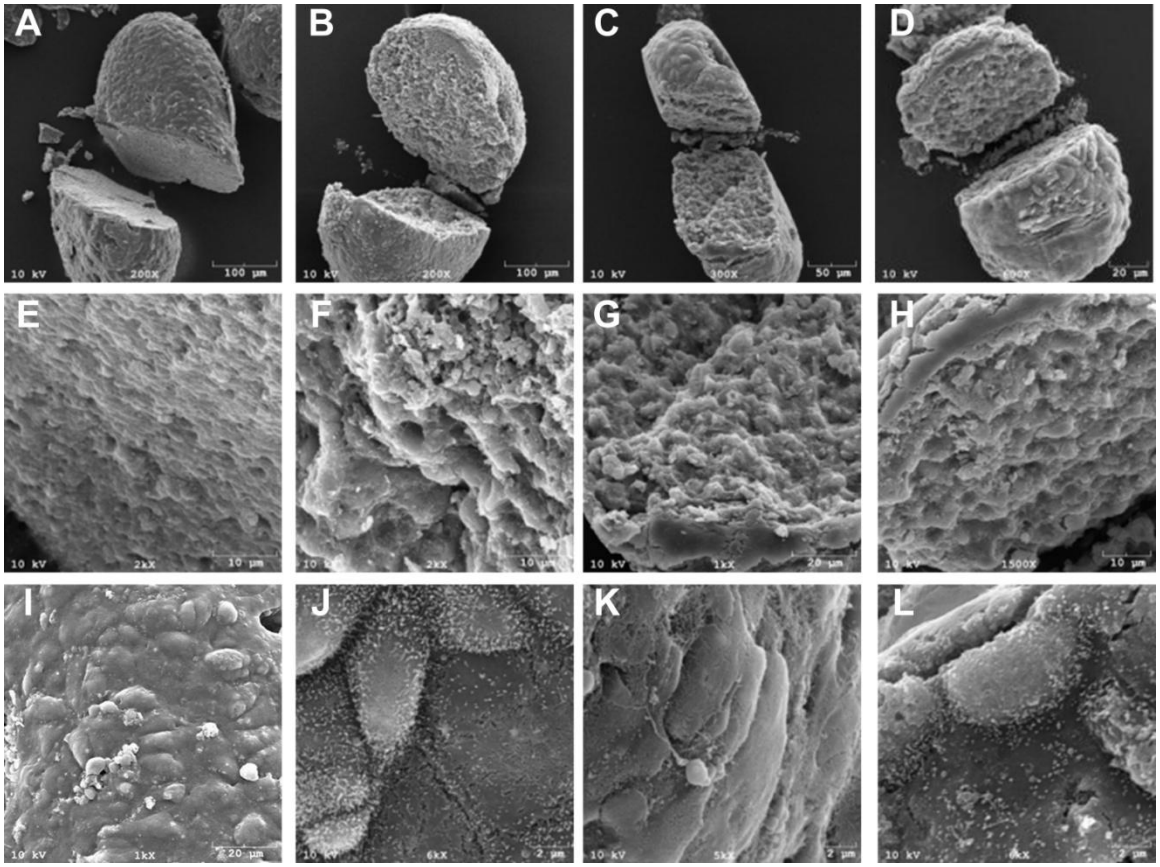

Figure 3.9: SEM analysis of embryoid body structure. Scanning electron microscopy images of static (A,E,I), 25 rpm (B,F,J), 40 rpm (C,G,K), and 55 rpm (D,H,L) EBs at day 7 of differentiation reveal the structure of the global appearance (A-D), cross-sectional area (E-H), and exterior surface (I-L). Differences between static and rotary EB interior and exterior were apparent at high magnification. scale bar = 100 µm (A&B), 50 µm (C), 20 µm (D,G,I), 10 µm (E,F,H), 2 µm (J,K,L).

Hydrodynamic Conditions Modulate Embryoid Body Gene Expression

Potential differences in differentiation between different EB populations (25, 40, 55, or 0 rpm) were assessed using gene expression analyses. Global gene expression was analyzed using the Mouse Stem Cell RT^2 Profiler™ PCR array after 7 days of differentiation in suspension culture based on the morphological differences evident between EBs at this time point (Figure 5 C,F,I,L). Of the 84 genes on the array, 52 genes

exhibited a minimum of a 3-fold change compared to undifferentiated ESCs (Figure 6A). Each of the EB groups exhibited a decrease in *growth differentiation factor 3 (Gdf3)* expression, a molecule expressed by pluripotent ESCs [19-20]. *Brachyury T* expression, a transiently expressed marker of mesoderm, was also decreased within all EB groups. Expression of phenotypic markers of the three germ layers, such as *forkhead box A2 (Foxa2), pancreatic and duodenal homeobox 1 (Pdx1), islet 1 (Isl1),* and *keratin (Krt15),* increased in all EB groups compared to ESCs, as did signaling molecules implicated in differentiation processes, including *bone morphogenetic protein 2 (Bmp2), growth differentiation factor 2 (Gdf2), notch 1 and 2, delta-like ligand 1 (Dll1), frizzled 1 (Frd1),* and *wingless-type1 (Wnt1).* The increased expression of differentiated markers of all three germ layers indicated that rotary orbital conditions did not inhibit the progression of differentiation, consistent with previous observations [15]. Two-way hierarchical clustering of the data grouped experimental replicates from each condition together, indicating the similarity in gene expression profiles between like samples and highlighting the differences between static and hydrodynamic conditions. Of the 52 genes that increased or decreased at least 3-fold compared to ESCs, 31 genes exhibited significant differences ($p \leq 0.05$) in expression levels between the different EB culture conditions (Figure 6B). Phenotypic markers of ectoderm differentiation, including *neural cell adhesion molecule 1 (Ncam1), neurogenin 2 (Neurog2), and S100b*, were increased in static EBs compared to rotary EBs (Figure 6B, bolded box).

The clear separation of culture conditions by hierarchical clustering suggested differences in gene expression not only between static and rotary, but also between the rotary orbital speeds; these differences are highlighted by differential intensity across 25,

40, and 55 rpm groups for certain genes, such as *bone gamma carboxyglutamate protein 1* (*Bglap1*) and several cyclin dependent genes and collagens (Figure 6B, bolded box). Hierarchical clustering of gene expression from rotary orbital groups exhibiting a 3-fold difference compared to static conditions indicated two distinct clusters of genes that were either increased or decreased by rotary culture (Figure 6C). Again, several cyclin dependent genes (*Cd4, Cd8a, Cd8b1, and Cd19*) were decreased within all rotary speeds compared to static culture (decreased 4 to 24 fold), as were some collagens (decreased 4 to 16 fold) and neural maker *S100b* (decreased 10 to 16 fold). Genes indicative of endo and mesoderm differentiation (including phenotypic markers *brachyury T*, *Foxa2,* and signaling molecules *Dll1, Dll3, Fzd1, Wnt1,* and *Jag1*) were increased in rotary conditions compared to static culture. Additionally, 25 and 40 rpm clustered more closely together than 55 rpm, suggesting that gene expression profiles from 25 and 40 rpm EBs were more similar, and several genes exhibited subtle intensity differences across the rotary speeds, including *Cd8a*, which appeared more decreased at 25 and 40 rpm conditions (25 and 40 rpm: ~8 fold decrease, 55 rpm: ~4 fold decrease compared to static), and *Jag1* and *Wnt1*, which appeared more increased by 55 rpm conditions (55 rpm: ~9 fold and ~13 fold increase respectively, 25 and 40 rpm: ~4 fold increase and $\geq$ 1.2 fold decrease respectively compared to static). Thus, the introduction of hydrodynamic forces to EB suspension culture significantly impacts differentiated gene expression profiles as compared to static culture, and furthermore, subtle differences between hydrodynamic conditions differentially affect EB differentiation.

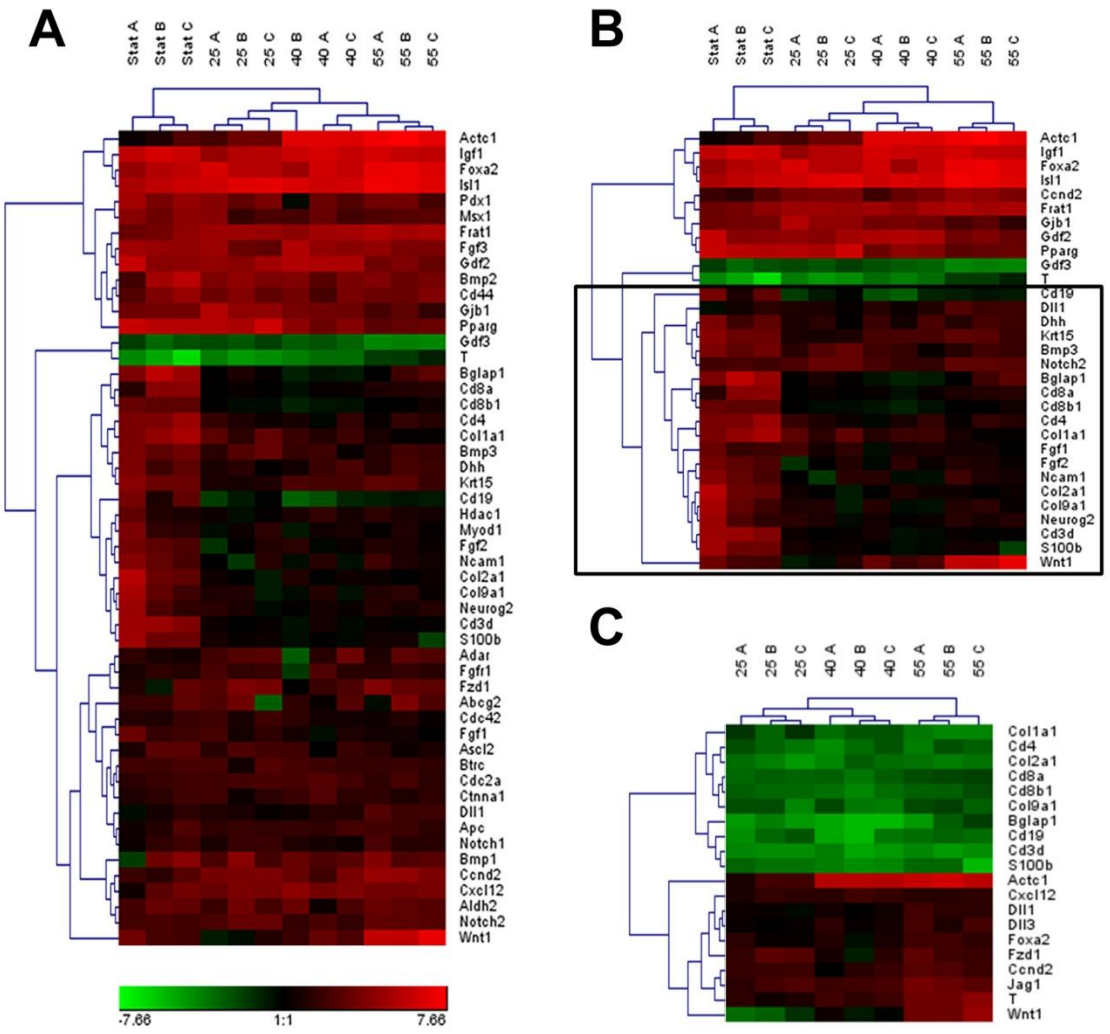

Figure 3.10: Low density, global gene analysis. Gene expression profiles of EBs from suspension cultures at 25, 40, 55, and 0 rpm (static) at day 7 of differentiation were performed using PCR SuperArrays. Hierarchical clustering displayed clear grouping of culture conditions with genes expression levels $\geq$ 3-fold compared to ESCs (A). Several genes from the array exhibited significantly different expression levels between culture conditions (B), specifically phenotypic and signaling related genes were different between static and rotary conditions (boxed area, B). Rotary conditions exhibited distinct classes of genes either decreased (green) or increased (red) compared to static culture conditions (C), and there were variable expression levels between rotary orbital speeds as well. n = 3

Discussion

In this study, the effects of initiating and maintaining embryoid bodies (EBs) in different hydrodynamic environments created by rotary orbital culture were examined by

assessing EB formation, structure, and differentiation. EB size and yield were controlled by rotary orbital speed due to different cell aggregation kinetics modulated by hydrodynamic conditions. The hydrodynamic forces experienced by EBs within the orbiting Petri dishes were characterized by CFD analysis and found to be spatially uniform, but distinctly different depending on rotary speed. Differences between static and rotary conditions, as well as between different rotary speeds, were reflected by changes in the organization and morphology of cells within EBs. In addition to variations of the global gene expression profile between static and rotary conditions, specific genes related to signaling pathways and germ lineage differentiation were noted between EB populations cultured at different rotary speeds. Overall, the results of this study indicate that ESC aggregation and differentiation can be modulated by hydrodynamic environments to which EBs are exposed during suspension culture.

The hydrodynamic properties of rotary orbital culture clearly affected the assembly and maintenance of EBs in suspension. Horizontal rotary orbital motion improves the overall homogeneity and prevents agglomeration of individual EBs formed from single-cell suspensions of mouse ESCs compared to static culture [15, 21]. The modulation of EB formation by rotary orbital suspension culture speed reported in this study is consistent with the performance of other EB suspension culture systems that have illustrated the dependence of EB size and yield on mixing conditions imposed by various types of bioreactors [22-24]. Thus, overall it appears that mixing conditions, created by rotary orbital culture or other means of agitation, generally control the physical association of individual cells and clusters, thereby promoting more homogeneous and efficient aggregation compared to static batch suspension culture

methods. Additionally, lower-shear conditions created by slower rotary orbital speeds result in more rapid initial cell aggregate formation of single-cell suspensions and subsequently larger EBs compared to faster orbital speeds (Figures 3.1 – 3.5). The effects of hydrodynamic properties on initial EB formation is an important parameter to consider due to the fact that EB size (i.e. number of cells/EB) can influence the relative proportions of differentiated cells [25-28]. However, in contrast to most techniques, hydrodynamic control of EB formation is a scalable approach to direct cell spheroid assembly in a massively parallel manner in suspension culture conditions.

In addition to regulating EB formation and size, EB structure and cellular morphology were also affected by hydrodynamic conditions imposed by rotary orbital culture. Larger EBs from lower speeds contained larger necrotic cores, while the smaller EBs from faster speeds exhibited more homogeneous nuclear distribution throughout (Figure 3.8). Although EB size can inherently limit the diffusion of oxygen and molecules throughout ESC aggregates, hydrodynamic conditions generally improve nutrient and waste transport. In past studies, increased internal cell viability within EBs cultured in mixed bioreactor systems compared to static culture conditions has been attributed to enhanced access to nutrients and removal of metabolic by-products from the differentiating ESC spheroids [22-24, 29]. Transport properties are an important, yet often overlooked consideration for EB differentiation studies due to the fact that even small molecules do not readily diffuse from the surrounding media homogeneously within the 3D cell spheroids [30-31]. Additionally, the appearance of cilia on the exterior of rotary EBs suggests transport may be modulated by cellular means as well as hydrodynamic conditions. The differences in EB structure observed between static

culture and different rotary orbital speeds also suggest that subtle changes in hydrodynamic properties impact the internal organization of the cells within EBs. Regional differences in the density of cells due to hydrodynamic forces could affect the extent of coupling and interaction mediated via intercellular receptors. This in turn could affect signal transduction events mediated by of cell-cell adhesions that instruct cell fate decisions during the course of differentiation [32-35]. One of the most interesting findings of the present study is that the differentiation of ESCs was modulated by culturing EBs in different hydrodynamic environments. Although the most prominent differences in ESC differentiation occurred between static and rotary culture conditions, significant differences in gene expression also resulted from culturing EBs at different rotary orbital speeds (Figure 3.10), indicating that hydrodynamic culture may provide a method to regulate ESC differentiation.

Biomechanical forces created by hydrodynamic conditions could be partially responsible for differences in EB differentiation, as well as formation and structure. Shear stress imposed on 2-D cultures of adult and embryonic stem cells has been reported to regulate differentiation, especially with regards to enhancing hematopoietic development in the range of shear stresses of 1.5 - 15 dyn/cm^2 [36-39]. CFD modeling of the 3D fluid mechanics within orbiting culture dishes can be used to define the range of shear stresses created by different rotary orbital speeds [17]. In the current examination of low rotary speeds (25-55 rpm), the resulting shear stresses (~0.7 – 2.5 dyn/cm^2) imposed on EB populations were sufficient to modulate the expression of markers from all three germ lineages, suggesting that hydrodynamic forces influence more than just hematopoietic or mesoderm development. Other 3D suspension culture systems, such as

STLV or stirred-bioreactors, have illustrated the ability to produce differentiated cells from ESCs such as hematopoietic cells [14, 22] or cardiomyocytes [24] equivalent to static culture. However, manipulation of hydrodynamic parameters to facilitate or inhibit the differentiation of EBs in suspension culture is an entirely new and novel approach to direct cell fate decisions that has yet to be fully explored.

This study demonstrates, for the first time, that the hydrodynamic environment created within culture vessels can significantly affect not only EB formation and structure, but also the global differentiation profiles. Thus, hydrodynamic modulation of ESC differentiation represents a novel and scalable approach to integrate into the design and engineering of strategies for ESC propagation and differentiation in suspension culture. Since hydrodynamics forces are inherently created by mixed or stirred bioreactors, this parameter should be considered along with other environmental factors, such as culture media components, oxygen tension, and pH, in the development of controlled systems for stem cell bioprocessing.

References

1. Evans, M.J. and M.H. Kaufman, *Establishment in culture of pluripotential cells from mouse embryos.* Nature, 1981. 292(5819): p. 154-6.

2. Martin, G.R., *Isolation of a pluripotent cell line from early mouse embryos cultured in medium conditioned by teratocarcinoma stem cells.* Proc Natl Acad Sci U S A, 1981. 78(12): p. 7634-8.

3. Thomson, J.A., J. Itskovitz-Eldor, S.S. Shapiro, M.A. Waknitz, J.J. Swiergiel, V.S. Marshall, and J.M. Jones, *Embryonic stem cell lines derived from human blastocysts.* Science, 1998. 282(5391): p. 1145-7.

4. Doetschman, T.C., H. Eistetter, M. Katz, W. Schmidt, and R. Kemler, *The in vitro development of blastocyst-derived embryonic stem cell lines: Formation of visceral yolk sac, blood islands and myocardium.* J Embryol Exp Morphol, 1985. 87: p. 27-45.

5. Doevendans, P.A., S.W. Kubalak, R.H. An, D.K. Becker, K.R. Chien, and R.S. Kass, *Differentiation of cardiomyocytes in floating embryoid bodies is comparable to fetal cardiomyocytes.* J Mol Cell Cardiol, 2000. 32(5): p. 839-51.

6. Hopfl, G., M. Gassmann, and I. Desbaillets, *Differentiating embryonic stem cells into embryoid bodies.* Methods Mol Biol, 2004. 254: p. 79-98.

7. Itskovitz-Eldor, J., M. Schuldiner, D. Karsenti, A. Eden, O. Yanuka, M. Amit, H. Soreq, and N. Benvenisty, *Differentiation of human embryonic stem cells into embryoid bodies compromising the three embryonic germ layers.* Mol Med, 2000. 6(2): p. 88-95.

8. Keller, G.M., *In vitro differentiation of embryonic stem cells.* Curr Opin Cell Biol, 1995. 7(6): p. 862-9.

9. Coucouvanis, E. and G.R. Martin, *Signals for death and survival: A two-step mechanism for cavitation in the vertebrate embryo.* Cell, 1995. 83(2): p. 279-87.

10. Maltsev, V.A., A.M. Wobus, J. Rohwedel, M. Bader, and J. Hescheler, *Cardiomyocytes differentiated in vitro from embryonic stem cells developmentally express cardiac-specific genes and ionic currents.* Circ Res, 1994. 75(2): p. 233-44.

11. Wiese, C., G. Kania, A. Rolletschek, P. Blyszczuk, and A.M. Wobus, *Pluripotency: Capacity for in vitro differentiation of undifferentiated embryonic stem cells.* Methods Mol Biol, 2006. 325: p. 181-205.

12. Yoon, B.S., S.J. Yoo, J.E. Lee, S. You, H.T. Lee, and H.S. Yoon, *Enhanced differentiation of human embryonic stem cells into cardiomyocytes by combining hanging drop culture and 5-azacytidine treatment.* Differentiation, 2006. 74(4): p. 149-59.

13. Ng, E.S., R.P. Davis, L. Azzola, E.G. Stanley, and A.G. Elefanty, *Forced aggregation of defined numbers of human embryonic stem cells into embryoid bodies fosters robust, reproducible hematopoietic differentiation.* Blood, 2005. 106(5): p. 1601-3.

14. Dang, S.M., M. Kyba, R. Perlingeiro, G.Q. Daley, and P.W. Zandstra, *Efficiency of embryoid body formation and hematopoietic development from embryonic stem cells in different culture systems.* Biotechnol Bioeng, 2002. 78(4): p. 442-53.

15. Carpenedo, R.L., C.Y. Sargent, and T.C. McDevitt, *Rotary suspension culture enhances the efficiency, yield, and homogeneity of embryoid body differentiation.* Stem Cells, 2007. 25(9): p. 2224-34.

16. Sargent, C.Y., G.Y. Berguig, and T.C. McDevitt, *Cardiomyogenic differentiation of embryoid bodies is promoted by rotary orbital suspension culture.* Tissue Eng Part A, 2009. 15(2): p. 331-342.

17. Berson, R.E., M.R. Purcell, and M.K. Sharp, *Computationally determined shear on cells grown in orbiting culture dishes.* Adv Exp Med Biol, 2008. 614: p. 189-98.

18. Sargent, C.Y., G.Y. Berguig, M.A. Kinney, L.A. Hiatt, R.L. Carpenedo, R.E. Berson, and T.C. McDevitt, *Hydrodynamic modulation of embryonic stem cell differentiation by rotary orbital suspension culture.* Biotechnol Bioeng, 2010. 105(3): p. 611-26.

19. Levasseur, D.N., J. Wang, M.O. Dorschner, J.A. Stamatoyannopoulos, and S.H. Orkin, *Oct4 dependence of chromatin structure within the extended nanog locus in es cells.* Genes Dev, 2008. 22(5): p. 575-80.

20. Levine, A.J. and A.H. Brivanlou, *Gdf3, a bmp inhibitor, regulates cell fate in stem cells and early embryos.* Development, 2006. 133(2): p. 209-16.

21. Zweigerdt, R., M. Burg, E. Willbold, H. Abts, and M. Ruediger, *Generation of confluent cardiomyocyte monolayers derived from embryonic stem cells in suspension: A cell source for new therapies and screening strategies.* Cytotherapy, 2003. 5(5): p. 399-413.

22. Cameron, C.M., W.S. Hu, and D.S. Kaufman, *Improved development of human embryonic stem cell-derived embryoid bodies by stirred vessel cultivation.* Biotechnol Bioeng, 2006. 94(5): p. 938-48.

23. Gerecht-Nir, S., S. Cohen, and J. Itskovitz-Eldor, *Bioreactor cultivation enhances the efficiency of human embryoid body (heb) formation and differentiation.* Biotechnol Bioeng, 2004. 86(5): p. 493-502.

24. Schroeder, M., S. Niebruegge, A. Werner, E. Willbold, M. Burg, M. Ruediger, L.J. Field, J. Lehmann, and R. Zweigerdt, *Differentiation and lineage selection of mouse embryonic stem cells in a stirred bench scale bioreactor with automated process control.* Biotechnol Bioeng, 2005. 92(7): p. 920-33.

25. Bauwens, C.L., R. Peerani, S. Niebruegge, K.A. Woodhouse, E. Kumacheva, M. Husain, and P.W. Zandstra, *Control of human embryonic stem cell colony and aggregate size heterogeneity influences differentiation trajectories.* Stem Cells, 2008. 26(9): p. 2300-10.

26. Messana, J.M., N.S. Hwang, J. Coburn, J.H. Elisseeff, and Z. Zhang, *Size of the embryoid body influences chondrogenesis of mouse embryonic stem cells.* J Tissue Eng Regen Med, 2008. 2(8): p. 499-506.

27. Park, J., C.H. Cho, N. Parashurama, Y. Li, F. Berthiaume, M. Toner, A.W. Tilles, and M.L. Yarmush, *Microfabrication-based modulation of embryonic stem cell differentiation.* Lab Chip, 2007. 7(8): p. 1018-28.

28. Wobus, A.M., K. Guan, H.T. Yang, and K.R. Boheler, *Embryonic stem cells as a model to study cardiac, skeletal muscle, and vascular smooth muscle cell differentiation.* Methods Mol Biol, 2002. 185: p. 127-56.

29. Wang, X., G. Wei, W. Yu, Y. Zhao, X. Yu, and X. Ma, *Scalable producing embryoid bodies by rotary cell culture system and constructing engineered cardiac tissue with es-derived cardiomyocytes in vitro.* Biotechnol Prog, 2006. 22(3): p. 811-8.

30. Carpenedo, R.L., A.M. Bratt-Leal, R.A. Marklein, S.A. Seaman, N.J. Bowen, J.F. McDonald, and T.C. McDevitt, *Homogeneous and organized differentiation within embryoid bodies induced by microsphere-mediated delivery of small molecules.* Biomaterials, 2009. 30(13): p. 2507-15.

31. Sachlos, E. and D.T. Auguste, *Embryoid body morphology influences diffusive transport of inductive biochemicals: A strategy for stem cell differentiation.* Biomaterials, 2008. 29(34): p. 4471-80.

32. Krtolica, A., O. Genbacev, C. Escobedo, T. Zdravkovic, A. Nordstrom, D. Vabuena, A. Nath, C. Simon, K. Mostov, and S.J. Fisher, *Disruption of apical-basal polarity of human embryonic stem cells enhances hematoendothelial differentiation.* Stem Cells, 2007. 25(9): p. 2215-23.

33. Metallo, C.M., J.C. Mohr, C.J. Detzel, J.J. Pablo, B.J. Wie, and S.P. Palecek, *Engineering the stem cell microenvironment.* Biotechnol Prog, 2007. 23(1): p. 18-23.

34. Mogi, A., H. Ichikawa, C. Matsumoto, T. Hieda, D. Tomotsune, S. Sakaki, S. Yamada, and K. Sasaki, *The method of mouse embryoid body establishment affects structure and developmental gene expression.* Tissue Cell, 2009. 41(1): p. 79-84.

35. Sheardown, S.A. and M.L. Hooper, *A relationship between gap junction-mediated intercellular communication and the in vitro developmental capacity of murine embryonic stem cells.* Exp Cell Res, 1992. 198(2): p. 276-82.

36. Wang, H., G.M. Riha, S. Yan, M. Li, H. Chai, H. Yang, Q. Yao, and C. Chen, *Shear stress induces endothelial differentiation from a murine embryonic mesenchymal progenitor cell line.* Arterioscler Thromb Vasc Biol, 2005. 25(9): p. 1817-23.

37. Yamamoto, K., T. Sokabe, T. Watabe, K. Miyazono, J.K. Yamashita, S. Obi, N. Ohura, A. Matsushita, A. Kamiya, and J. Ando, *Fluid shear stress induces differentiation of flk-1-positive embryonic stem cells into vascular endothelial cells in vitro.* Am J Physiol Heart Circ Physiol, 2005. 288(4): p. H1915-24.

38. Yamamoto, K., T. Takahashi, T. Asahara, N. Ohura, T. Sokabe, A. Kamiya, and J. Ando, *Proliferation, differentiation, and tube formation by endothelial progenitor cells in response to shear stress.* J Appl Physiol, 2003. 95(5): p. 2081-8.

39. Adamo, L., O. Naveiras, P.L. Wenzel, S. McKinney-Freeman, P.J. Mack, J. Gracia-Sancho, A. Suchy-Dicey, M. Yoshimoto, M.W. Lensch, M.C. Yoder, G. Garcia-Cardena, and G.Q. Daley, *Biomechanical forces promote embryonic haematopoiesis.* Nature, 2009. 459(7250): p. 1131-5.

CHAPTER 4

CARDIOMYOCYTE DIFFERENTIATION IS PROMOTED WITHIN EMBRYONIC STEM CELL SPHEROIDS CULTURED IN ROTARY ORBITAL SUSPENSION AND IS ALTERED VIA ROTARY ORBITAL SPEED*

Introduction

Myocardial infarction due to an ischemic episode results in significant death of heart muscle cells (cardiomyocytes) that support normal cardiac contractility. Mature cardiomyocytes are incapable of significant (if any) proliferation, thus adult mammals fail to regenerate functional myocardial tissue in response to tissue injury or insult [1-3]. Severe myocardial ischemia initiates a cascade of cellular and molecular remodeling

---

*Modified from:

CY Sargent, GY Berguig, MA Kinney, LA Hiatt, RL Carpenedo, RE Berson, TC McDevitt. *Hydrodynamic Modulation of Embryonic Stem Cell Differentiation by Rotary Orbital Culture.* Biotechnology and Bioengineering, 2010, 105(3):611-626.

and

CY Sargent, GY Berguig, TC McDevitt. *Cardiomyogenic Differentiation of Embryoid Bodies is Promoted by Rotary Orbital Suspension Culture*. Tissue Engineering Part A 15(2):331-342.

events within the heart, such as protease activity, extracellular matrix synthesis and degradation, chamber dilatation, thinning of the ventricular wall, and ultimately fibrotic scar formation [4-5]. Structural changes to the geometry of the heart, along with a significant decrease in the number of contractile muscle cells, leads to decreased cardiac output volume and eventually culminates in heart failure and mortality [4-8]. The emphasis of most current clinical therapies to treat myocardial infarction is on re-vascularization strategies to restore normal blood flow, protect residual cells and slow the normal progression of heart failure. However, current clinical treatment options do not adequately address the need to replace contractile cardiomyocytes that are lost due to cardiac disease or injury.

Tissue engineering and regenerative cellular therapies capable of replacing cardiomyocytes to injured myocardium offer a promising approach to restore functional tissue; however, an appropriate cell source should have the potential to produce large yields of cardiomyocytes capable of functionally incorporating within the host tissue. Attempts thus far to employ cell therapies to achieve these rigorous criteria have been minimally successful. Skeletal myoblasts and bone marrow-derived cells transplanted within the infarcted heart have elicited small improvements in cardiac function, but have not generated significant amounts of integrated muscle tissue [9-14]. The identification and recent characterization of a putative cardiac stem cell population within the heart represents a novel cell source for cardiac regenerative therapies, but inefficient isolation and cultivation methods for these cells currently limit their therapeutic utility [15-18]. In contrast to these other cell types, ESCs are capable of significant expansion *in vitro* and inherently retain the ability to differentiate into definitive contractile cardiomyocytes that

can survive and electromechanically couple with host cells of the heart [19-22]. However, before ESC-derived cardiomyocytes can be realistically implemented as a viable cell therapy, efficient methods of differentiating ESCs to cardiomyocytes using scalable techniques must be developed to yield the large numbers of cells (10^9/heart) expected to be clinically necessary [23].

ESC differentiation is commonly initiated via spontaneous aggregation of single-cell suspensions into clusters of cells termed embryoid bodies (EBs). EBs recapitulate many of the cellular morphogenic events similar to those of pre-implantation stage embryos, eventually leading to formation of primitive cell types comprising the three germ lineages (ectoderm, endoderm and mesoderm) and further differentiation into specialized cells types, including cardiomyocytes [24-29]. For experimental studies, hanging drop cultures are typically employed to study mesoderm differentiation because of the high frequency with which cardiogenic differentiation can be readily observed [30-31]. However, the number of EBs formed per dish (~100 per 10 cm plate) is limited by surface area, and thus, hanging drops are not readily amenable to scale-up procedures [31-33]. In contrast, static suspension cultures yield larger numbers of EBs with less effort than hanging drops, but ESCs in static suspension form a heterogeneous population of EBs that readily agglomerate, thereby further increasing the heterogeneity of differentiation and reducing the overall efficiency of cell differentiation [34], including the frequency of cardiomyogenic differentiation. Recently our lab developed a novel EB formation and culture method whereby suspension ESC dishes are placed onto rotary orbital shakers [35]. Compared to hanging drop and static suspension methods, constant rotary orbital motion (40 rpm) applied continuously for 7 days of EB suspension culture

enhanced the initial efficiency of cellular incorporation during EB formation and resulted in a significantly greater number of individual EBs and EB-derived cells. Compared to static suspension cultures, rotary orbital shaking yielded more uniformly-sized EBs, and agglomeration of individual EBs after formation was inhibited, similar to hanging drop methods [35]. Additionally, rotary orbital culture has been shown to regulate EB size through the application of different rotary orbital speeds [35-36]. In addition to controlling EB size, rotary orbital speed also affects EB formation kinetics, and early evidence has suggested that differentiation pathways are modulated by these hydrodynamic conditions [35-36].

Based on these previous observations between different EB culture methods, the objective of this study was to specifically examine the cardiomyogenic differentiation of EBs cultured in rotary orbital suspension compared to both hanging drop and static suspension cultures, as well as cultured at different rotary orbital speeds. EBs were cultured for 7 days in suspension via rotary, static, or hanging drop conditions and cardiomyogenic differentiation was assessed based on spontaneous contractile activity, gene expression, and sarcomeric protein expression. The results indicate that rotary orbital suspension culture enhances the endogenous cardiomyogenic differentiation of EBs compared to static batch-culture methods and the extent of cardiomyocyte differentiation may be modulated by rotary orbital speed. Thus, rotary orbital suspension culture is a simple means of promoting cardiomyocyte differentiation from ESCs for regenerative cardiac therapies.

Materials and Methods

Embryonic Stem Cell Culture

Murine embryonic stem cells (line D3) were expanded on 0.1% gelatin-coated (Sigma) tissue culture plates (Corning) with Dulbecco's modified eagle medium (DMEM) (Mediatech) supplemented with 15% fetal bovine serum (Hyclone, Logan, UT), 2 mM L-glutamine (Mediatech), 0.1 mM β-mercaptoethanol (Fisher Chemical, Fairlawn, NJ), 1x non-essential amino acids (Mediatech), penicillin-streptomycin (Mediatech) and 10^3 U/ml leukemia inhibitory factor (LIF) (Chemicon International). ESCs were re-fed with fresh media every other day, and ESCs were routinely passaged every 2-3 days prior to reaching 70% confluence.

Embryoid Body Formation and Culture

In order to form embryoid bodies (EBs), ESCs were detached from culture dishes using 0.05% trypsin-EDTA solution (Mediatech) before reaching 70% confluence and suspended in differentiation media (same as undifferentiated ESC media but without LIF). Hanging drop EBs were formed by suspending 600 cells/15 µl drop from the lid of square Petri dishes (10 cm x 10 cm) (Nunc). To prevent evaporation of the hanging drops, 10 ml of a sterile 1% solution of BSA in PBS was added to the bottom of each dish. Suspension EB cultures (static and rotary) were inoculated with 2-4 x 10^5 cells/ml in 10 ml differentiation media in 100 x 15 mm non-tissue culture treated polystyrene (i.e. bacteriological grade) Petri dishes (Becton Dickinson Biosciences). A thin layer of sterile 2% agar (Sigma) was used to pre-coat static plates to prevent cell attachment. Static and rotary suspension culture media was refreshed every other day, but hanging drop media was not changed during the 7 day suspension period. Rotary suspension EBs

were placed on rotary orbital shakers (Lab-Line Lab Rotator, Model #2314, Barnstead International) set at a range of speeds (25, 40, or 55 rotations per minute) and calibrated daily for the entire suspension culture period to ensure consistent speed was maintained throughout the studies.

Spontaneous Contractile Activity Assessment

After 7 days of suspension culture, EBs from each formation method were collected and individually plated onto 0.1% gelatin-coated 48-well tissue culture dishes to prevent the spreading of individual EB colonies into one another. The development of contractile foci within EB colonies was monitored every other day (8, 10, 12, and 14) to assess the frequency of cardiomyogenic differentiation. Suspension EBs were collected by diluting 200 µl of EBs into 5 ml fresh media within a new Petri dish, and hanging drop EBs were collected by harvesting 1 100 x 100 dish (~50 EBs) and placing into 5 ml media within a new Petri dish. Individual EBs were selected from the diluted suspension with 1 ml, wide bore pipet tips (Rainin, Oakland, CA; 100 µl volume), dispersed into individual gel-coated wells of a 48-well plate and an additional 400 µl of media was added for a final volume of 500 µl per well. After 24 hours, wells were visually inspected to ensure each well contained at least one EB; in cases where 2 or 3 EBs occupied the same well (~2% of wells; no wells contained >3 EBs), merged EBs were excluded from the contractile analysis. Blinded counts of EB colonies with one or more spontaneously beating foci were scored as "contractile" and the percentage of contractile EBs relative to the total number of plated EBs was calculated (minimum of 30 EBs per experimental sample; >90 EBs total assessed per condition).

Real-Time PCR Analysis

Total RNA was extracted from undifferentiated ESCs and EBs from each of the different formation methods at various time points of differentiation using the RNeasy Mini kit (Qiagen Incorporated). Reverse transcription for complementary DNA synthesis was performed using the iScript cDNA synthesis kit (Bio-Rad), and quantitative PCR was performed with SYBR green technology on the MyiQ cycler (Bio-Rad). Primers, sequences and annealing temperatures are listed in Table 1 for *Oct-4*, *Nanog*, *Brachyury T*, *Gata4*, *Nkx2.5*, *Myocyte enhancer factor-2c* (*Mef2c*), *Myosin light chain-2 ventricle* (*MLC-2v*), *α-myosin heavy chain* (*α-MHC*), *myogenic factor 5* (*Myf5*), *alpha-fetoprotein* (*AFP*), and *glyceraldhyde-3-phosphate-dehydrogenase* (*GAPDH*). Each primer set was designed with Beacon Designer software (Invitrogen), and validated with appropriate cell controls. Relative gene expression levels of *Oct-4* and *Nanog* (pluripotent ESC markers) were internally normalized to *GAPDH* (housekeeping gene) and quantified relative to undifferentiated ESC expression levels using the Pfaffl method of quantification [37]. For differentiation cell markers, absolute gene expression concentrations were calculated against standard curves and internally normalized versus levels of *GAPDH* expression.

Table 4.1: Primer Sequences and Annealing Temperatures

Gene	Forward sequence	Reverse sequence	Temp.
Oct-4	CCG TGT GAG GTG GAG TCT GGA G	GCG ATG TGA GTG ATC TGC TGT AGG	63.0°C
Nanog	GAA ATC CCT TCC CTC GCC ATC	CTC AGT AGC AGA CCC TTG TAA GC	60.5°C
Brachyury-T	GAC TCC AGC CTT CCT TCC	CAC ACC ACT GAC GCA CAC	60.5°C
Gata4	TGC TTT GAT GCT GGA TTT AAT TTC G	CGG GTG TGC GGA ACT GTC	59.0°C
Nkx2.5	CAA GTG CTC TCC TGC TTT CC	GGC TTT GTC CAG CTC CAC T	62.0°C
Mef2c	CCC AAT CTT CTG CCA CTG	GGT TGC CGT ATC CAT TCC	59.0°C
α-MHC	GGT CCA CAT TCT TCA GGA TTC TC	GCG TTC CTT CTC TGA CTT TCG	64.3°C
MLC-2v	GAC CAT TCT CAA CGC ATT CAA G	CTT CTC CGT GGG TAA TGA TGT G	64.3°C
Myf5	GGA ACA GGT GGA GAA CTA TTA C	CTT TCG GGA CCA GAC AGG	62.0°C
AFP	CAC ACC CGC TTC CCT CAT CC	TTC TTC TCC GTC ACG CAC TGG	60.5°C
Nestin	GGA GAA GCA GGG TCT ACA G	AGC CAC TTC CAG ACT AAG G	60.5°C
GAPDH	GCC TTC CGT GTT CCT ACC	GCC TGC TTC ACC ACC TTC	60.5°C

Histology and Immunohistochemistry

Suspension EBs were sampled from each group at day 7 of differentiation, and at day 10 (after EB plating), EBs were scraped from gelatin-coated dishes for immunohistochemical analysis. The samples were fixed for 30 minutes in formalin (4% formaldehyde), embedded in Histogel® (Richard Allen Scientific) and polymerized for 2 hours at 4° C in cryomolds (10mm x 10mm x 5mm, Sakura Finetek). After polymerization, the EBs entrapped within Histogel® were dehydrated through a graded series of alcohol solutions (70-100%) and xylene and embedded in paraffin. Five-micron sections were obtained using a rotary microtome (Microm HM 355S) with 80 μm intervals between sections to ensure that unique EBs were analyzed within the different sections, and histological slides were de-paraffinized prior to staining. For

morphological assessment, slides were stained with hemotoxylin and eosin using a Lieca Autostainer XL.

For immunohistochemical analysis, de-paraffinized samples were incubated for 1 hour in a 0.05% (weight/volume) Triton X solution of 2% horse serum in PBS at room temperature in order to permeabilize and block the sections. A primary anti- α-sarcomeric actin antibody (1:5000, 5c5, Sigma) was incubated overnight at 4°C, followed by three PBS rinses. A secondary biotinylated horse anti-mouse antibody (1:400, Vector Laboratories) was incubated at room temperature for 30-60 minutes, followed by three rinses in PBS. The avidin-biotinylated alkaline phosphatase complex was incubated in solution for 30 minutes at room temperature prior to application, per vendor's instructions (VECTASTAIN ABC-AP kit, Vector Laboratorie), and applied to histological sections for 30 minutes at room temp, rinsed twice with PBS and once in 100 mM Tris, pH 8.2 prior to developing with the chromagen, Vector Red SK-5100 (Vector Labs). Cell nuclei were counterstained with hematoxylin (Lieca AutoStainer XL), dehydrated with alcohol and xylene, mounted with Cytoseal™ 60 mounting medium (Richard Allen Scientific), cover-slipped, and imaged on a Nikon 80i upright microscope with a SpotFlex camera. Four to six independent fields were imaged per slide, and images were used to quantify the percentage of cardiomyogenic EBs. Sections of mouse heart and intestine were included with each batch of immunostaining as positive and negative controls, respectively.

Image Analysis

For quantitative analysis, only distinct cell clusters $\geq$ 2500 μm^2 were considered to be individual EBs. Smaller groups of cells (< 2500 μm^2) representing partial EBs or

debris from scraping were excluded from the quantitative analysis. Blinded counts were performed of the total number of EBs and the number of EBs with positive regions of α-sarcomeric actin expression in order to report the percentage of "cardiomyogenic" EBs. Immunohistochemical EB count data from independent experiments were combined (n = 4 for hanging drop and rotary EBs; n = 3 for static EBs), and a minimum of 40 EBs per condition was assessed. Within NIH ImageJ, a threshold for colorimetric staining was determined according to positive and negative control slide staining intensity and used to define the areas of positive α-sarcomeric actin staining within EBs. A macro program was written and employed within NIH ImageJ to measure the relative cross-sectional area of positively stained cells within individual EBs (as defined by the threshold), as well as the total EB cross-sectional area, and the relative area of α-sarcomeric actin immunoreactivity was calculated for individual EBs.

Immuno-Cytometry

EBs either plated at day 7 of differentiation or maintained in suspension were trypsinized (0.25% trypsin-EDTA) 3 days later (day 10 of differentiation) or 5 days later (day 12) and triturated every 10 minutes for a total of 30 minutes to attain single-cell suspensions for flow cytometric analysis. Cell suspensions were centrifuged at 200 rcf for 5 minutes to collect the cells, re-suspended in 1 ml PBS, transferred to 1.5 ml centrifuge tubes, centrifuged again at 3,500 rcf for 8 minutes, and re-suspended in 1 ml formalin for 5 minutes with rotation at room temperature. Cells were collected by centrifugation (8 min, 3,500 rcf) and rinsed three times with PBS; after the final rinse and centrifugation, the cell-pellet was re-suspended in 1 ml of working buffer (0.3% BSA, 0.1% Tween-20 in 1x PBS) supplemented with 0.05% Triton X-100 and 10% serum to

provide permeablize cells and block non-specific antibody binding, and rotated for 30 minutes at room temperature. Cell suspensions were divided into equal quantities of 5 x 10^5 cells for further antibody incubations and analysis, and cells were rinsed and centrifuged three times with working buffer. The resulting cell-pellets were re-suspended in 300 µl of antibody solution in working buffer and rotated for 30 minutes at room temperature, followed by successive rinse and centrifugation steps. The cell pellet was re-suspended in 300 µl of secondary antibody solution in working buffer with rotation in the dark for 30 minutes at room temperature followed by a series of three rinses in working buffer and centrifugation. Antibodies and concentrations used were: mouse monoclonal 5c5 (Sigma), anti-α-sarcomeric actin (1:500) with goat-anti-mouse secondary (Dako) (1:20), rabbit polyclonal anti-human AFP (Dako) (1:200) with goat-anti-rabbit secondary (Southern Biotech) (1:200), and mouse monoclonal anti-p63 (Chemicon) (1:200) with goat-anti-mouse secondary (1:200). For control comparison for background fluorescent levels, unlabeled Ig anti-mouse antibody was used in place of primary antibody incubation. The final cell-pellet was re-suspended in 500 µL of PBS, filtered through the 35 µm cell-strainer cap of a BD Flacon™ 5 mL polystyrene round-bottom tube (BD Falcon), and run on a digital flow cytometer to capture a minimum of 10,000 events (BD LSR, BD Immunocytometry Systems). Analysis was performed using FlowJo software (Tree Star Inc.), and positive gates were set at 2% of the Ig isotype control population.

Statistical Analysis

Experimental conditions were examined with triplicate samples in independent experiments and data values presented reflect the mean value ± standard deviation.

Analysis of variance was performed to determine statistical significance ($p<0.05$) between experimental groups, and where significant, was followed by post-hoc Tukey analysis to define statistical differences ($p<0.05$) between specific experimental variables.

Results

Rotary Orbital Culture Enhances Cardiomyocyte Differentiation

Embryoid Body Contractility is Enhanced via Rotary Orbital Culture

The development of spontaneously contractile, rhythmically-beating foci within EBs is a commonly observed indication of cardiomyogenic differentiation. The onset of spontaneous beating was detected within EBs from hanging drop, static, and rotary culture typically one day after plating onto gelatin-coated dishes (Figure 4.1). Hanging drop culture consistently yielded the highest frequency of contractile EBs compared to either static or rotary culture methods, with > 60% of hanging drop EBs beating at 8 days of differentiation and reaching 89.4 ± 6.7% by day 10 of differentiation. EBs generated by rotary orbital suspension culture demonstrated a significantly greater occurrence of spontaneous beating activity compared to EBs cultured in static suspension at each time point observed ($p < 0.01$). At 8 days of differentiation, 37.4 ± 23.7% of rotary EBs exhibited contractile foci, while only 5.9 ± 4.1% of static EBs contained beating areas. By 10 days of differentiation, 50.7 ± 16.7% of rotary EBs contained contractile activity, whereas static culture only achieved 20.7 ± 11.2% contractile EBs (Figure 4.1). About 50% of rotary EBs retained contractile activity through day 12 of differentiation, but a slight decline in the percentage of contractile EBs was observed by 14 days, similar to hanging drop EBs, which also exhibited a slight decline in spontaneous contraction after

12 days of differentiation. The significant differences in spontaneous beating activity of EBs observed between the different culture methods suggested an increased potential of cardiomyogenesis was induced by rotary orbital culture compared to static suspension culture.

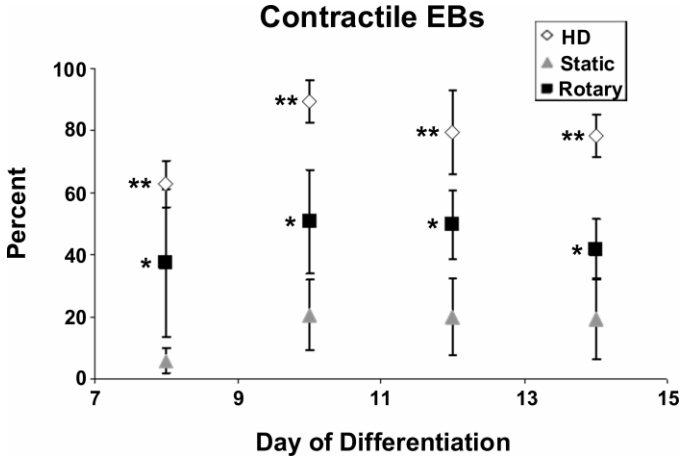

Figure 4.1: Percent Contractile EBs. After day 8 of differentiation, rotary EBs consistently exhibited approximately 50% contractile EBs (days 10 and 12), while static EBs only achieved a maximum of about 20% (days 10, 12, and 14). Hanging drop (HD) EBs consistently exhibited beating foci in $\geq$ 80% of EBs, between days 10 – 14 of differentiation. By day 14, both hanging drop and rotary EBs slightly decreased contractile EB percentages. Data points represent the combined sum of data from 3 independent experiments, n = 9 (HD and rotary) or 6 (Static), $p \leq 0.01$, * = compared to static, ** = compared to static and rotary. From Sargent et al. 2009 [38].

Rotary Orbital Culture Modulates Cardiomyogenic-Associated Gene Expression

Based upon the differences observed in contractile activity of EBs elicited by the different formation methods, quantitative gene expression analysis of cardiac differentiation was performed. The expression of pluripotent genes, *Oct-4* and *Nanog*, progressively decreased over the course of EB differentiation such that by 7 days of suspension culture, negligible levels remained detectable and no significant differences in pluripotent gene expression were observed between EBs from the different formation

methods (Figure 4.2 A&B). Hanging drop and rotary EBs exhibited significantly decreased expression of *Nanog* by day 4 compared to static EBs (Figure 4.2 B), and hanging drop EBs expressed significantly less levels of *Oct-4* at day 4 of differentiation compared to rotary and static culture methods (Figure 4.2 A). *Brachyury T*, a transiently expressed mesoderm transcription factor, was expressed by EBs formed by each of the different methods at day 4 of differentiation, but at significantly greater levels by rotary EBs compared to hanging drop and static EBs (Figure 4.2 C). The cardiac transcription factors *Gata4*, *Nkx2.5*, and *Mef2c* were expressed by rotary, static, and hanging drop EBs, although the onset and extent of expression differed. Hanging drop and rotary EBs exhibited significantly increased levels of *Gata4* at day 4 or 7 (respectively) compared to either of the other culture methods (Figure 4.2 D). By day 7 of differentiation, rotary and hanging drop EBs exhibited a significant increase in expression of *Nkx2.5* compared to static EBs (27x and 44x, respectively) (Figure 4.2 E). Similar to patterns of *Nkx2.5* expression, levels of *Mef2c* expression were significantly greater in hanging drop EBs at day 4 of differentiation and expression of *Mef2c* by rotary EBs was increased by day 7 of differentiation, relative to either hanging drop or static suspension cultures (Figure 4.2 F). In addition to cardiac transcription factors, rotary and hanging drop EBs expressed transcripts for sarcomeric muscle proteins, *α-MHC* and *MLC-2v*, at comparable levels at day 7 of differentiation (~9x-fold and ~6x-fold greater than static EBs) (Figure 4.2 G&H). *Myf5*, an early skeletal muscle-specific transcription factor, was not expressed until 14 days of EB differentiation, indicating that expression of sarcomeric muscle markers prior to 14 days was specific for cardiac muscle, similar to previous reports [39].

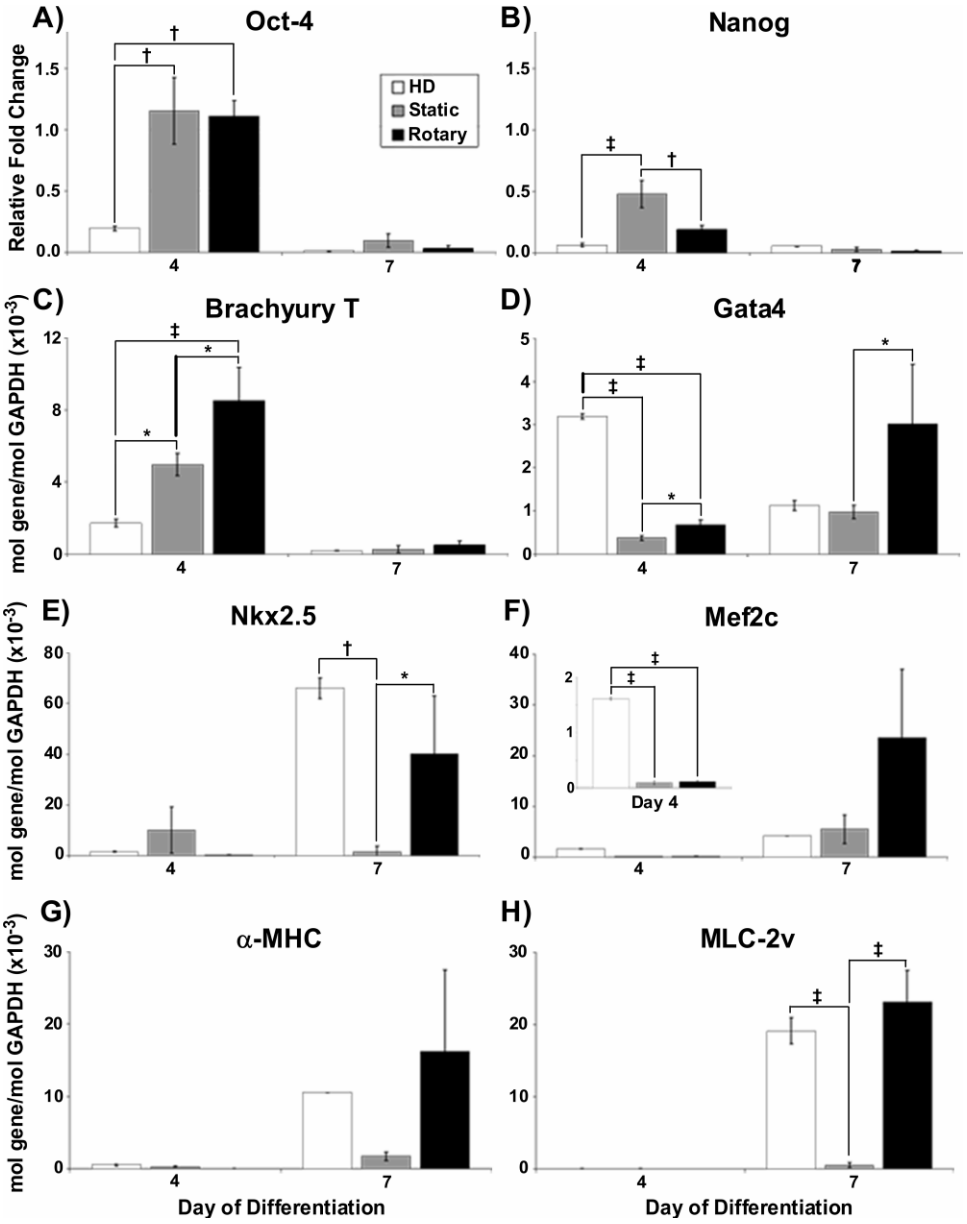

Figure 4.2: Gene Expression. Hanging drop (HD) EBs exhibited a decrease in Oct-4 (A) expression compared to rotary and static at day 4 of differentiation, while both hanging drop and rotary EBs expressed lower levels of Nanog (B) compared to static at day 4. B-T (C) expression was greatest within rotary EBs at day 4, and both hanging drop and rotary EBs exhibited increased Gata4 (D) at days 4 and 7 respectively compared to static EBs, which maintained relatively low levels of Gata4 expression. Nkx2.5 (E) expression was increased within hanging drop and rotary EBs at day 7, and rotary EBs also exhibited the greatest expression of Mef2c (F) at day 7. Additionally, both α-MHC (G) and MLC-2v (H) expression was increased the most within hanging drop and rotary EBs, while static EBs maintained only low expression levels at day 7. n = 3, * = $p \leq 0.05$, † = $p \leq 0.01$, ‡ = $p \leq 0.001$. Modified from Sargent et al. 2009 [38].

Altogether, the expression profiles of genes directing EB cardiomyogenic differentiation indicated that rotary orbital suspension promoted a cardiomyogenic genotype similar to hanging drop culture more robustly than static suspension methods.

Rotary Orbital Culture Enhances Cardiogenic Protein Expression

Immunohistochemical (IHC) staining for α-sarcomeric actin was performed to identify and confirm the presence of developing cardiomyocytes within EBs. At early stages of EB differentiation (before 14 days), immunostaining for α-sarcomeric actin is a reliable phenotypic marker of cardiomyocyte differentiation by ESCs because of the coincident absence of early skeletal muscle transcription factors, as previously noted [39]. By day 10 of differentiation, clusters of α-sarcomeric actin+ cells were readily observed in cross-sections of many rotary and hanging drop EBs, but few static EBs stained positive for α-sarcomeric actin (Figure 4.3, top row). In addition, α-sarcomeric actin+ regions appeared to occupy a larger portion of the cross-sectional area of rotary EBs, occasionally comprising a majority of the EB interior (Figure 4.3, middle row). The morphology of α-sarcomeric actin+ cells within rotary and hanging drop EBs was consistent with that of immature cardiomyocytes prior to the development of distinct, organized sarcomeres or myofibrils (Figure 4.3, bottom row). Quantitative assessment of cardiomyogenic (α-sarcomeric actin+) EBs confirmed a significantly increased percentage was attained with rotary and hanging drop methods (78 ± 18% and 66 ± 25%, respectively) compared to static suspension culture (7 ± 8%, Figure 4.4 A) at day 10 of differentiation. Furthermore, rotary EBs contained 36.9 ± 27.8% of sarcomeric actin+ area, whereas hanging drop and static EBs contained 13.5 ± 2.1% and 18.8 ± 4.7%

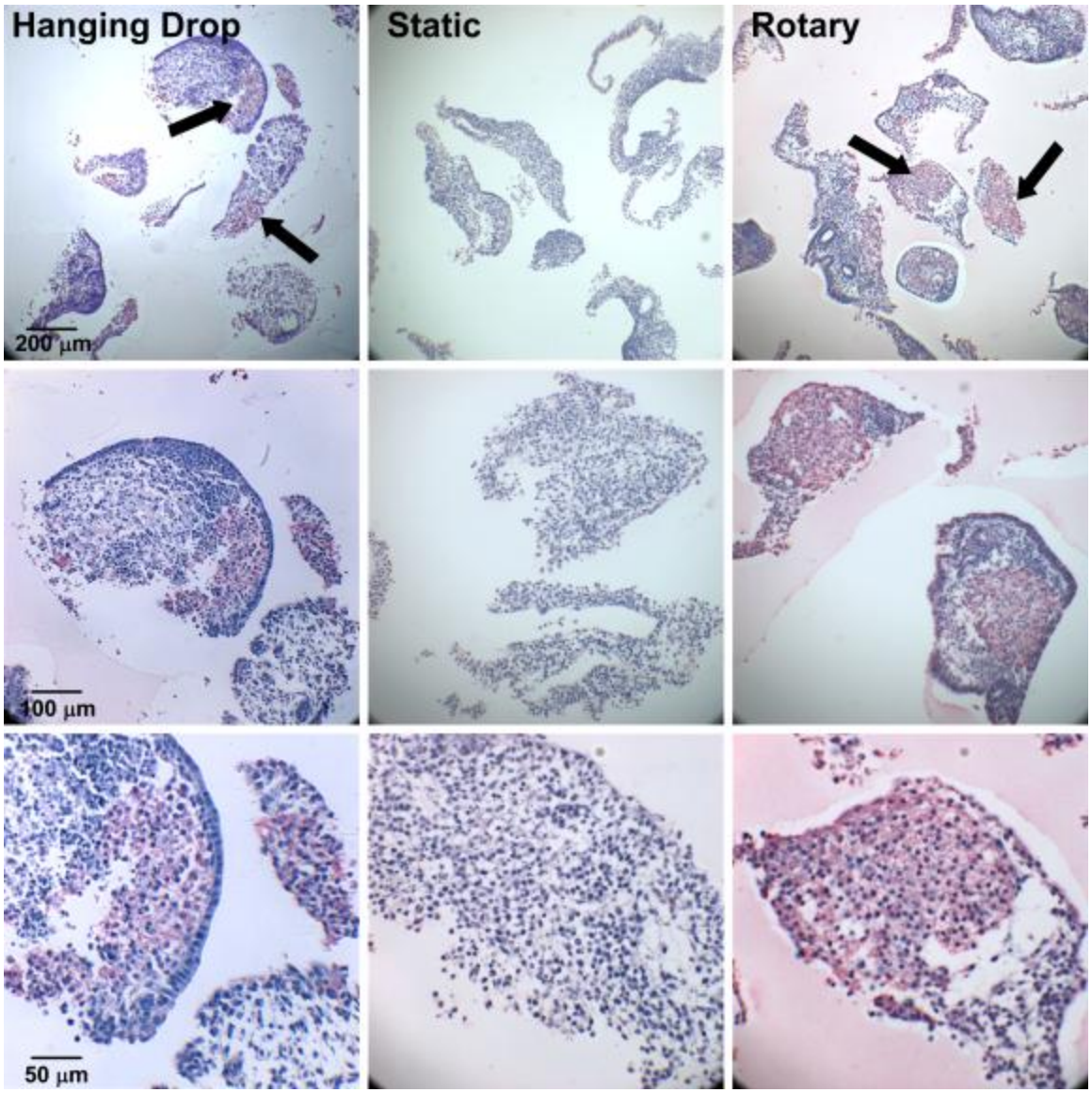

Figure 4.3: Sarcomeric Protein Staining. α-sarcomeric actin IHC staining using 5c5 antibody within hanging drop (Left), static (Center), and 40 rpm rotary (Right) EBs. Pink/red staining indicates 5c5 + clusters of cells within hanging drop and rotary EBs, but no apparent positive areas in static EBs. Top row low magnification (scale bar = 200 µm), middle row bottom row high magnification (scale bar = 100 µm and 50 µm, respectively). Black arrows = positive stain. From Sargent et al. 2009 [38].

respectively (Figure 4.4 B). Thus, IHC staining analysis, consistent with spontaneous contractile activity and cardiac gene expression, suggested that rotary orbital culture

promoted the differentiation of cardiomyocytes to a greater extent than static suspension culture conditions.

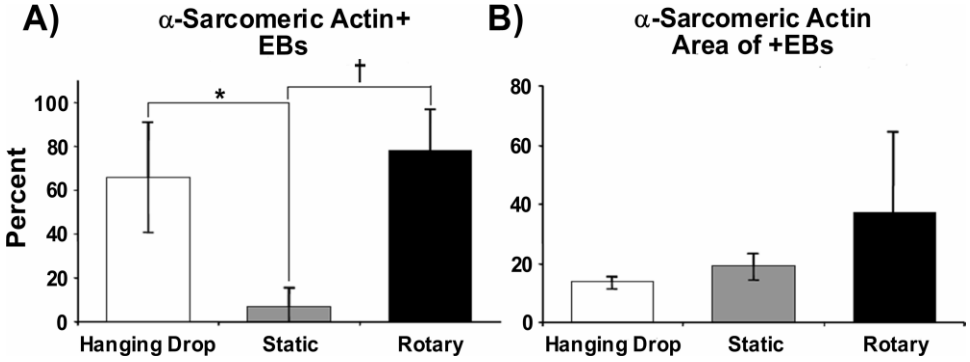

Figure 4.4: Quantification of Sarcomeric Protein Staining. Percent of EBs stained positive for α-sarcomeric actin at day 10 of differentiation from hanging drop, static, and rotary culture conditions (A). Percent of positive area within positively stained EBs from hanging drop, static, and rotary culture conditions (B). Combined data from two independent experiments, n = 4 (hanging drop and rotary), n= 3 (static), * = $p \leq 0.05$, † = $p \leq 0.005$. From Sargent et al. 2009 [38].

Rotary Orbital Culture Modulates Cardiogenic Cell Phenotype

Flow cytometry analysis for cardiac myocyte immunoreactivity of dissociated EBs was performed to assess the percent of α-sarcomeric actin+ cells yielded by the different EB culture methods. Based on histogram analysis, the population of cells from rotary and hanging drop EBs exhibited a distinct positive shift in fluorescent signal intensity compared to static EBs and immunostaining controls (Figure 4.5 A). Static EBs contained 3.54 ± 3.07% α-sarcomeric actin+ cells, whereas hanging drop EBs contained 6.71 ± 3.63% and rotary EBs possessed 13.08 ± 7.37% α-sarcomeric actin+ cells (Figure 4.5 B). The average value of α-sarcomeric actin+ cells was calculated by quantifying the positive number of gated fluorescent events relative to the overall population of cells (Figure 4.5 C). Thus, consistent with the results of gene expression and IHC staining,

flow cytometry studies suggested that rotary orbital culture enriched the number of cardiomyocytes within EBs compared to the other culture techniques examined.

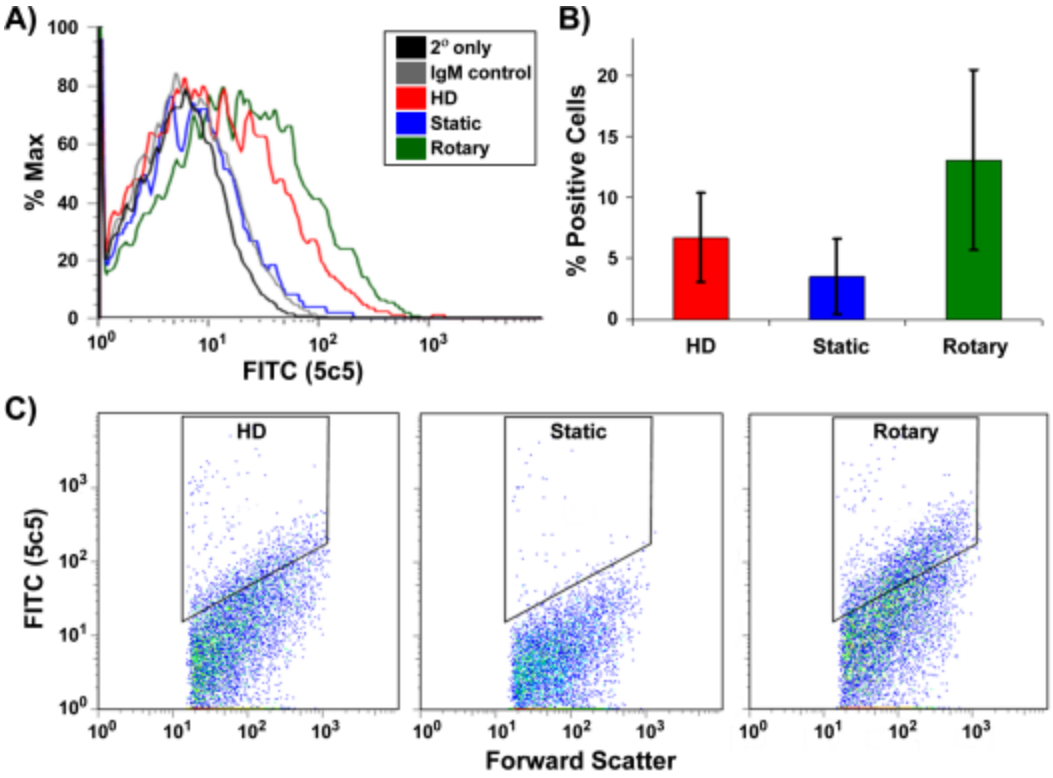

Figure 4.5: Sarcomeric Protein Immunocytometry. Histogram representation of associated α-sarcomeric actin expression within dissociated EBs from hanging drop, static, and rotary orbital culture at day 10 of differentiation (A). Percent of α-sarcomeric actin+ cells within EBs from hanging drop, static, and rotary conditions (B). Dot plot representation of 10,000 events captured, gated on 1% of the IgM isotype control (C). n = 3, data representative of a minimum of two independent experiments. From Sargent et al. 2009 [38].

Hydrodynamic Conditions from Rotary Orbital Culture Modulate Cardiogenic Differentiation

Hydrodynamic Conditions Affect Contractility of EBs

Spontaneous beating was detected within EBs from rotary orbital culture one day after plating onto gelatin-coated dishes (Figure 4.6). Similar to previous results (Figure 4.1), rotary EBs exhibited increased contractile percentages compared to static EBs at all time points examined ($p \leq 0.005$), except at day 14 of differentiation when contractile activity of 25 rpm EBs was reduced to levels similar to static EBs. Lower rotary speeds of 25 and 40 rpm consistently generated to highest frequency of contractile EBs, approaching nearly 100% between days 8 and 12 of differentiation. The faster rotary orbital speed examined (55 rpm) produced a lower percentage of contractile EBs between days 8 and 12 of differentiation compared to 25 and 40 rpm ($p \leq 0.05$), but EBs from 55 rpm still exhibited increased beating activity as compared to static EBs between days 8 and 12 of differentiation ($p \leq 0.05$). Similar to previous results (Figure 4.1), rotary orbital EBs exhibited slight decreases in contractile frequency at day 14 of differentiation. Additionally, spontaneous beating within static EBs appeared delayed compared to rotary EBs, requiring at least 12 days of differentiation before contractile foci were observed (Figure 4.6). The differences in beating frequency between rotary and static conditions agree with previously reported data. Interestingly, rotary conditions did not induce spontaneous beating to equal extents, and increased contractile activity correlated to lower rotary orbital speeds, suggesting that the different hydrodynamic environments created by different rotary speed may modulate cardiomyocyte differentiation.

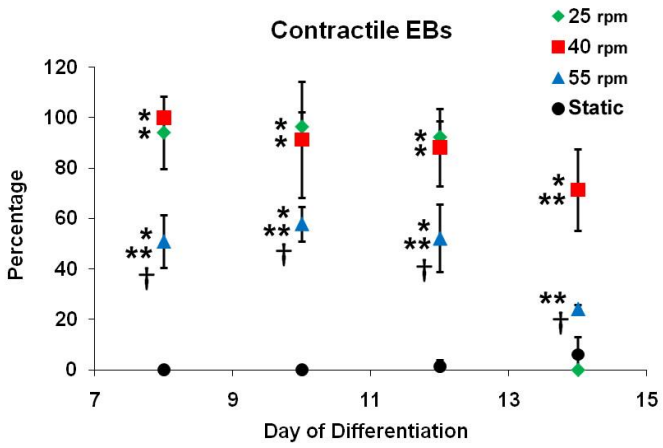

Figure 4.6: Development of Spontaneous Beating in Variable Speed EBs. After day 8 of differentiation, rotary EBs consistently exhibited increased contractile activity compared to static EBs. EBs from lower rotary speeds exhibited the highest percentages of contractile EBs, approaching 100%, while faster rotary speeds generated EBs with reduced development of spontaneously beating EBs, but still greater than the percentage of contractile static EBs. Static EBs required at least 12 days of differentiation to exhibit beating foci. n = 3, $p \leq 0.05$, * = compared to static, ** = compared to 25 rpm, † = compared to 40 rpm.

Hydrodynamic Conditions Alter Gene Expression Patterns

Temporal gene expression analysis for specific phenotypic markers of undifferentiated ESCs and each of the three germ lineages (ecto-, endo-, mesoderm) was also performed in order to examine the effects of rotary orbital culture on ESC differentiation kinetics. As expected, the expression of pluripotent genes *Oct-4* and *nanog* decreased over time for each of the different EB populations, regardless of rotary speed (Figure 4.7 A&B), further indicating that rotary orbital culture does not inhibit the progressive loss of pluripotent marker expression by EBs under differentiation conditions. However, EBs from static culture exhibited significantly higher *Oct-4* (days 4 and 7) and *nanog* expression (day 4) compared to EBs from rotary culture conditions

($p \leq 0.05$), suggesting a slight acceleration in the onset of differentiation with hydrodynamic culture conditions. Additionally, gene expression levels for markers generally associated with the different germ layers (i.e *brachyury T* (*B-T*) for mesoderm, *nestin* for ectoderm, and *Gata-4* and *AFP* for endoderm) increased with time in EBs from both static and rotary orbital cultures. Levels of *B-T* expression were transiently increased within rotary conditions (at all speeds) at days 2 and 4, while static EBs exhibited increased expression only after 4 days of differentiation. As expected, *B-T* expression was reduced by day 7 of differentiation at each of the experimental conditions examined. The expression of markers from each germ layer to varying extents indicates that the hydrodynamic environments examined did not inhibit EB differentiation from proceeding in a normal fashion (Figure 4.7 C-I).

Several differences in the expression of differentiated gene markers were detected between static and rotary EBs. For example, independent of rotary speed, orbital culture enhanced the expression of cardiomyogenic genes such as *Nkx2.5, α-myosin heavy chain* (*α-MHC*), and *myosin light chain 2-ventricle* (*MLC-2v*) compared to static conditions (Figure 7 D-F). Expression of *Nkx2.5* and *α-MHC* was significantly increased in 25 rpm EBs compared to static EBs ($p \leq 0.05$) at day 7 of differentiation, but not significantly greater than either of the other rotary speeds examined (Figure 4.7 D&E). However, after 12 days of differentiation, all of the rotary speeds exhibited significantly increased levels of *α-MHC* expression compared to static EBs (Figure 4.7 E). At each time point examined, rotary EBs expressed significantly higher levels of *MLC-2v* compared to static culture ($p \leq 0.005$) (Figure 4.7 E). In addition, at day 10 of differentiation, rotary EBs at 40 and 55 rpm expressed higher levels of *MLC-2v* than 25 rpm EBs, and by day 12 of

differentiation, 55 rpm EBs expressed *MLC-2v* greater than either of the other rotary speeds or static cultures.

Similarly, rotary speed also modulated EB expression of endoderm and ectoderm-associated genes as a function of time. At day 7 of differentiation, *Gata-4* expression was significantly higher in 25 rpm EBs than static and 55 rpm EBs ($p \leq 0.05$), and at day 10, 25 rpm EBs expressed significantly higher levels of *Gata-4* compared to all other experimental conditions ($p \leq 0.005$). However, by day 12 of EB differentiation, *Gata-4* expression levels in 40 rpm EBs were similar to 25 rpm EBs and significantly greater than static EBs (Figure 4.7 G). At day 10 of differentiation, 25 rpm EBs also expressed significantly higher levels of *AFP* than all other conditions ($p \leq 0.01$), but by day 12, *AFP* expression by 40 rpm EBs was significantly higher than both static and 55 rpm EBs ($p \leq 0.05$). In addition to differences in mesoendoderm gene expression levels, 40 and 55 rpm EBs expressed significantly higher levels of *nestin* (a potential ectoderm marker) than static or 25 rpm EBs at days 10 ($p \leq 0.005$) and 12 ($p \leq 0.05$) of differentiation. Although the specifity of *nestin* expression to ectoderm versus endoderm derivatives has been questioned [40-41], endoderm associated genes were expressed to a lesser degree in 55 rpm EBs compared to 25 and 40 rpm EBs (Fig 7 G&H), suggesting that in this instance, *nestin* expression may be indicative of more ectoderm differentiation than endoderm. Taken together, the results of gene expression analysis indicate that expression of differentiated germ layer markers is modulated by rotary orbital speed and thus, hydrodynamic states can influence the differentiation of EBs.

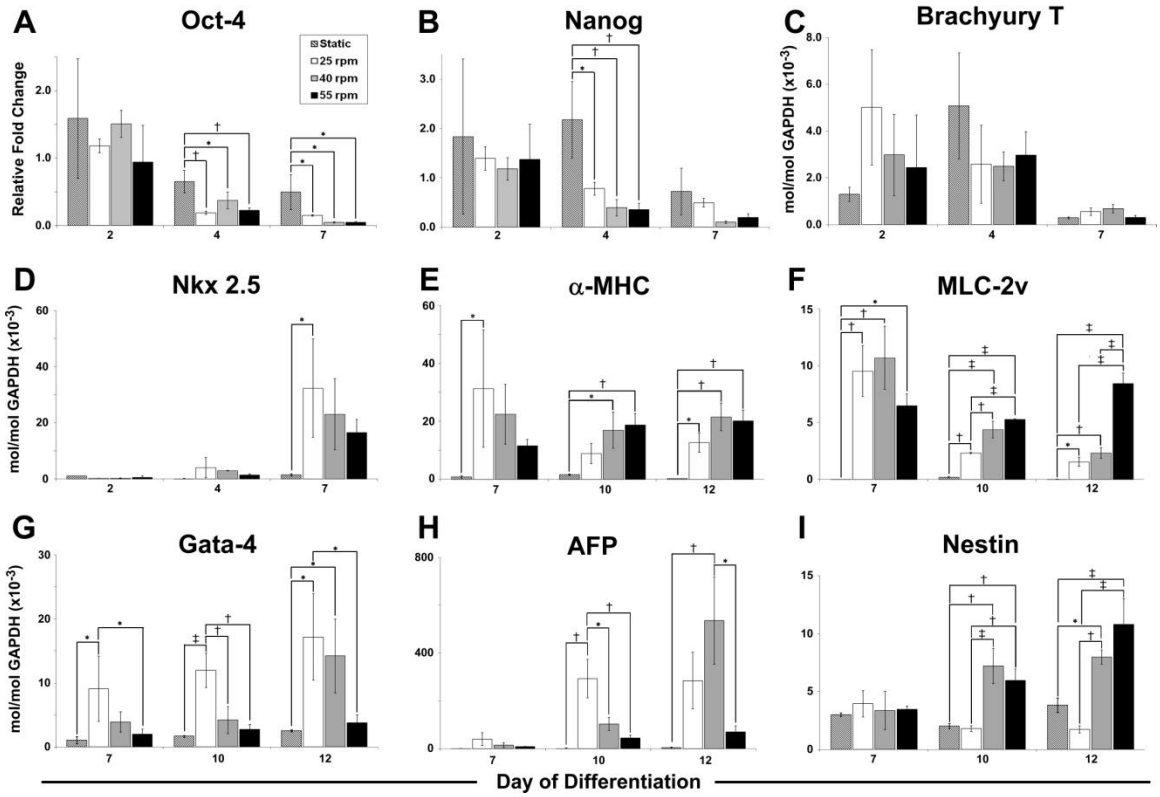

Figure 4.7: Temporal gene expression analysis of embryoid bodies. By days 4 and 7, all EBs exhibited deceased levels of pluripotent gene expression (*Oct-4* and *Nanog*) (A&B). EBs from each culture condition expressed some level of mesoderm (C-F), endoderm (G&H), and ectoderm (I) during the time course of differentiation, suggesting that rotary orbital speed did not preclude normal EB differentiation into the three germ layers. *Gata-4* (mes/endoderm) was expressed earlier and at a higher level in 25 rpm EBs, with 40 rpm obtaining similar expression levels by day 12, and 55 rpm EBs maintained significantly less *Gata-4* expression throughout the time course of differentiation (G). EBs formed at 25 rpm also exhibited increased levels of *AFP* expression (endoderm) at earlier differentiation time points than 40 or 55 rpm. While 40 rpm EBs attained similar expression levels to 25 rpm by day 12, 55 rpm *AFP* expression remained significantly lower (H). EBs formed at higher speeds (40 & 55 rpm) exhibited increased levels of *Nestin* (ectoderm) expression compared to 25 rpm EBs. n = 3. * = $p<0.05$, † = $p<0.01$, ‡ = $p<0.001$. Modified from Sargent et al. 2010 [36].

Hydrodynamic Conditions Affect Differentiating Cell Phenotypes

In order to quantify the relative amounts of different cell phenotypes comprising EBs, dissociated cell populations were assessed by immunocytometry. Cell derivatives of mesoderm (α-sarcomeric actin), endoderm (AFP), and ectoderm (p63) were assessed

from EBs after 12 days of differentiation. Consistent with gene expression analysis, each of the EB culture conditions yielded populations of differentiated cells that expressed markers indicative of the three germ layers (Figure 4.8 A-C). Similar to gene expression analysis, the largest differences in cell phenotype populations were between static and rotary groups, and although the rotary groups (25, 40, and 55 rpm) exhibited similar percentages of cell derivatives from each germ layer (Figure 4.8 D), a few differences between rotary orbital speeds were evident. Cell populations from 25 rpm EBs exhibited significantly more AFP+ cells compared to 40 rpm ($p \leq 0.05$) and more p63+ cells compared to all other conditions ($p \leq 0.05$ - static or 55 rpm EB, $p = 0.07$ - 40 rpm). The population mean fluorescent intensity values of the EB derived cells indicated that differentiation of α-sarcomeric actin+ cells was increased at 25 rpm compared to static cultures (Figure 4.8 E), and that differentiation of p63+ cells was enhanced at 25 rpm compared to all other culture conditions ($p \leq 0.05$) (Figure 4.8 F). Overall, cytometry results indicate that hydrodynamic modulation of EBs in suspension culture differentially affects the relative populations of ESC differentiated phenotypes.

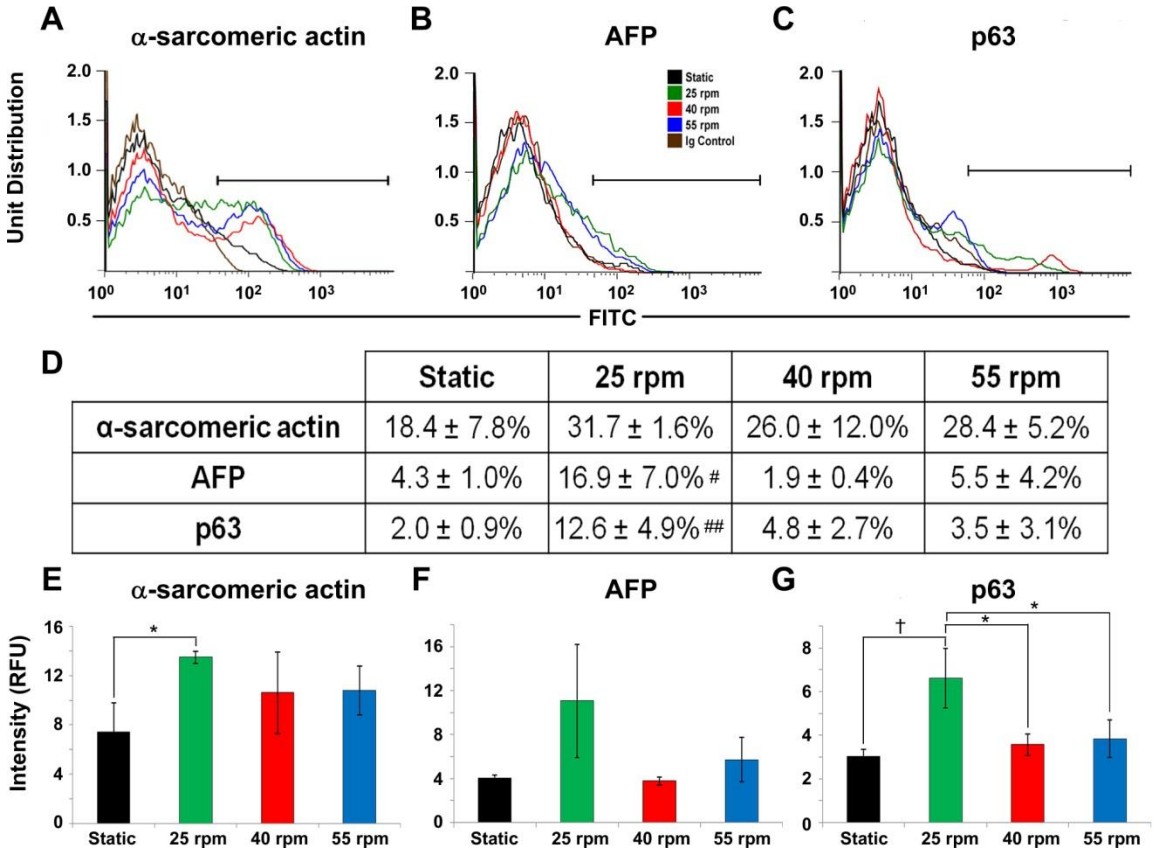

D

	Static	25 rpm	40 rpm	55 rpm
α-sarcomeric actin	18.4 ± 7.8%	31.7 ± 1.6%	26.0 ± 12.0%	28.4 ± 5.2%
AFP	4.3 ± 1.0%	16.9 ± 7.0% #	1.9 ± 0.4%	5.5 ± 4.2%
p63	2.0 ± 0.9%	12.6 ± 4.9% ##	4.8 ± 2.7%	3.5 ± 3.1%

Figure 4.8: Immunocytometry analysis of cell phenotypes within EBs. Cells from dissociated EBs at each culture condition (25, 40, 55, and 0 rpm) were assessed for derivatives of the three germ lineages via immunocytometry at day 12 of differentiation. Histograms of α-sarcomeric actin (A), AFP (B), and p63 (C) are representative of 3 independent flow cytometry runs. Generally, rotary conditions elicited a subtle enhancement of α-sarcomeric actin+ (A,D,E), AFP+ (B,D,F), and p63+ (C,D,G) cell populations compared to static EBs and isotype controls. Additionally, the percentage of AFP+ cells from 25 rpm EBs was significantly higher than 40 rpm EBs, and percentage of p63+ from 25 rpm EBs was greater than either static or 55 rpm conditions (D). The geometric mean of the histograms, also suggested increased populations of α-sarcomeric actin+ cells within 25 rpm EBs compared to static (E) and increased p63+ populations from 25 rpm EBs compared to all other culture conditions (G). n = 3. # = $p \leq 0.05$ compared to 40 rpm, ## = $p \leq 0.05$ compared to static and 55 rpm EBs. * = $p \leq 0.05$, † = $p<0.01$. Modified from Sargent et al. 2010 [36].

Discussion

In this study, the effects of rotary orbital suspension culture speed on cardiomyocyte differentiation within EBs were assessed compared to hanging drop and

static suspension culture methods. Suspension culture of EBs under all rotary orbital conditions for 7 days resulted in a significantly greater frequency of spontaneous contractile EBs than static culture, and the percent of beating EBs was modulated by rotary speed, with slower speeds exhibiting increased contractile percentages (Figures 4.1 & 4.6). Differentiation proceeded within EBs from each formation method, but rotary EBs exhibited significant increases in the expression of genes associated with mesoderm and cardiac differentiation, similar to hanging drops. Rotary orbital culture also increased the proportion of α-sarcomeric actin+ EBs and augmented the relative size of sarcomeric actin+ regions within individual EBs, as well as the percent of α-sarcomeric actin+ cells within rotary EBs as determined by immunocytometric analysis. Additionally, hydrodynamic conditions generated by different rotary orbital speeds influenced the temporal gene expression pattern of differentiation markers, and modulated the relative percentage of cells expressing distinct germ lineage markers (Figures 4.7 & 4.8). These results indicate that rotary orbital suspension culture promotes enhanced cardiomyogenesis of EBs relative to static suspension and slower rotary speeds generate the most pronounced increase of cardiomyogensis, suggesting that not all hydrodynamic environments affect EB differentiation in the same way.

The endogenous yield of cardiomyocytes from spontaneously differentiating ESCs is typically only 1-5% of the total differentiated cell population [23, 42]. It is conventionally accepted that hanging drop culture increases cardiomyogenic differentiation compared to static suspension [30-31, 43], suggesting that the method of EB formation can impact the proportion of cell phenotypes within EBs. Despite these observations, currently there is a lack of direct quantitative comparisons of

cardiomyogenesis between different formation techniques. The 3.5% of α-sarcomeric actin+ cells within static EBs at day 10 of differentiation reported in this study (Figure 4.5) is similar to previous reports of 3.9% sarcomeric myosin+ cells (Mab MF20) at day 9 of differentiation [42] and 2% at day 14 of differentiation [44] from statically cultured EBs using the mouse ESC D3 cell-line. In this study, cardiomyogenic differentiation was enhanced almost 4-fold by hydrodynamic culture conditions created by rotary orbital mixing (40 rpm) compared to static suspension in the same culture vessel. The differences in efficiency of cardiomyocyte differentiation between EB formation methods implicate the ability of microenvironmental conditions to dictate endogenous levels of cell differentiation.

One of the most interesting findings of the present study is that the differentiation of ESCs was modulated by culturing EBs in different hydrodynamic environments. Continuous culture at different rotary orbital speeds affected the relative magnitude of expression of differentiation genes in a temporally dependent manner (Figure 4.7). Interestingly, several significant differences in gene expression were exhibited after the cessation of rotary culture, suggesting that the hydrodynamic environment to which EBs are initially exposed can alter the course of subsequent differentiation (Figure 4.7). In addition to modulating gene expression, the culture of EBs in different hydrodynamic environments changed the relative numbers of differentiated cells constituting each of the different germ lineages (Figure 4.8). Altogether, the aforementioned results demonstrate that hydrodynamic conditions imposed during EB suspension culture can affect the resulting differentiated phenotypes.

Several elements of the microenvironment can simultaneously impact stem cell differentiation including soluble cytokines and nutrients, cell-matrix and cell-cell adhesions, and mechanical forces [45-46]. Co-culture of EBs with endoderm explants and visceral endoderm-like cells or treatment with conditioned media from endoderm cells increases cardiomyogenic differentiation, presumably due to secreted factors [47-49]. Similarly, other directed differentiation techniques rely on exogenous addition of specific soluble factors capable of enhancing cardiomyogenesis of EBs, such as bone morphogenic protein 2 (BMP-2) [47, 50], transforming growth factor beta-1 (TGFβ-1) [50] insulin-like growth factor 1 (IGF-1) [51], and retinoic acid [42, 52], several of which are secreted from developing endoderm. The fact that rotary culture alone promotes cardiomyocyte differentiation of EBs suggests that endogenous production of cardiomyogenic molecules within EBs may be enhanced. Previous studies indicated that rotary orbital culture increased endoderm differentiation [35], thus, rotary orbital suspension culture may promote endoderm derived-cardiomyogenic factors locally within EBs. Rotary suspension, specifically at reduced speeds, may create a "pro-cardiomyogenic" microenvironment within EBs that could potentially be further enhanced by additional supplementation of cardiac-inductive molecules to the culture media.

Genetic modification and physical separation techniques can be used to increase the purity of cardiomyocytes attained from differentiating EBs. For example, the resulting purity of mouse ESC-derived cardiomyocytes can be increased to 70% or greater (from <5% originally) by either positive or negative selection strategies used in conjunction with genetically engineered cell lines [21, 42, 53]. Physical separation of

cells by density centrifugation, such as Percoll gradients, has been used to increase the purity of cardiomyocytes derived from both mouse and human ESCs [26, 53-54]. However, an increase in cell purity does not actually reflect an increase in cell yield derived from ESCs, but rather, simply an enrichment of a particular cell phenotype (i.e. cardiomyocytes) relative to the overall differentiated cell population. As noted previously, the rotary orbital culture method alone can increase the total yield of differentiating cells from EBs compared to static suspension culture inoculated at equivalent starting densities [35]. Based on the present study, rotary culture also endogenously enhances cardiomyocyte differentiation and selection techniques could be easily integrated downstream of rotary orbital suspension culture to further increase the purity, as well as the yield of cardiomyocytes obtained from this method.

Mixing speed is one novel environmental parameter introduced by rotary suspension culture to ESC differentiation. Although, it was previously recognized that rotary orbital shaking promotes initial ESC aggregation and accelerates the kinetics of EB formation compared to static culture and rotational speed further modulation formation kinetics (Chapter 3) [35], the present study indicates that cardiomyocyte development from EBs is also enhanced by rotary culture. Although differences in EB size, agglomeration, and necrotic core formation have been observed within EBs from hanging drop, static, and rotary orbital suspension culture [35], no apparent links between these morphological features and cardiomyocyte differentiation were clearly observed. Hydrodynamic mixing conditions imposed on EBs by rotary culture also introduces fluid shear stresses that may directly impact ESC, and more specifically, cardiovascular differentiation; however, these shear stresses were shown to be mild ($\leq$ 2.5 dyn/cm^2) in at

all rotary speeds examined (Figure 3.7). In contrast to the wealth of studies examining the response of somatic (differentiated) cell types to fluid mechanical forces, very little is known about the characteristics or effects of fluid mechanics that may impact cardiogenesis during early mammalian development. Interestingly, intracardiac flow and the resultant shear forces are required during embryonic development to achieve normal cardiogenesis in zebrafish [55]. Recent work has also demonstrated that differentiating, adherent ESCs exposed to laminar shear stress via a cone-plate viscometer exhibited significant histone modification and subsequent increases in *Mef2c* and α-sarcomeric actin expression [56]. Other stirred suspension systems, including slow turning lateral vessel (STLV) and spinner flask bioreactors, have been used to form EBs and differentiate cardiomyocytes; however only 5.5% of cells were reported to be sarcomeric myosin+ within spinner flask conditions prior to genetic selection [42], and relatively small increases in human cardiomyocyte yield (1.5 – 2 fold > static suspension) were achieved after the implementation of selection methods [57-60]. Although the mechanism remains unclear, hydrodynamic forces created by rotary orbital culture provide a simple, batch-culture system capable of promoting the endogenous cardiomyogenic differentiation of ESCs. Thus, the findings of the present study demonstrate a novel approach for engineering stem cell fate using hydrodynamic conditioning and provide design criteria to implement in the creation of novel bioreactors used to scale-up the production of differentiated cardiomyocytes from stem cells.

References

1. Pasumarthi, K.B. and L.J. Field, *Cardiomyocyte cell cycle regulation.* Circ Res, 2002. 90(10): p. 1044-54.

2. Steinhelper, M.E., N.A. Lanson, Jr., K.P. Dresdner, J.B. Delcarpio, A.L. Wit, W.C. Claycomb, and L.J. Field, *Proliferation in vivo and in culture of differentiated adult atrial cardiomyocytes from transgenic mice.* Am J Physiol, 1990. 259(6 Pt 2): p. H1826-34.

3. Soonpaa, M.H. and L.J. Field, *Survey of studies examining mammalian cardiomyocyte DNA synthesis.* Circ Res, 1998. 83(1): p. 15-26.

4. Weisman, H.F. and B. Healy, *Myocardial infarct expansion, infarct extension, and reinfarction: Pathophysiologic concepts.* Prog Cardiovasc Dis, 1987. 30(2): p. 73-110.

5. Swynghedauw, B., *Molecular mechanisms of myocardial remodeling.* Physiol Rev, 1999. 79(1): p. 215-62.

6. Lutgens, E., M.J. Daemen, E.D. de Muinck, J. Debets, P. Leenders, and J.F. Smits, *Chronic myocardial infarction in the mouse: Cardiac structural and functional changes.* Cardiovasc Res, 1999. 41(3): p. 586-93.

7. Pfeffer, J.M., M.A. Pfeffer, P.J. Fletcher, and E. Braunwald, *Progressive ventricular remodeling in rat with myocardial infarction.* Am J Physiol, 1991. 260(5 Pt 2): p. H1406-14.

8. Pfeffer, M.A. and E. Braunwald, *Ventricular remodeling after myocardial infarction. Experimental observations and clinical implications.* Circulation, 1990. 81(4): p. 1161-72.

9. Dib, N., R.E. Michler, F.D. Pagani, S. Wright, D.J. Kereiakes, R. Lengerich, P. Binkley, D. Buchele, I. Anand, C. Swingen, M.F. Di Carli, J.D. Thomas, W.A. Jaber, S.R. Opie, A. Campbell, P. McCarthy, M. Yeager, V. Dilsizian, B.P. Griffith, R. Korn, S.K. Kreuger, M. Ghazoul, W.R. MacLellan, G. Fonarow, H.J. Eisen, J. Dinsmore, and E. Diethrich, *Safety and feasibility of autologous myoblast transplantation in patients with ischemic cardiomyopathy: Four-year follow-up.* Circulation, 2005. 112(12): p. 1748-55.

10. Menasche, P., A.A. Hagege, J.T. Vilquin, M. Desnos, E. Abergel, B. Pouzet, A. Bel, S. Sarateanu, M. Scorsin, K. Schwartz, P. Bruneval, M. Benbunan, J.P. Marolleau, and D. Duboc, *Autologous skeletal myoblast transplantation for*

severe postinfarction left ventricular dysfunction. J Am Coll Cardiol, 2003. 41(7): p. 1078-83.

11. Perin, E.C., H.F. Dohmann, R. Borojevic, S.A. Silva, A.L. Sousa, C.T. Mesquita, M.I. Rossi, A.C. Carvalho, H.S. Dutra, H.J. Dohmann, G.V. Silva, L. Belem, R. Vivacqua, F.O. Rangel, R. Esporcatte, Y.J. Geng, W.K. Vaughn, J.A. Assad, E.T. Mesquita, and J.T. Willerson, *Transendocardial, autologous bone marrow cell transplantation for severe, chronic ischemic heart failure.* Circulation, 2003. 107(18): p. 2294-302.

12. Siminiak, T., D. Fiszer, O. Jerzykowska, B. Grygielska, N. Rozwadowska, P. Kalmucki, and M. Kurpisz, *Percutaneous trans-coronary-venous transplantation of autologous skeletal myoblasts in the treatment of post-infarction myocardial contractility impairment: The poznan trial.* Eur Heart J, 2005. 26(12): p. 1188-95.

13. Strauer, B.E., M. Brehm, T. Zeus, M. Kostering, A. Hernandez, R.V. Sorg, G. Kogler, and P. Wernet, *Repair of infarcted myocardium by autologous intracoronary mononuclear bone marrow cell transplantation in humans.* Circulation, 2002. 106(15): p. 1913-8.

14. Wollert, K.C., G.P. Meyer, J. Lotz, S. Ringes-Lichtenberg, P. Lippolt, C. Breidenbach, S. Fichtner, T. Korte, B. Hornig, D. Messinger, L. Arseniev, B. Hertenstein, A. Ganser, and H. Drexler, *Intracoronary autologous bone-marrow cell transfer after myocardial infarction: The boost randomised controlled clinical trial.* Lancet, 2004. 364(9429): p. 141-8.

15. Beltrami, A.P., L. Barlucchi, D. Torella, M. Baker, F. Limana, S. Chimenti, H. Kasahara, M. Rota, E. Musso, K. Urbanek, A. Leri, J. Kajstura, B. Nadal-Ginard, and P. Anversa, *Adult cardiac stem cells are multipotent and support myocardial regeneration.* Cell, 2003. 114(6): p. 763-76.

16. Cai, C.L., X. Liang, Y. Shi, P.H. Chu, S.L. Pfaff, J. Chen, and S. Evans, *Isl1 identifies a cardiac progenitor population that proliferates prior to differentiation and contributes a majority of cells to the heart.* Dev Cell, 2003. 5(6): p. 877-89.

17. Laugwitz, K.L., A. Moretti, J. Lam, P. Gruber, Y. Chen, S. Woodard, L.Z. Lin, C.L. Cai, M.M. Lu, M. Reth, O. Platoshyn, J.X. Yuan, S. Evans, and K.R. Chien, *Postnatal isl1+ cardioblasts enter fully differentiated cardiomyocyte lineages.* Nature, 2005. 433(7026): p. 647-53.

18. Torella, D., G.M. Ellison, I. Karakikes, and B. Nadal-Ginard, *Resident cardiac stem cells.* Cell Mol Life Sci, 2007. 64(6): p. 661-73.

19. Hodgson, D.M., A. Behfar, L.V. Zingman, G.C. Kane, C. Perez-Terzic, A.E. Alekseev, M. Puceat, and A. Terzic, *Stable benefit of embryonic stem cell therapy*

in myocardial infarction. Am J Physiol Heart Circ Physiol, 2004. 287(2): p. H471-9.

20. Kehat, I., L. Khimovich, O. Caspi, A. Gepstein, R. Shofti, G. Arbel, I. Huber, J. Satin, J. Itskovitz-Eldor, and L. Gepstein, *Electromechanical integration of cardiomyocytes derived from human embryonic stem cells.* Nat Biotechnol, 2004. 22(10): p. 1282-9.

21. Klug, M.G., M.H. Soonpaa, G.Y. Koh, and L.J. Field, *Genetically selected cardiomyocytes from differentiating embronic stem cells form stable intracardiac grafts.* J Clin Invest, 1996. 98(1): p. 216-24.

22. Xue, T., H.C. Cho, F.G. Akar, S.Y. Tsang, S.P. Jones, E. Marban, G.F. Tomaselli, and R.A. Li, *Functional integration of electrically active cardiac derivatives from genetically engineered human embryonic stem cells with quiescent recipient ventricular cardiomyocytes: Insights into the development of cell-based pacemakers.* Circulation, 2005. 111(1): p. 11-20.

23. Murry, C.E., H. Reinecke, and L.M. Pabon, *Regeneration gaps: Observations on stem cells and cardiac repair.* J Am Coll Cardiol, 2006. 47(9): p. 1777-85.

24. Coucouvanis, E. and G.R. Martin, *Signals for death and survival: A two-step mechanism for cavitation in the vertebrate embryo.* Cell, 1995. 83(2): p. 279-87.

25. Doetschman, T.C., H. Eistetter, M. Katz, W. Schmidt, and R. Kemler, *The in vitro development of blastocyst-derived embryonic stem cell lines: Formation of visceral yolk sac, blood islands and myocardium.* J Embryol Exp Morphol, 1985. 87: p. 27-45.

26. Doevendans, P.A., S.W. Kubalak, R.H. An, D.K. Becker, K.R. Chien, and R.S. Kass, *Differentiation of cardiomyocytes in floating embryoid bodies is comparable to fetal cardiomyocytes.* J Mol Cell Cardiol, 2000. 32(5): p. 839-51.

27. Hopfl, G., M. Gassmann, and I. Desbaillets, *Differentiating embryonic stem cells into embryoid bodies.* Methods Mol Biol, 2004. 254: p. 79-98.

28. Itskovitz-Eldor, J., M. Schuldiner, D. Karsenti, A. Eden, O. Yanuka, M. Amit, H. Soreq, and N. Benvenisty, *Differentiation of human embryonic stem cells into embryoid bodies compromising the three embryonic germ layers.* Mol Med, 2000. 6(2): p. 88-95.

29. Keller, G.M., *In vitro differentiation of embryonic stem cells.* Curr Opin Cell Biol, 1995. 7(6): p. 862-9.

30. Kurosawa, H., *Methods for inducing embryoid body formation: In vitro differentiation system of embryonic stem cells.* J Biosci Bioeng, 2007. 103(5): p. 389-98.

31. Yoon, B.S., S.J. Yoo, J.E. Lee, S. You, H.T. Lee, and H.S. Yoon, *Enhanced differentiation of human embryonic stem cells into cardiomyocytes by combining hanging drop culture and 5-azacytidine treatment.* Differentiation, 2006. 74(4): p. 149-59.

32. Maltsev, V.A., A.M. Wobus, J. Rohwedel, M. Bader, and J. Hescheler, *Cardiomyocytes differentiated in vitro from embryonic stem cells developmentally express cardiac-specific genes and ionic currents.* Circ Res, 1994. 75(2): p. 233-44.

33. Wiese, C., G. Kania, A. Rolletschek, P. Blyszczuk, and A.M. Wobus, *Pluripotency: Capacity for in vitro differentiation of undifferentiated embryonic stem cells.* Methods Mol Biol, 2006. 325: p. 181-205.

34. Dang, S.M., M. Kyba, R. Perlingeiro, G.Q. Daley, and P.W. Zandstra, *Efficiency of embryoid body formation and hematopoietic development from embryonic stem cells in different culture systems.* Biotechnol Bioeng, 2002. 78(4): p. 442-53.

35. Carpenedo, R.L., C.Y. Sargent, and T.C. McDevitt, *Rotary suspension culture enhances the efficiency, yield, and homogeneity of embryoid body differentiation.* Stem Cells, 2007. 25(9): p. 2224-34.

36. Sargent, C.Y., G.Y. Berguig, M.A. Kinney, L.A. Hiatt, R.L. Carpenedo, R.E. Berson, and T.C. McDevitt, *Hydrodynamic modulation of embryonic stem cell differentiation by rotary orbital suspension culture.* Biotechnol Bioeng, 2010. 105(3): p. 611-26.

37. Pfaffl, M.W., *A new mathematical model for relative quantification in real-time rt-pcr.* Nucleic Acids Res, 2001. 29(9): p. e45.

38. Sargent, C.Y., G.Y. Berguig, and T.C. McDevitt, *Cardiomyogenic differentiation of embryoid bodies is promoted by rotary orbital suspension culture.* Tissue Eng Part A, 2009. 15(2): p. 331-342.

39. McDevitt, T.C., M.A. Laflamme, and C.E. Murry, *Proliferation of cardiomyocytes derived from human embryonic stem cells is mediated via the igf/pi 3-kinase/akt signaling pathway.* J Mol Cell Cardiol, 2005. 39(6): p. 865-73.

40. Lobo, M.V., M.I. Arenas, F.J. Alonso, G. Gomez, E. Bazan, C.L. Paino, E. Fernandez, B. Fraile, R. Paniagua, A. Moyano, and E. Caso, *Nestin, a neuroectodermal stem cell marker molecule, is expressed in leydig cells of the*

human testis and in some specific cell types from human testicular tumours. Cell Tissue Res, 2004. 316(3): p. 369-76.

41. Wiese, C., A. Rolletschek, G. Kania, P. Blyszczuk, K.V. Tarasov, Y. Tarasova, R.P. Wersto, K.R. Boheler, and A.M. Wobus, *Nestin expression--a property of multi-lineage progenitor cells?* Cell Mol Life Sci, 2004. 61(19-20): p. 2510-22.

42. Zandstra, P.W., C. Bauwens, T. Yin, Q. Liu, H. Schiller, R. Zweigerdt, K.B. Pasumarthi, and L.J. Field, *Scalable production of embryonic stem cell-derived cardiomyocytes.* Tissue Eng, 2003. 9(4): p. 767-78.

43. Boheler, K.R., J. Czyz, D. Tweedie, H.T. Yang, S.V. Anisimov, and A.M. Wobus, *Differentiation of pluripotent embryonic stem cells into cardiomyocytes.* Circ Res, 2002. 91(3): p. 189-201.

44. Toumadje, A., K. Kusumoto, A. Parton, P. Mericko, L. Dowell, G. Ma, L. Chen, D.W. Barnes, and J.D. Sato, *Pluripotent differentiation in vitro of murine es-d3 embryonic stem cells.* In Vitro Cell Dev Biol Anim, 2003. 39(10): p. 449-53.

45. Engler, A.J., S. Sen, H.L. Sweeney, and D.E. Discher, *Matrix elasticity directs stem cell lineage specification.* Cell, 2006. 126(4): p. 677-89.

46. Metallo, C.M., J.C. Mohr, C.J. Detzel, J.J. Pablo, B.J. Wie, and S.P. Palecek, *Engineering the stem cell microenvironment.* Biotechnol Prog, 2007. 23(1): p. 18-23.

47. Bin, Z., L.G. Sheng, Z.C. Gang, J. Hong, C. Jun, Y. Bo, and S. Hui, *Efficient cardiomyocyte differentiation of embryonic stem cells by bone morphogenetic protein-2 combined with visceral endoderm-like cells.* Cell Biol Int, 2006. 30(10): p. 769-76.

48. Rudy-Reil, D. and J. Lough, *Avian precardiac endoderm/mesoderm induces cardiac myocyte differentiation in murine embryonic stem cells.* Circ Res, 2004. 94(12): p. e107-16.

49. Stary, M., W. Pasteiner, A. Summer, A. Hrdina, A. Eger, and G. Weitzer, *Parietal endoderm secreted sparc promotes early cardiomyogenesis in vitro.* Exp Cell Res, 2005. 310(2): p. 331-43.

50. Behfar, A., L.V. Zingman, D.M. Hodgson, J.M. Rauzier, G.C. Kane, A. Terzic, and M. Puceat, *Stem cell differentiation requires a paracrine pathway in the heart.* FASEB J, 2002. 16(12): p. 1558-66.

51. Sachinidis, A., B.K. Fleischmann, E. Kolossov, M. Wartenberg, H. Sauer, and J. Hescheler, *Cardiac specific differentiation of mouse embryonic stem cells.* Cardiovasc Res, 2003. 58(2): p. 278-91.

52. Wobus, A.M., G. Kaomei, J. Shan, M.C. Wellner, J. Rohwedel, G. Ji, B. Fleischmann, H.A. Katus, J. Hescheler, and W.M. Franz, *Retinoic acid accelerates embryonic stem cell-derived cardiac differentiation and enhances development of ventricular cardiomyocytes.* J Mol Cell Cardiol, 1997. 29(6): p. 1525-39.

53. Muller, M., B.K. Fleischmann, S. Selbert, G.J. Ji, E. Endl, G. Middeler, O.J. Muller, P. Schlenke, S. Frese, A.M. Wobus, J. Hescheler, H.A. Katus, and W.M. Franz, *Selection of ventricular-like cardiomyocytes from es cells in vitro.* FASEB J, 2000. 14(15): p. 2540-8.

54. Xu, C., S. Police, N. Rao, and M.K. Carpenter, *Characterization and enrichment of cardiomyocytes derived from human embryonic stem cells.* Circ Res, 2002. 91(6): p. 501-8.

55. Hove, J.R., *In vivo biofluid dynamic imaging in the developing zebrafish.* Birth Defects Res C Embryo Today, 2004. 72(3): p. 277-89.

56. Illi, B., A. Scopece, S. Nanni, A. Farsetti, L. Morgante, P. Biglioli, M.C. Capogrossi, and C. Gaetano, *Epigenetic histone modification and cardiovascular lineage programming in mouse embryonic stem cells exposed to laminar shear stress.* Circ Res, 2005. 96(5): p. 501-8.

57. Gerecht-Nir, S., S. Cohen, and J. Itskovitz-Eldor, *Bioreactor cultivation enhances the efficiency of human embryoid body (heb) formation and differentiation.* Biotechnol Bioeng, 2004. 86(5): p. 493-502.

58. Schroeder, M., S. Niebruegge, A. Werner, E. Willbold, M. Burg, M. Ruediger, L.J. Field, J. Lehmann, and R. Zweigerdt, *Differentiation and lineage selection of mouse embryonic stem cells in a stirred bench scale bioreactor with automated process control.* Biotechnol Bioeng, 2005. 92(7): p. 920-33.

59. Wang, X., G. Wei, W. Yu, Y. Zhao, X. Yu, and X. Ma, *Scalable producing embryoid bodies by rotary cell culture system and constructing engineered cardiac tissue with es-derived cardiomyocytes in vitro.* Biotechnol Prog, 2006. 22(3): p. 811-8.

60. Niebruegge, S., A. Nehring, H. Bar, M. Schroeder, R. Zweigerdt, and J. Lehmann, *Cardiomyocyte production in mass suspension culture: Embryonic stem cells as a source for great amounts of functional cardiomyocytes.* Tissue Eng Part A, 2008.

CHAPTER 5

CULTURE HYDRODYNAMICS ALTER BETA-CATENIN SIGNALING THEREBY MODULATING DOWNSTREAM EMBRYONIC STEM CELL DIFFERENTIATION

Introduction

Much effort has been made to elucidate mechanisms that regulate embryonic stem cell (ESC) fate decisions since ESCs have the promise of providing therapies for many degenerative and chronic diseases in which the normal tissue is damaged beyond endogenous abilities for repair. Many programming paradigms from embryonic development are conserved within embryonic stem cell differentiation, and embryoid body (EB) differentiation methods are often employed because they mimic some the early signaling events of post-implantation embryos [1]. Beta-catenin signaling is an important pathway active in early embryonic development, aiding in the regulation of embryonic patterning, axis formation, primitive streak formation, and mesoderm differentiation [2-3]. Similarly, in ESCs, β-catenin signaling is required both for maintenance of pluripotency [4-5], as well as self-organization, axis formation, and initial mesoderm differentiation within EBs [6-7]. Two pools of β-catenin are present within cells: 1- β-catenin sequestered within cell adherens junctions, specifically with E-cadherin at the cell membrane [8-10], and 2 – stabilized cytoplasmic β-catenin that can translocate to the nucleus, and associate with T-cell factor/Leukemia enhancer factor (TCF/LEF) to mediate transcription [11-14]. Thus, β-catenin is a central component in

both cell-cell interactions and gene transcription, both of which are highly important in regulating embryonic development and ESC differentiation.

Recent studies in genetically modified mice and mESCs have illustrated that activation of the β-catenin pathway can play both inductive and repressive roles in cardiomyogenesis depending on the temporal aspect of stimulation. Activation of β-catenin by the presence of Wnt during early EB differentiation (between days 2 and 5 of differentiation) increases cardiomyocyte differentiation, while late-stage activation prevents early cardiac committed cells from terminally differentiating into cardiomyocytes [15-16]. The converse is also true; early inhibition of Wnt/β-catenin suppresses cardiac differentiation, while later inhibition increases cardiomyogenesis. It is currently thought that early activation of β-catenin signaling increases the proliferation of early mesoderm and cardiomyocyte progenitors [17-20], but to proceed to more definitive cardiomyocyte differentiation, inhibition of β-catenin signaling is required.

Several methods are commonly used to initiate EB formation, including hanging drop culture, where individual EBs are suspended in small volume media droplets from the lid of Petri dish, static suspension culture, where single cell suspensions of ESCs spontaneously aggregate in non-adherent bacteriological dishes, and more recently hydrodynamic culture, which employs fluid mixing to produce and maintain increased yields of EBs [21-24]. It is widely accepted that methods of EB formation may affect differentiation, as hanging drop culture typically enhances mesoderm development and the contractile phenotype of cells [21-22, 24-25]; however, little is known about the mechanisms responsible for propagating these observed variations. Rotary orbital suspension culture enhances cardiomyocyte differentiation compared to static suspension culture, to similar levels attained within hanging drop culture, while producing larger yields of EBs (Figures 4.1, 4.2, 4.5) [25]. Additionally, the extent of cardiomyogenic differentiation is further modulated by rotary orbital speed (Figures 4.6, 4.7, 4.8) [26],

suggesting that the rotary orbital suspension culture system may provide a model to interrogate potential mechanisms responsible for the regulation of cardiomyocyte differentiation. Interestingly, rotary orbital speeds that resulted in increased formation kinetics (Figure 3.5) also exhibited increased cardiomyocyte differentiation [26].

Due to β-catenin's dual roles in cell-cell contacts mediating EB formation and in transcriptional activity regulating cardiomyocyte differentiation, the object of the present study was to investigate the presence and transcriptional activity of β-catenin within EB formed under static and rotary orbital conditions (25, 40, and 55rpm). A stably transduced luciferase TCF/LEF reporter ESC line was generated to quantitatively assess β-catenin transcription, and immuno-staining for total and dephosphorylated β-catenin was performed in conjunction with immune-blotting of cytoplasmic and nuclear protein fractions to determine the presence and location of β-catenin within differentiating EBs from static and rotary conditions. Additionally, gene expression related to both β-catenin signaling and cardiomyocyte differentiation was analyzed to determine if the changes in presence and location of β-catenin corresponded to alteration of gene expression. The results of this study indicate that the location and phosphorylation state of β-catenin are temporally modulated by hydrodynamic conditions. Additionally, this temporal regulation of β-catenin signaling appears to alter the progression of cardiomyocyte differentiation. These findings provide evidence of a developmentally-relevant, mechanistic pathway that is modulated by hydrodynamic conditions and EB formation methods.

Materials and Methods

Embryonic Stem Cell Culture

Murine ESCs (D3 cell line) were cultured on tissue culture-treated dishes (Corning) pre-adsorbed with gelatin (0.1% solution in diH_2O). Culture media consisted

of Dulbecco's modified Eagle's medium (DMEM) supplemented with 15% fetal bovine serum (Hyclone), 100 U/mL penicillin, 100 ug/mL streptomycin and 0.25 ug/mL amphotericin (Mediatech), 2mM L-glutamine (Mediatech), 1x MEM nonessential amino acid solution (Mediatech), 0.1 mM 2-mercaptoethanol (Fisher Chemical), and 10^3 U/mL of leukemia inhibitory factor (LIF; ESGRO, Chemicon). Cultures were re-fed with fresh media every other day, and passaged at approximately 70% confluence.

Embryoid Body Formation and Culture

Embryoid bodies were formed by inoculating single-suspension ESCs at 2 x 10^5 cells/mL into 100 mm bacteriological grade polystyrene Petri dishes with 10 mL ESC media without LIF. Dishes were incubated at 37°C with 5% CO_2 either statically or placed on rotary orbital shakers (Lab-Line Lab Rotator, Barnstead International) at 25, 40, or 55 rpm to impart hydrodynamic conditions. Rotary speed was calibrated daily to maintain assigned speed. Media was exchanged every two days by collecting the EBs from the dish, allowing them to sediment to the bottom of 15 mL conical tubes, aspirating the old media from the tube and transferring the EBs back to their dish containing fresh media.

Luciferase Transduction

Lenti-viral transduction of D3-line ESCs with a luciferase TCF/LEF reporter construct was used to generate stably transduced ESC clones that induced luciferase expression following β-catenin signaling. Cignal™ TCF/LEF luciferase reporters (SA Biosciences) are replication incompetent, VSV-g pseudotyped lentivirus particles that express both firefly luciferase under the control of a minimal CMV promoter and tandem repeats of the TCF/LEF transcriptional response element (TRE) and puromycin resistance gene under the control of the human phosphoglycerate kinase eukaryotic promoter such that selection for transduced cells can be performed with puromycin treatment. ESCs

were plated at 50,000 cells/well on 0.1% gelatin-coated tissue culture treated 6-well dishes (Corning) and maintained undifferentiated (in the presence of LIF) for 24 hours prior to the introduction of Cignal Lenti vectors.

Stable transduction of D3 ESCs with puromycin resistance and luciferase reporter for TCF/LEF transcription was accomplished by incubating cells with Cignal™ Lenti TCF/LEF vectors at three Multiplicity of Infection (MOI) levels (3, 10, or 25) for 24 hours in the presence of 1 mg/mL polybrene (Sigma) to enhance cellular uptake of the virus [27]. MOI was calculated as the number of transducing units per well divided by the number of cells per well. After 24 hours of incubation with the lentivirus particles, media was exchanged and cells were maintained for 72 hours prior to puromycin selection [27-28]. Seventy-two hours post-transduction 3 µg/mL puromycin (Sigma) was supplemented in the media to select for cells that had incorporated the Cignal Lenti TCF/LEF luciferase gene. Prior to purocymin treatment, a kill curve was generated using non-transduced ESCs treated with 0.5, 1.0, and 3.0 µg/mL puromycin to determine concentrations required for cell death. Surviving cells were cultured in the presence of puromycin for 6 days, at which time 23 individual colonies were selected using cloning rings and 0.05% trypsin-EDTA to detach the colonies and plated onto 0.1% gelatin-coated tissue culture treated 100 mm dishes. The selected clones were cultured for 24 hours to allow for adherence and then were maintained in undifferentiated media supplemented with 3 µg/mL puromycin for an additional 2 weeks. Clones were assessed for luciferase expression via anti-luciferase immunostaining and protein lysate luciferase activity with the Luciferase Assay System (Promega) as well as for the maintenance of alkaline phosphatase activity. The clone with highest expression of luciferase in response to LiCl stimulation was used for further experiments.

Luciferase Activity Quantification

Prior to collection, samples to be used as positive controls were cultured in undifferentiated media supplemented with of 50mM LiCl [4] for 24 hours to inhibit the GSK-3β complex from phosyphorylating beta-catenin, ultimately resulting in increased luciferase expression within transduced cells. Luciferase activity was quantified using the Luciferase Assay System (Promega), according to directions. Briefly, undifferentiated transduced ESCs or EBs were rinsed 3x in PBS, lysed in 0.5mL 1X Cell Culture Lysis Buffer with rotation at 4 °C for 10 minutes, vortexed for 5 seconds, and centrifuged at 10,000 rcf for 5 minutes. The supernant was collected and transferred to a pre-chilled microcentrifuge tube. Twenty microliters of the cell lysate was added to 100 µL of Luciferase Assay Reagent and luminescence was detected using a Femtomaster FB12 luminometer (Zylux Corporation) set for a 2-second delay and 10 second measurement read. Relative light units (RLUs) were normalized to µg DNA per sample as determined by Quant-It PicoGreen assay.

Immuno-staining

ESCs were plated on gelatin-coated tissue culture treated polystyrene cover slips and maintained undifferentiated in the presence of LIF. At ~70% confluence, ESCs were fixed with formalin (4% formaldehyde), rinsed with PBS 3x, permeablized and blocked with 0.05% Triton X-100/2% BSA/PBS solution for 1 hour at room temperature, and incubated overnight at 4°C with polyclonal rabbit anti-β-catenin (Millipore, 1:200) and monoclonal mouse anti-active β-catenin (Millipore, 1:50) specific to dephosphorylated Ser-33 and Thr-41 [29]. Cells were rinsed with PBS 3x, and then incubated with Alexa Fluor 546 conjugated anti-rabbit and Alexa Fluor 488 conjugated anti-mouse (Invitrogen

1:200) for 2 hours at room temperature, rinsed 3x, counterstained with Hoechst, rinsed, mounted and coverslipped. Images were acquired with a laser scanning confocal microscope (Zeiss LSM 510).

Undifferentiated, transduced clones were cultured on gelatin-adsorbed (0.1% gelatin in di H_2O) tissue culture treated polystyrene 6-well dishes. At ~70% confluence, cells were rinsed 3x with PBS, formalin fixed in the wells for 10 minutes, and rinsed again with PBS. Cells were permeabilized and blocked using a 0.05% Triton X-100/2% BSA/PBS solution for 30 minutes at room temperature, incubated with polyclonal goat anti-luciferase (Promega, 1:100) and polyclonal rabbit anti-β-catenin (Millipore, 1:200) for 2 hours at room temperature, rinsed 3x with PBS, and incubated with FITC-conjugated anti-goat secondary antibody (Southern Biotech, 1:200) for 1 hour at room temperature. Cells were again rinsed 3x with PBS, mounted, and coverslipped for imaging using a Nikon TE 2000 inverted microscope (Nikon Inc.) with a SpotFlex camera (Diagnostic Instruments).

Alkaline Phosphatase Staining

Undifferentiated ESCs were cultured on 0.1% gelatin-adsorbed tissue culture treated polystyrene 6- well dishes, and at ~70% confluence cells were fixed and stained for alkaline phosphatase activity using the Sigma 86C kit. Briefly, were rinsed 3x with PBS and fixed with 25% Citrate Buffer/63% Acetone/12% Formaldehyde solution for 10 minutes at room temperature. After fixation, cells were rinsed with diH_2O 3x, and fast blue base-alkaline solution was added to allow color development for 15 minutes at room temperature protected from light. Following color development, cells were rinsed 3x in diH_2O, mounted and coverslipped. Images were captured using brightfield settings on a

Nikon TE 2000 inverted microscope (Nikon Inc.) with a SpotFlex camera (Diagnostic Instruments).

Whole-mount Embryoid Body Immuno-staining

Embryoid bodies were collected by sedimentation at days 1, 2, 4, and 7 of differentiation, rinsed 3x with PBS, and formalin (4% formaldehyde) fixed at room temperature for 45 minutes with rotation. EBs were then rinsed 3x (5 minutes with rotation) in EB wash/block buffer (2% BSA/0.1% Tween-20 in PBS) and permeabilized in 0.05% Triton X-100 and 2% BSA solution for 1 hour at 4°C with rotation. EBs were re-fixed in formalin for 15 minutes and blocked in wash/block buffer for 2 hours at 4°C with rotation. After permeablization and blocking, EBs were incubated with polyclonal rabbit anti-β-catenin (Millipore, 1:200) and monoclonal mouse anti-Active β-catenin (anti-ABC, Millipore, 1:50) or with polyclonal anti-β-catenin (Millipore, 1:200) and monoclonal rat anti-E-cadherin (Sigma, 1:200) at 4°C overnight with rotation, rinsed 3x in wash buffer, and incubated with secondary antibodies (Alex Fluor 488 anti-rabbit and Alexa Fluor 546 anti-mouse, Invitrogen, 1:200) for 4 hours at 4°C with rotation. EBs were rinsed in wash buffer 3x, counterstained with Hoechst (10 min at 4°C with rotation), rinsed again 3x, and imaged with a laser scanning confocal microscope (Zeiss LSM 510). Images were acquired at equal settings across all samples as sets of Z-stacks and slices ~16 to 22 μm deep are shown.

Protein Fractionation

Undifferentiated ESCs (with or without LiCl stimulation) and EBs were collected at days 1, 2, 3, and 4 of differentiation for protein collection and western blot analysis. The NE-PER cell fractionation kit (Pierce) was used to separate the cytoplasmic and

nuclear fractions of undifferentiated cells and differentiating EBs. Briefly, cells and EBs were rinsed 3x in ice cold PBS and first lysed with ice cold CER I reagent supplemented with 500x protease inhibitor cocktail (Calbiochem 535140) and 50x phosphatase inhibitor cocktail (Calbiochecm 524629). Lysate solutions were transferred to pre-chilled microcentrifuge tubes, vortexed for 15 sec, and placed on ice for 10 minutes. CER II reagent was then added, samples were vortexed again for 15 seconds and then centrifuged at 16,000x g for 10 minutes at 4°C. The supernatant containing the cytoplasmic fraction was transferred to pre-chilled microcentrifuge tubes and stored at -80°C. The nuclear pellet was rinsed in ice cold PBS, incubated on ice with the NER reagent containing 500x protease and 50x phosphatase inhibitor cocktail, vortexed for 15 seconds every 10 minutes for 40 minutes, and centrifuged at 16,000x g for 10 minutes at 4°C. The supernatant containing the nuclear fraction was transferred to pre-chilled microcentrifuge tubes and stored at -80°C.

Electrophoresis

Sample protein concentration was determined using the BCA Protein Quantification kit (Pierce); equal amounts of protein (10 µg) per sample were mixed with loading buffer (0.1 M Tris-HCl containing SDS, glycerol, biomophenol blue, and 2-mercaptoethanol), incubated at 95°C for 5 minutes, and loaded in 10% Tris-HCl polyacrylamide precast gels (Bio-Rad). Vertical electrophoresis was performed using the Mini-PROTEAN Treta Cell (Bio-Rad) system with SDS/PAGE running buffer (Tris base/glycine/SDS solution) run at 100V for 1 hour to separate the protein samples by molecular weight. A protein ladder (Precision Plus Protein Kaleidoscope, 10-250kD, Bio-Rad) was also loaded into each gel as a reference for protein products.

Immuno-blotting and Densitometry

Following SDS/PAGE separation, gels were removed from the electrophoresis tank, equilibrated in cold transfer buffer (Tris base/glycine/methanol solution), and loaded into transfer cassettes. Gels were placed directly beside a PVDF membrane (Immobilon-P, Millipore) and sandwiched between filter paper within the cassettes to allow for protein transfer from the gel onto the PVDF membrane. Protein transfer was run in transfer buffer overnight at 4°C with 30V. Once protein transfer was complete, membranes were removed and equilibrated in PBS prior to immunostaining. Blots were stained using the Snap ID system (Bio-Rad). Membranes were placed in Snap ID blot holders, and Near Infrared blocking medium (30 mL per well, Rockland Immunochemicals) was pulled through the well by vacuum. Membranes were then incubated with anti-β-catenin (1:200), anti-ABC (1:100), and anti-β-actin (loading control, Rockland Immunochemicals, 1:300) for 1 hour at room temperature before being pulled through by vacuum. Primary antibody incubation was followed by continuous vacuum rinse with 0.01% Tween-20/PBS solution, and membranes were incubated with IR secondary antibodies (680 anti-mouse and 800 anti-rabbit, LiCor Biosciences, 1:2500), followed by continuous vacuum rinse with 30 mL PBS/0.1% Tween-20 solution. Stained membranes were removed from the staining wells and rinsed 2 more times in PBS with gentle rocking for 10 minutes at room temperature. Blots were imaged using the Odyssey Infrared imager (LiCor Biosciences) for dual secondary visualization.

Blot images were converted to grayscale to obtain black protein bands on a white background for densitometry analysis using Scion Image (Windows version of NIH image, ScionCorp). Bands corresponding to the molecular weights of β-catenin (92 kD)

and β-actin (42 kD) were digitally cut from the blot image, opened in Scion image, and run with the Gelplot2 macro (standard macro in Scion Image) to generate plots corresponding to band intensity. Area under the curve for each β-catenin band plot was calculated and normalized to the corresponding calculated intensity of β-actin to semi-quantitatively represent the relative amount of β-catenin present in each sample.

Quantitative PCR Analysis

Total RNA was extracted from undifferentiated ESCs prior to differentiation and from EBs at days 2, 4, 6, 8, and 10 of differentiation using the RNeasy Mini kit (Qiagen Incorporated, Valencia, CA). Reverse transcription for complementary DNA synthesis was performed from 1 µg RNA using the iScript cDNA synthesis kit (Bio-Rad, Hercules, CA), and quantitative PCR was performed with SYBR green technology on the MyiQ cycler (Bio-Rad). Primers sequences and annealing temperatures are listed in Table 5.1 for *Wnt-1*, *Wnt-3a*, *Dickkopf-1* (*Dkk-1*), *Brachyury T* (*B-T*), *mesoderm posterior 1* (*Mesp-1*), *myocyte enhancer factor-2c* (*Mef-2c*), *Nkx2.5*, *α-myosin heavy chain* (*α-MHC*), *myosin light chain-2 ventricle* (*MLC-2v*), and *18S ribosome*. Each primer set was designed with either Beacon Designer software (Invitrogen, Carlsbad, CA) (*B-T, Mesp-1, Mef-2c, α-MHC, and MLC-2v)* or the Integrated DNA technologies INC design website (www.idtdna.com) (*Wnt11, Wnt3a, Dkk-1, Nkx2.5*) and validated with appropriate cell controls. Absolute gene expression concentrations were calculated against standard curves and represented per µg RNA. All samples contained equivalent concentrations of 18S expression, indicating that all PCR reactions ran equally across samples.

Table 5.1: Primer sequences and annealing temperatures.

Gene	Forward sequence	Reverse sequence	Temp.
Wnt 11	AGG GTG AGG ACA GAC GTC TTG AAA	TGG CTG TGC TGT AAG AAT GTC CCT	57.9 °C
Wnt3a	GTC TTC TGC CTG GAA CTT TGC GTT	TGT CTA AAT CCA GTG GTG GGT GGA	57 °C
Dkk1	GCG GCA GCT GTC CGG TTC TT	GAG AAC TCC CGG CGC CAC AC	58 °C
B-T	GAC TCC AGC CTT CCT TCC	CAC ACC ACT GAC GCA CAC	56.5 °C
Mesp1	GAC CCA TCG TTC CTG TAC	CTG AAG AGC GGA GAT GAG	56.5 °C
Mef2c	CCC AAT CTT CTG CCA CTG	GGT TGC CGT ATC CAT TCC	57 °C
Nkx2.5	ATG CCC TGT CCC TCA GAT TTC ACA	AAG TGG GAT GGA TCG GAG AAA GGT	60.5 °C
α-MHC	GGT CCA CAT TCT TCA GGA TTC TC	GCG TTC CTT CTC TGA CTT TCG	58 °C
MLC-2v	GAC CAT TCT CAA CGC ATT CAA G	CTT CTC CGT GGG TAA TGA TGT G	56.5 °C
18S	CTC TAG TGA TCC CTG AGA AGT TCC	ACT CGC TCC ACC TCA TCC TC	58 °C

Statistical Analysis

Experimental conditions were examined with triplicate samples in independent experiments and data values presented reflect the mean value ± standard deviation. Analysis of variance was performed to determine statistical significance ($p<0.05$) between experimental groups, and where significant, was followed by post-hoc Tukey analysis to define statistical differences ($p<0.05$) between specific experimental variables.

Results

Embryonic Stem Cells and Embryoid Bodies Express β-catenin

Embryonic stem cell colonies maintained in an undifferentiated state exhibited positive staining for β-catenin (Figure 5.1 A). The presence of β-catenin appeared mainly intercellular, presumably on the cell membrane, but some intrecellular staining was noted, in agreement with previous studies indicating low levels of β-catenin are required to maintain the undifferentiated state of ESCs [4]. Additionally, β-catenin was expressed by differentiating ESCs within EBs; again, the appearance of β-catenin was mainly at the cell membrane and co-localized with membrane cell adhesion protein E-cadherin (Figure 5.1 B). Both ESCs and EBs expressed β-catenin at the cell membrane, suggesting that β-catenin is involved with cell-cell adhesion through E-cadherin, but β-catenin can also be involved with transcription regulation when it translocated to the nucleus.

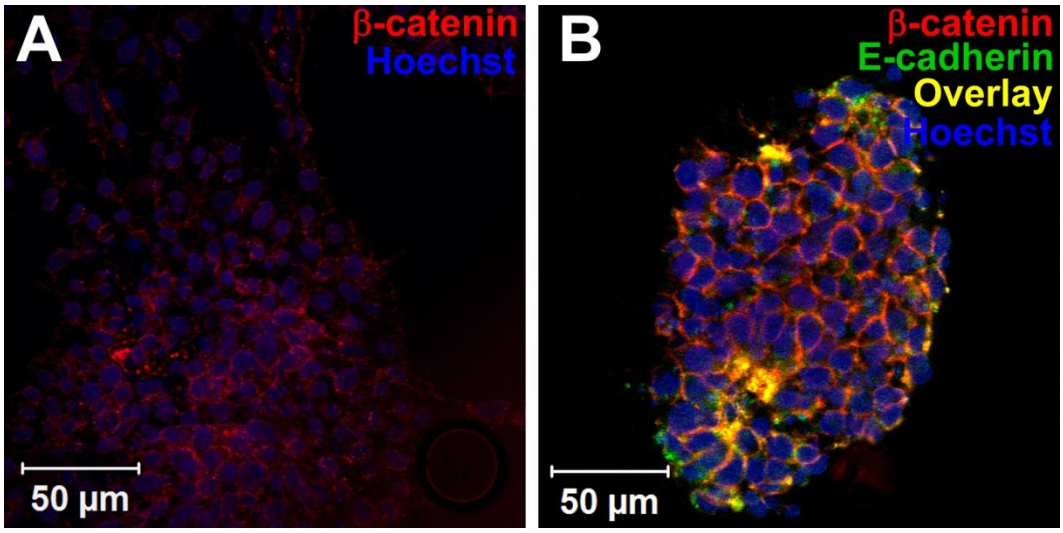

Figure 5.1: β-catenin expression within ESCs and EBs. Undifferentiated ESCs (A) exhibited β-catenin+ staining mainly between cells at the cell membrane. β-cateinin expression was maintained upon EB formation, and localized on the cell membrane with adhesion protein E-cadherin. Red = β-cateinin, Green = E=cadherin, Yellow = β-cateinin/E-cadherin overlay, Blue = Nuclei. Scale bar = 50 µm.

Luciferase Transduction

To address whether β-catenin is also present as a regulator of transcription, studies were completed examining levels of luciferase reporter in transduced ESCs. Embryonic stem cells retained typical morphological appearance 24 hours after incubation with Cignal™ TCF/LEF Lenti particles at all MOI levels examined (Figure 5.2 A-C). However, after treatment with puromycin for selection of transduced cells, only ESCs from 10 and 25 MOI remained (Figure 5.2 D-F). After selection with puromycin for one week, a total of 23 colonies were selected and clonally maintained in the presence of puromycin for an additional 6 days to ensure stable transduction.

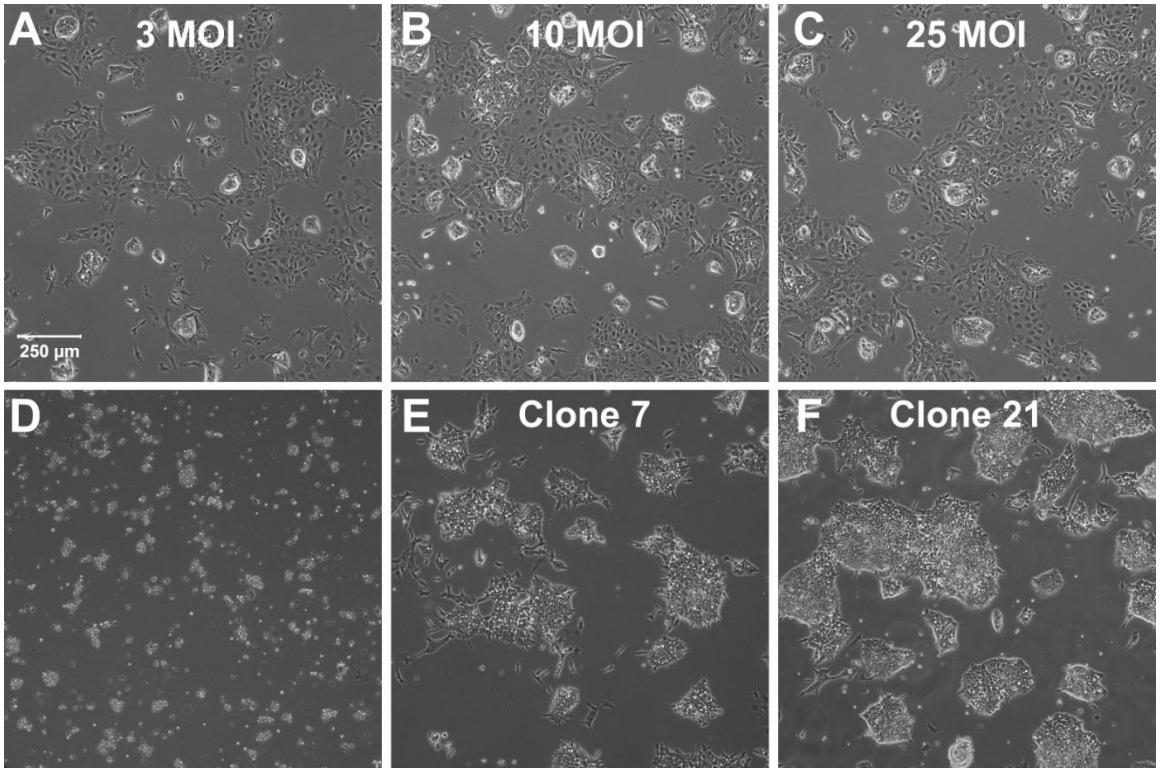

Figure 5.2: ESC transduction. ESCs were incubated with lenti particles containing the luciferase TCF/LEF reporter construct for 24 hours at 3 (A), 10 (B), and 25 (C) MOI. Selection with puromycin resulted in no transduced colonies from 3 MOI (D), but colonies from 10 MOI (E) and 25 MOI (F) remained after 1 week of puromycin treatment. Scale bar = 250 µm.

These 23 clones were assessed for morphological appearance, alkaline phosphatase activity (indicative of undifferentiated embryonic stem cells), luciferase expression, and ability to form embryoid bodies. Of the 23 clones, 13 were excluded due to changes in growth rate (either increased or reduced doubling times compared to non-transduced ESCs) or a differentiated appearance during culture. The 10 remaining clones were stained for alkaline phosphatase (Figure 5.3 A&C) and luciferase protein (Figure 5.3 B&D). All clones exhibited positive alkaline phosphatase staining, but only 2 of the 10 clones stained positive for luciferase, and clone 7 (C7) appeared to contain increased positive staining compared to clone 21 (C21). Additionally, C7 cells exhibited the highest level of luciferase activity upon LiCl treatment (exogenous stimulation of β-catenin regulated transcription) compared to C21, while both C7 and C21 cells displayed increased luciferase activity compared to non-transduced ESCs (which were similar to background levels) (Figure 5.3 E). Again, the low occurrence of luciferase expression without LiCl treatment is consistent with the fact that ESCs maintain low levels of β-catenin regulated transcription in their undifferentiated state [4]. All clones also formed EBs similar in size and appearance to EBs formed from non-transduced ESCs at various rotary speeds and static conditions (represented by C7, Figure 5.4 A-D). The sum of these results indicate that C7 and C21 stably transduced ESCs maintained their undifferentiated state and ability to form EBs while expressing the luciferase reporter in response to activation of the β-catenin pathway. Since C7 exhibited higher luciferase activity compared to C21, experiments examining the response of the β-catenin pathway to hydrodynamic conditions were performed with the C7 ESCs.

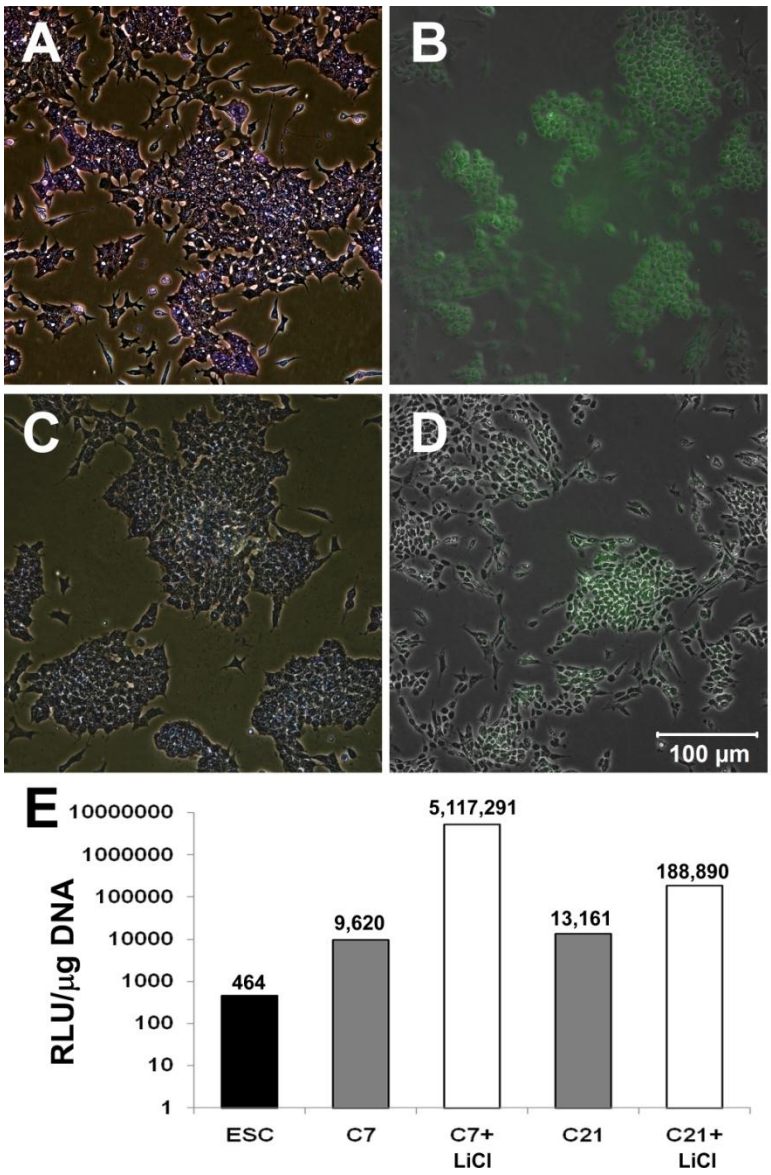

Figure 5.3: Luciferase expression within transduced ESCs. Transduced clones C7 and C21 maintained alkaline phosphatase activity (A&C) and exhibited luciferase+ staining (B&D) when maintained in an undifferentiated state. C7 and C21 cells also exhibited increased luciferase activity compared to non-transduced ESCs, and upon 50 mM LiCl stimulation, C7 cells exhibited the highest levels of luciferase activity (E). Scale bar = 100 µm.

Luciferase Expression is Altered via Hydrodynamic Conditions

Embryoid bodies were formed with a single-cell suspension of C7 ESCs at 2 x 10^5 cells/mL in 100 mm dishes with 10 mL media and cultured statically or under rotary orbital conditions at 25, 40, or 55 rpm (Figure 5.4 A-D). At days 2, 3, 4, and 6 of differentiation, EBs were collected and protein was harvested for luciferase activity analysis (Figure 5.4 E). After 2 days of EB differentiation, static and 25 rpm EBs exhibited the greatest amount of luciferase activity compared to 40 and 55 rpm ($p \leq 0.05$). By day 3, EBs from all rotary conditions had increased amounts of luciferase compared to static ($p \leq 0.05$), and 25 rpm EBs expressed significantly more luciferase than the other rotary conditions ($p \leq 0.05$). Although EBs from rotary orbital culture

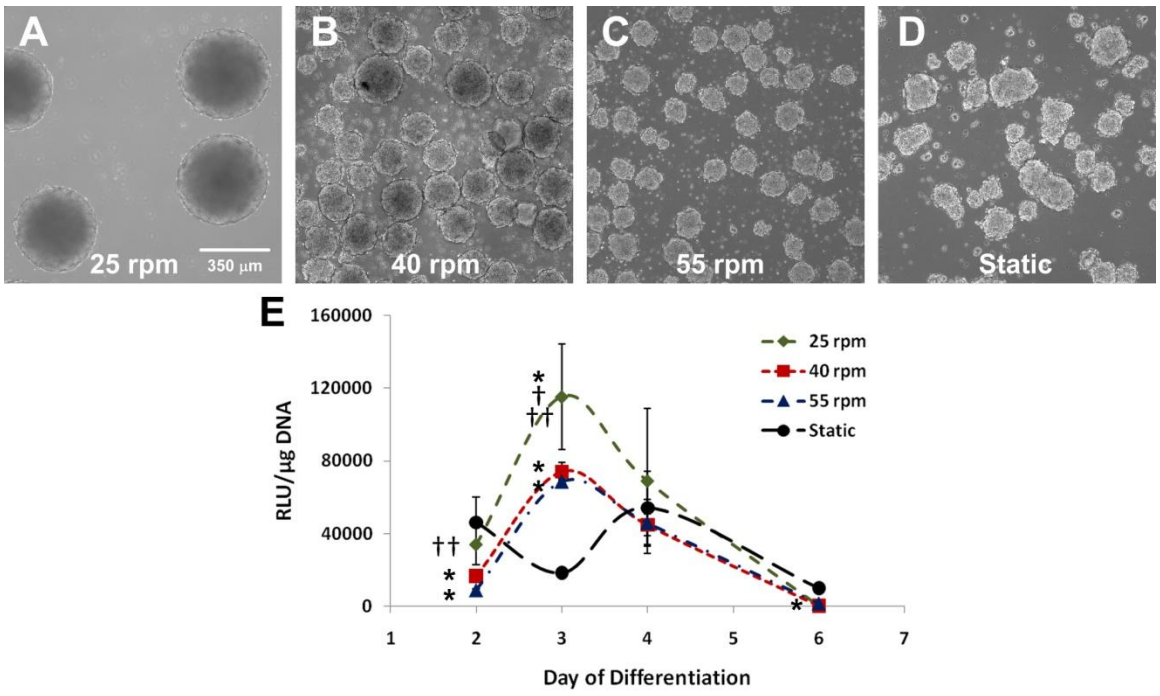

Figure 5.4: Luciferase expression in differentiating EBs. C7 ESCs formed EBs at rotary and static conditions (Day 3, A-D). Culture conditions modulated luciferase expression (E), and EBs from rotary conditions exhibited increased luciferase activity compared to static EBs, with 25 rpm generating the largest increase in luciferase expression from EBs. Scale bar = 350 µm, n = 3, $p \leq 0.05$, * = compared to static, ** = compared to 25 rpm, † = compared to 40 rpm, and †† = compared to 55 rpm.

increased luciferase expression from day 2 to day 3, static EBs exhibited a decrease in luciferase between days 2 and 3 of differentiation (Figure 5.4 E). At day 4 of differentiation, luciferase activity within EBs from all rotary orbital culture decreased from day 3, while expression within static EBs increased compared to day 3; however, there was no significant difference in expression levels between the culture conditions. Within 6 days of differentiation, luciferase activity from all EBs had decreased to below initial day 2 levels, but static EBs maintained more luciferase expression than any of the rotary orbital conditions ($p \leq 0.05$) (Figure 5.4 E). These results indicate through expression of the TCF/LEF luciferase reporter that β-catenin regulated transcription is most active within the first 4 days of differentiation and is differentially modulated due to EB culture conditions. Rotary orbital culture appears to increase β-catenin transcription compared to static with 25 rpm rotary orbital culture resulting in the highest level of β-catenin transcription.

Hydrodynamics Affect the Temporal and Spatial Expression β-catenin

To confirm the presence of signaling active β-catenin (dephosphorylated) within cells of differentiating EBs from static and rotary conditions (25, 40, and 55 rpm) and to visualize the location of β-catenin, whole-mount immunostaining for both total (β-catenin+, red in Figure 5.5) and dephosphorylated β-catenin (ABC+, green in Figure 5.5) was performed at days 1, 2, 4, and 7 of differentiation since studies with transduced cells indicated that β-catenin transcription was most active at early time points of differentiation. In general, differences in staining intensity and location were observed between EB culture conditions and were temporally regulated (Figure 5.5). Static EBs exhibited less spatial regulation compared to rotary conditions, represented by less

specific ABC+ staining appearance with time (Figure 5.5 A,E,&I), especially at day 2 of differentiation. EBs from rotary orbital suspension culture on the other hand, appeared to exhibit tightly regulated expression patterns of β-catenin+ and ABC+ cells, distinctly located within the nucleus or at the cell membrane (Figure 5.5, B-D, F-H, J-L, N-P). The nuclear location of ABC+ staining implies potential regulation of β-catenin controlled transcription events, while the intercellular location of β-catenin, presumably with E-cadherin, indicates less availability for transcriptional regulation.

EBs from static conditions exhibited some nuclear expression of ABC+ cells at day 1 of differentiation (Figure 5.5 A, inset), accompanied by intercellular β-catenin+ staining at the cell membrane. At day 2, static EBs appeared to maintain expression of ABC within cells, but with less regulation over location (nuclear or cytoplasmic) (Figure 5.5 E, inset), and by day 4, the majority of β-catenin expression (dephosphorylated or not) appeared to be limited to the cell membrane (evidenced by yellow appearance, Figure 5.5 I) and reduced within in the nucleus (Figure 5.5 I, inset). EBs from 25 rpm rotary conditions appeared to contain the greatest number of cells with ABC+ nuclear staining at day 1 of differentiation (Figure 5.5 B, inset) compared to either static or other rotary conditions (40 and 55 rpm, Figure 5.5 A,C,D, insets), and also exhibited distinct intercellular β-catenin+ staining at the cell membrane. The increased nuclear location of ABC+ staining suggests increased levels of β-catenin regulated transcription and is in agreement with the increased luciferase protein expression exhibited by 25 rpm EBs compared to other rotary conditions at days 2 and 3 of differentiation (Figure 5.4 E). By day 2, however, less nuclear ABC+ was observed within 25 rpm EBs (Figure 5.5 F, inset), and ABC+ staining appeared to be sequestered at the cell membrane (Figure 5.5 F,

yellow staining). Again, a change in location of ABC+ staining within 25 rpm EBs was noted at day 4 of differentiation with the reappearance of ABC+ nuclei, accompanying the presence of ABC+ staining at the cell membrane (Figure 5.5 J), suggesting potential over-lapping regulation between nuclear and membrane-bound β-catenin. Similar to 25 rpm expression patterns of ABC+ staining, 40 rpm EBs also exhibited nuclear ABC+ staining at day 1 of differentiation (Figure 5.5 C, inset), although to a lesser extent than 25 rpm EBs. At day 2 of differentiation, ABC+ staining appeared to be mostly at the cell membrane (Figure 5.5 G, yellow staining), and by day 4, ABC+ staining was again observed within the nucleus in addition to the cell membrane of 40 rpm EBs (Figure 5.5 K). In general 55 rpm EBs appeared to exhibit little if any ABC+ staining, and the majority of β-catenin+ staining was restricted to the cell membrane at days 1, 2, and 4 of differentiation (Figure 5.5 D,H,L). However, at day 7 of differentiation, 55 rpm EBs contained mainly intercellular ABC+ staining (Figure 5.5 P, yellow/green appearance). Indeed, at day 7 of differentiation little to no nuclear staining of β-catenin was observed in any of the culture conditions (Figure 5.5 M-P), suggesting that transcriptional responses governed by β-catenin are diminished by day 7 of differentiation. This observation is in agreement with the reduction of luciferase activity exhibited by EBs from all culture conditions at day 6 of differentiation (Figure 5.4 E). In total, the assessment of β-catenin staining within differentiating EBs indicates that rotary culture conditions may modulate both the phosphorylation state and location of β-catenin, and therefore may alter the gene expression profile of differentiating cells.

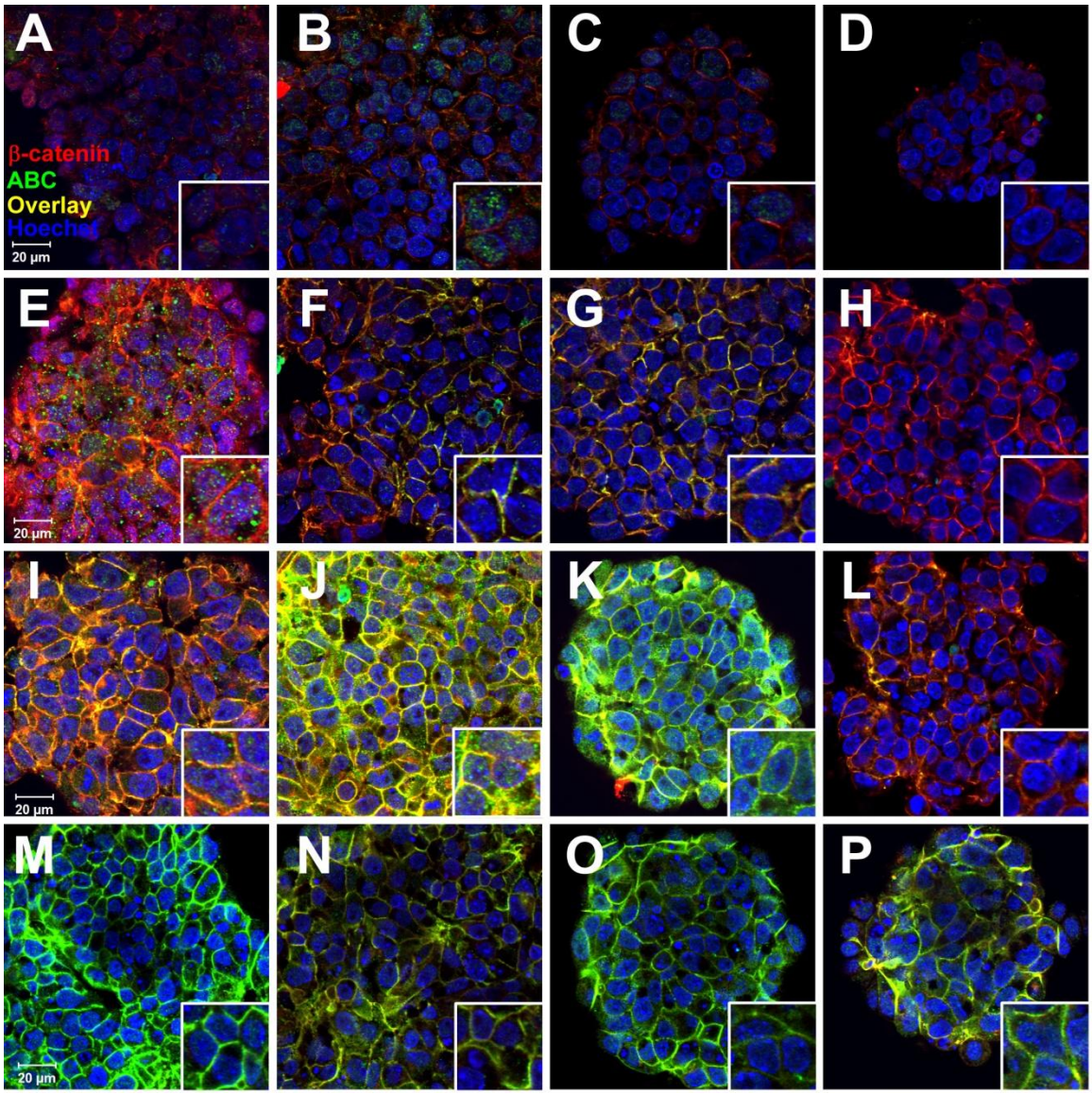

Figure 5.5: Location and phosphorylation state of β-catenin. Static (A,E,I,M) and rotary EBs at 25 (B,F,J,N), 40 (C,G,K,O), and 55 rpm (D,H,L,P) were stained for β-catenin+ and ABC+ cells at days 1 (A-D), 2 (F-H), 4 (I-L), and 7 (M-P) of differentiation. Differences in the staining patterns of β-catenin were observed between culture conditions and time point examined, suggesting that β-catenin phosphorylation and location may be regulated by hydrodynamic conditions. Scale bar = 20 μm. Red = β-catenin, Green = ABC, Yellow = β-catenin/ABC overlay, Blue = Nuclei

The phosphorylation state and location of β-catenin were further confirmed by western blot analysis of cytoplasmic and nuclear protein fractions from static and rotary

(25, 40, and 55 rpm) EBs at days 1, 2, 3, and 4 of differentiation (Figure 5.6 A,D). Densitometry analysis was used to semi-quantitatively compare total and dephosphorylated β-catenin expression within the cytoplasmic and nuclear fractions and expression levels were normalized to β-actin expression in each sample (Figure 5.6 B,C,E,F). EBs from all conditions expressed β-catenin in both the cytoplasm and nucleus at time points examined (Figure 5.6 A); however, the presence of dephosphorylated β-catenin in the nucleus was not observed at all time points (Figure 5.6 D). The largest fluctuations of total β-catenin expression were exhibited within 25 rpm EBs over the first 4 days of differentiation (Figure 5.6 B&C). Additionally, expression levels of dephosphorylated β-catenin (ABC) changed with time in both the cytoplasmic and nuclear fractions of 25 rpm EBs (Figure 5.6 E,F), with similar expression patterns to those observed by confocal staining (Figure 5.5 B,F,J). Compared to other culture conditions, 25 rpm appeared to exhibit the most total and dephosphorylated β-catenin from days 2 to 4 of differentiation. EBs from 40 rpm rotary culture exhibited similar cytoplasmic expression patterns of total and dephosphorylated β-catenin to EBs from 25 rpm but with somewhat reduced levels, and 55 rpm EBs also maintained similar trends, but with the lowest expression levels (Figure 5.6 B&E). EBs from static conditions expressed similar trends of total β-catenin and ABC in the cytoplasm, but levels were consistently lower than those from rotary conditions (Figure 5.6 B,E). Total β-catenin was expressed at relatively consistent levels within the nucleus of 40 rpm EBs between days 1 and 2 of differentiation before decreasing slightly at days 3 and 4 (Figure 5.6 C). Similarly, dephosphorylated levels of nuclear β-catenin in 40 rpm EBs were highest at day 1 of differentiation, then dropped slightly and were maintained between days 2 and 3

before decreasing again at day 4 (Figure 5.6 F). EBs from 55 rpm conditions expressed the least nuclear β-catenin of the culture conditions, whether dephosphorylated or not (Figure 5.6 C&F). Interestingly, within all conditions except 55 rpm and static, increased total or dephosphorylated β-catenin in the cytoplasm were accompanied by decreased expression in the nucleus and vice versa (note expression levels from days 2 and 3 of 25 and 40 rpm, Figure 5.6 B,C,E,F), thus indicative of a link between β-catenin bound at the membrane and the level of β-catenin available for transcriptional regulation.

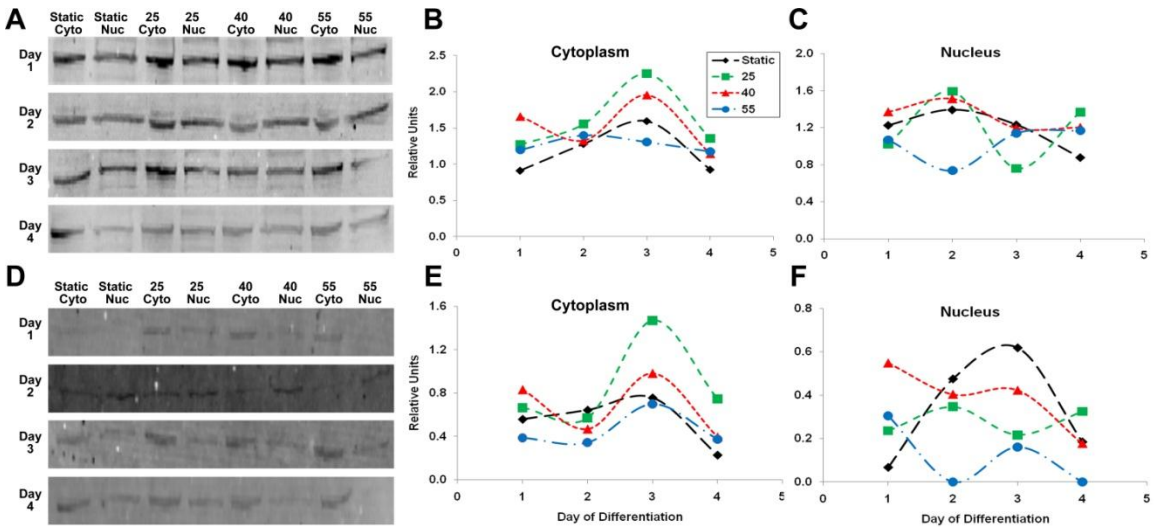

Figure 5.6: Western blot analysis of β-catenin expression. Cytoplasmic and nuclear protein fractions from static and rotary (25, 40, 55 rpm) EBs were collected at days 1, 2, 3, and 4 of differentiation for western blot analysis. Total (A) and dephosphorylated (D) β-catenin were immune-blotted and densitometry analysis was performed to compare expression levels of total β-catenin (B,C) and dephosphorylated β-catenin (E,F) with time between culture conditions.

Hydrodynamic Conditions Alter Expression of β-catenin-Related Genes

The combined results of β-catenin expression and location and luciferease activity suggested that regulation and availability of signaling active β-catenin by hydrodynamic conditions may alter transcription patterns within differentiating ESCs. Gene expression

levels of β-catenin-related genes were examined to assess if the changes in β-catenin expression corresponded with the modulation of gene profile patterns from EBs cultured under hydrodynamic conditions. Examination of *Wnt11*, a non-canonical Wnt that does act through β-catenin, and *Wnt3a*, a canonical Wnt implicated in early mesoderm and cardiac progenitor induction, revealed similar expression patterns (Figure 5.7 A,B). At day 2 of differentiation EBs from all culture conditions express equivilant amounts of both *Wnt11* and *Wnt3a*, but with continued culture, differences in *Wnt* expression emerge between culture conditions. Statically cultured EBs appeared to maintain similar levels of *Wnt11* and *Wnt3a* expression throughout the 8-day culture period (Figure 5.7 A,B). However, at day 4 of differentiation, 25 rpm EBs significantly decreased *Wnt11* expression compared to static and 55 rpm ($p \leq 0.05$, 0.01) and *Wnt3a* expression compared to 55 rpm ($p \leq 0.05$). At day 6 of differentiation, 40 rpm EBs exhibited increased *Wnt11* and *Wnt3a* expression levels compared to all other conditions ($p \leq 0.05$) (Figure 5.7 A,B). Interestingly, expression of *Dkk-1*, a canonical Wnt inhibitor, increased in 25 rpm EBs at day 4 compared to static and 55 rpm EBs ($p \leq 0.01$, 0.05) corresponding to the decrease in *Wnt* expression levels (Figure 5.7 A,B,C). In fact *Dkk-1* expression increased in all rotary conditions compared to static culture at day 4 of differentiation ($p \leq 0.05$), and static EBs exhibited less *Dkk-1* expression throughout the 8 day time course (Figure 5.7 C).

Expression of *brachyury T* (*B-T*), an early marker of mesoderm differentiation and associated with primitive streak formation, was increased significantly at day 2 of differentiation within 25 rpm EBs compared to all other culture conditions ($p \leq 0.05$), followed by increased expression at day 4 in all rotary conditions compared to static

culture ($p \leq 0.01$). Early mesoderm differentiation within ESCs requires β-catenin directed transcriptional events [6], and *mesoderm posterior 1* (*Mesp-I*) is a direct target of TCF/LEF regulated transcription [30]. Interestingly, 25 rpm EBs also exhibited the earliest increase in *Mesp-1* expression levels at day 4 of differentiation compared to all other culture conditions ($p \leq 0.001$); however, by 6 of differentiation this increase was diminished and expression levels between rotary and static conditions were not significant due to high variability of expression levels within static culture. Increased variability of expression levels within static EBs was common in several genes examined (Figure 5.7 D,E,,F).

Wnt/β-catenin signaling is not only required for early mesoderm differentiation but is also necessary of the differentiation of cardiomyocyte progenitor cells in development and within differentiating ESCs [15, 17, 19]. *Myocyte enhancer 2c* (*Mef-2c*) and *Nkx2.5* are early markers of cardiomyocyte progenitors and their expression levels were also modulated by hydrodynamic conditions (Figure 5.7 G,H). At day 4 of differentiation, *Mef-2c* expression was increased within 25 rpm EBs compared to static EBs ($p \leq 0.05$), and increased expression levels were maintained within 25 rpm EBs compared to all other culture conditions at day 10 of differentiation ($p \leq 0.01$). Likewise, 25 rpm EBs also expressed increased levels of *Nkx2.5* at day 6 of differentiation compared to static EBs ($p \leq 0.01$), and maintained increased expression levels at day 10 compared to other conditions ($p \leq 0.005$), similar to previously reported results (Sargent et al 2009 [25], Figure 4.7 D). Additionally at day 6, all rotary conditions expressed significantly more *Nkx2.5* than static ($p \leq 0.05$). Although β-catenin signaling is required for cardiomyocyte progenitor differentiation, continued Wnt activation of β-catenin

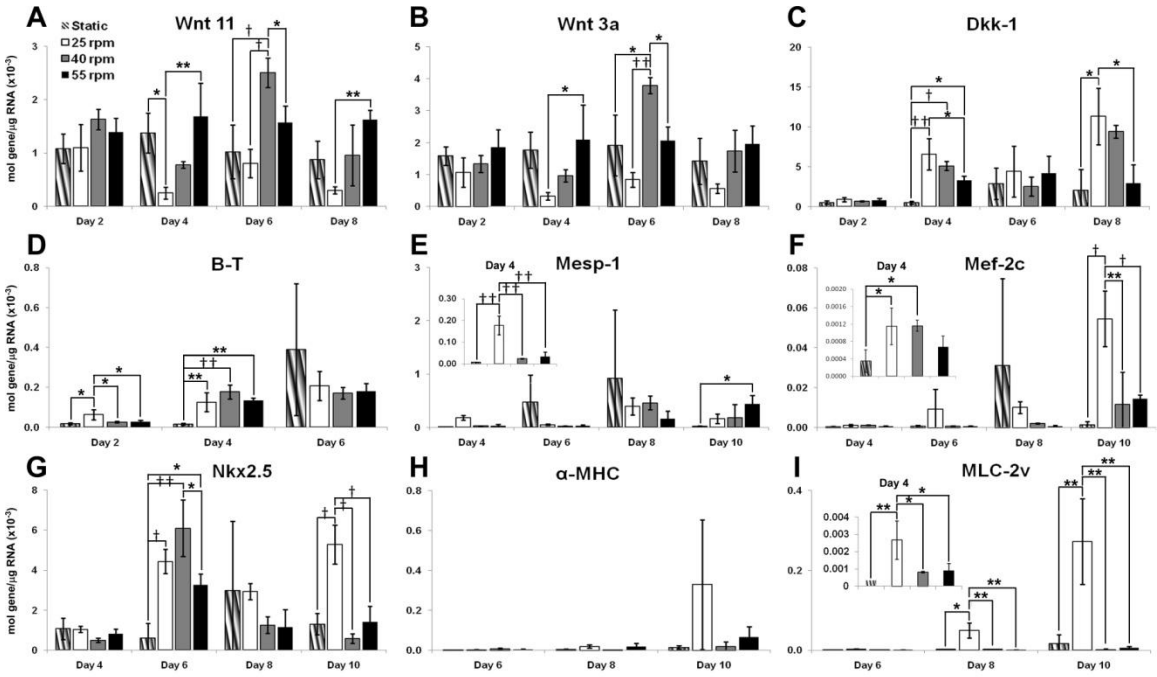

Figure 5.7: Expression of β-catenin-related genes within rotary and static EBs. qPCR analysis of RNA from static and rotary EBs (25, 40, 55 rpm) was performed at day 2, 4, 6, 8, and 10 of differentiation. Expression levels of non-canonical and canonical *Wnts* (A,B) was similar, but was modulated by culture condition, with 25 rpm rotary conditions exhibiting decreased levels of both *Wnt11* and *Wnt3a*. In contrast, Wnt inhibitor *Dkk-1* expression was increased within rotary EBs compared to static EBs (C), also corresponding to increased mesoderm-related gene expression within rotary conditions compared to static (D,E). Additionally, early cardiomyogenic markers *Mef-2c* and *Nkx2.5* were increased by rotary orbital culture (F,G), with 25 rpm conditions resulting in increased expression of sarcomeric muscle genes *α-MHC* and *MLC-2v* (H,I). n=3, * = $p \leq 0.05$, ** = $p \leq 0.01$, † = $p \leq 0.005$, and †† = $p \leq 0.001$.

transcription inhibits the further differentiation of a more mature cardiomyocyte phenotype [15-16]. Sarcomeric muscle related genes *α-myosin heavy chain* (*α-MHC*) and *myosin light chain 2 ventricle* (*MLC-2v*) represent more advanced cardiomyocyte differentiation, and expression of these genes was only observed within 25 rpm EBs (Figure 5.7 H,I). *MLC-2v* expression was significantly increased within 25 rpm EBs compared to other culture conditions ($p \leq 0.05$) as early as day 6 of differentiation, and *MLC-2v* expression increased with time in EBs from 25 rpm rotary orbital culture

compared to other culture conditions (day 8, $p \leq 0.05$; day 10 $p \leq 0.01$) (Figure 5.7 I). Taken together, these gene expression results indicate that transcriptional events related to β-catenin signaling are modulated by hydrodynamic conditions; specifically, targets of the Wnt/β-catenin pathway (*Mesp-1*, *Mef-2c*) appear to be increased earlier (day 4 of differentiation) within rotary orbital culture compared to static culture, and later inhibition of the Wnt/β-catenin pathway (through expression of *Dkk-1* and *Nkx2.5*) may be regulated by hydrodynamic conditions resulting in the modulation of cardiomyocyte differentiation.

Discussion

In this study the effects of hydrodynamic conditions from rotary orbital culture on β-catenin expression and cardiogenic gene transcription were examined by assessing TCF/LEF luciferase reporter expression, immuno-staining and immune-blotting for dephosphorylated β-catenin, and gene expression analysis of genes known to be directly and indirectly affected by β-catenin-regulated transcription. Lenti-viral transduction of D3-line ESCs with a luciferase TCF/LEF reporter construct was used to generate stably transduced ESC clones that induced luciferase expression following β-catenin signaling. Rotary orbital speed modulated both spatiotemporal location of β-catenin and the phosphorylation state of β-catenin, with slower rotary speeds resulting in earlier nuclear dephosphorylated β-catenin expression (Figures 5.5 and 5.6). Additionally, gene transcription directly regulated by β-catenin was increased initially within slower rotary speeds conditions (evidenced by increased luciferase activity and expression of *Mesp-1* and *Mef-2c*, Figures 5.4 E, 5.7 E,F). Hydrodynamic culture, in general, appeared to increase β-catenin-regulated transcription (Figures 5.4 E) and cardiogenic gene

expression (Figure 5.7 F,-I) compared to static culture conditions. Overall, this study illustrates how hydrodynamic conditions can modulate a developmentally relevant signaling pathway and result in differential regulation of downstream differentiation.

Early activation of β-catenin within differentiating ESCs has been linked to increased mesoderm differentiation and proliferation of Mesp-1+, Isl-1+, and Mef-2c+ cardiomyocyte progenitor cells [6, 15-20, 30-31]. However, continued β-catenin signaling (beyond day 4 of differentiation) has been shown to reduce or inhibit cardiomyocyte differentiation, while inhibition of β-catenin signaling through Wnt inhibitors (eg. Dkk-1) at these later time points of differentiation (day 4+) can increase cardiomyocyte development within EBs [15-16, 32]. Interestingly, the increased availability of signaling active nuclear β-catenin within slower rotary speed EBs at early time points of differentiation (days 1 and 2, Figures 5.5 and 5.6) correlated with significantly amplified expression luciferase at day 3 of differentiation (Figure 5.4) and significantly increased *Mesp-1* and *Mef-2c* expression (day 4) compared to other conditions (Figure 5.7). Expression of *Dkk-1* was also increased within slower rotary orbital speeds at the same time *Wnt* expression levels were decreased (days 4-6). The increase in *Dkk-1* expression may be due to the increased *Mesp-1* expression within low rotary speed EBs, as Mesp-1 is a transcription factor capable of directly increasing *Dkk-1* expression [30]. Dkk-1, along with Nkx2.5, inhibits the β-catenin signaling pathway [33]; thus the time course of *Mesp-1*, *Dkk-1*, and *Nkx2.5* expression within rotary EBs, particularly those from slower speeds, may allow for the inhibition of β-catenin signaling and further cardiomyocyte differentiation, as evidenced by increased *MLC-2v* expression at later time points of differentiation (Figure 5.7 I). Similar to previous results, rotary

orbital culture speed modulated the extent of cardiomyocyte differentiation (Figures 4.1, 4.2, 4.5, 4.7, 4.8) [25-26], and the results from this study suggest that the regulation of β-catenin signaling by rotary speed may be responsible for ultimately regulating cardiomyocyte differentiation.

Although many studies have linked EB formation methods to various differentiation capabilities, few have demonstrated a mechanistic cause of these observed differences. Rotary orbital suspension culture has been shown to modulate EB formation kinetics by the rotary speed applied, and slower speeds result in increased EB formation kinetics (Figure 3.5) [26, 34]. Initial ESC aggregation is dependent on E-cadherin, which also binds β-catenin on the cytoplasmic side of cell-cell contacts [35-38], and studies have illustrated the potential for cross-over between β-catenin associated with E-cadherin and its availability to participate in signaling/transcriptional activities [8, 39-40]; therefore, the modulation of EB formation may indirectly contribute to downstream β-catenin regulated transcription. The results from this study coupled with the developing understanding of the relationship between E-cadherin/β-catenin and β-catenin signaling support a proposed model linking EB aggregation, β-catenin signaling, and subsequent cardiomyocyte differentiation.

Possible Model: The aggregation of embryonic stem cells through E-cadherin binding facilitates the accumulation of stable β-catenin bound to E-cadherin, as the associatation of β-catenin with E-cadherin prevents the degradation of β-catenin by the GSK-3β/Axin/APC complex without the presence of Wnt. The β-catenin/E-cadherin complex can be endocytosed or destabilized upon phosphorylation by receptor tyrosine kinases [39-41], and in conjunction with Wnt binding to the Frizzled receptor [9, 39], β-

catenin is released from the catenin/cadherin complex and protected from degradation, allowing for its translocation to the nucleus to regulate transcription by coupling with TCF/LEF. β-catenin binding to TCF/LEF promotes transcription of early mesoderm and cardiac progenitor genes Mesp-1 and Isl-1, and in turn drives the transcription of Dkk-1, an inhibitor of the Wnt signaling pathway. Additionally, cardiac progenitor marker Nkx2.5 inhibits the transcription of β-catenin also reducing β-catenin signaling [33]. Culture conditions that facilitate/enhance ESC aggregation may increase the pool of stabilized β-catenin available for signaling upon Wnt activation. Therefore, the TCF/LEF regulated transcription response may be greater under such conditions (including hydrodynamic modulation of EB formation), possibly accounting for the modulation of mesoderm and cardiomyocyte differentiation observed. Although continued study of E-cadherin/ β-catenin dynamics are warranted, the study presented here offers a mechanistic explanation of how hydrodynamics, by way of EB formation kinetics, may modulate ESC differentiation, and as β-catenin signaling is implicated in numerous developmental pathways, hydrodynamic technologies could be designed to target several cell phenotypes.

References

1. Keller, G., *Embryonic stem cell differentiation: Emergence of a new era in biology and medicine.* Genes Dev, 2005. 19(10): p. 1129-55.

2. Nakaya, M.A., K. Biris, T. Tsukiyama, S. Jaime, J.A. Rawls, and T.P. Yamaguchi, *Wnt3a links left-right determination with segmentation and anteroposterior axis elongation.* Development, 2005. 132(24): p. 5425-36.

3. Rivera-Perez, J.A. and T. Magnuson, *Primitive streak formation in mice is preceded by localized activation of brachyury and wnt3.* Dev Biol, 2005. 288(2): p. 363-71.

4. Anton, R., H.A. Kestler, and M. Kuhl, *Beta-catenin signaling contributes to stemness and regulates early differentiation in murine embryonic stem cells.* FEBS Lett, 2007. 581(27): p. 5247-54.

5. James, D., A.J. Levine, D. Besser, and A. Hemmati-Brivanlou, *Tgfbeta/activin/nodal signaling is necessary for the maintenance of pluripotency in human embryonic stem cells.* Development, 2005. 132(6): p. 1273-82.

6. Lindsley, R.C., J.G. Gill, M. Kyba, T.L. Murphy, and K.M. Murphy, *Canonical wnt signaling is required for development of embryonic stem cell-derived mesoderm.* Development, 2006. 133(19): p. 3787-96.

7. ten Berge, D., W. Koole, C. Fuerer, M. Fish, E. Eroglu, and R. Nusse, *Wnt signaling mediates self-organization and axis formation in embryoid bodies.* Cell Stem Cell, 2008. 3(5): p. 508-18.

8. Gavard, J. and R.M. Mege, *Once upon a time there was beta-catenin in cadherin-mediated signalling.* Biol Cell, 2005. 97(12): p. 921-6.

9. Gottardi, C.J. and B.M. Gumbiner, *Distinct molecular forms of beta-catenin are targeted to adhesive or transcriptional complexes.* J Cell Biol, 2004. 167(2): p. 339-49.

10. Jamora, C. and E. Fuchs, *Intercellular adhesion, signalling and the cytoskeleton.* Nat Cell Biol, 2002. 4(4): p. E101-8.

11. Cadigan, K.M. and R. Nusse, *Wnt signaling: A common theme in animal development.* Genes Dev, 1997. 11(24): p. 3286-305.

12. Hecht, A., C.M. Litterst, O. Huber, and R. Kemler, *Functional characterization of multiple transactivating elements in beta-catenin, some of which interact with the tata-binding protein in vitro.* J Biol Chem, 1999. 274(25): p. 18017-25.

13. Hecht, A., K. Vleminckx, M.P. Stemmler, F. van Roy, and R. Kemler, *The p300/cbp acetyltransferases function as transcriptional coactivators of beta-catenin in vertebrates.* EMBO J, 2000. 19(8): p. 1839-50.

14. Barker, N., A. Hurlstone, H. Musisi, A. Miles, M. Bienz, and H. Clevers, *The chromatin remodelling factor brg-1 interacts with beta-catenin to promote target gene activation.* EMBO J, 2001. 20(17): p. 4935-43.

15. Naito, A.T., I. Shiojima, H. Akazawa, K. Hidaka, T. Morisaki, A. Kikuchi, and I. Komuro, *Developmental stage-specific biphasic roles of wnt/beta-catenin signaling in cardiomyogenesis and hematopoiesis.* Proc Natl Acad Sci U S A, 2006. 103(52): p. 19812-7.

16. Ueno, S., G. Weidinger, T. Osugi, A.D. Kohn, J.L. Golob, L. Pabon, H. Reinecke, R.T. Moon, and C.E. Murry, *Biphasic role for wnt/beta-catenin signaling in cardiac specification in zebrafish and embryonic stem cells.* Proc Natl Acad Sci U S A, 2007. 104(23): p. 9685-90.

17. Kwon, C., J. Arnold, E.C. Hsiao, M.M. Taketo, B.R. Conklin, and D. Srivastava, *Canonical wnt signaling is a positive regulator of mammalian cardiac progenitors.* Proc Natl Acad Sci U S A, 2007. 104(26): p. 10894-9.

18. Kwon, C., L. Qian, P. Cheng, V. Nigam, J. Arnold, and D. Srivastava, *A regulatory pathway involving notch1/beta-catenin/isl1 determines cardiac progenitor cell fate.* Nat Cell Biol, 2009. 11(8): p. 951-7.

19. Lin, L., L. Cui, W. Zhou, D. Dufort, X. Zhang, C.L. Cai, L. Bu, L. Yang, J. Martin, R. Kemler, M.G. Rosenfeld, J. Chen, and S.M. Evans, *Beta-catenin directly regulates islet1 expression in cardiovascular progenitors and is required for multiple aspects of cardiogenesis.* Proc Natl Acad Sci U S A, 2007. 104(22): p. 9313-8.

20. Qyang, Y., S. Martin-Puig, M. Chiravuri, S. Chen, H. Xu, L. Bu, X. Jiang, L. Lin, A. Granger, A. Moretti, L. Caron, X. Wu, J. Clarke, M.M. Taketo, K.L. Laugwitz, R.T. Moon, P. Gruber, S.M. Evans, S. Ding, and K.R. Chien, *The renewal and differentiation of isl1+ cardiovascular progenitors are controlled by a wnt/beta-catenin pathway.* Cell Stem Cell, 2007. 1(2): p. 165-79.

21. Boheler, K.R., J. Czyz, D. Tweedie, H.T. Yang, S.V. Anisimov, and A.M. Wobus, *Differentiation of pluripotent embryonic stem cells into cardiomyocytes.* Circ Res, 2002. 91(3): p. 189-201.

22. Kurosawa, H., *Methods for inducing embryoid body formation: In vitro differentiation system of embryonic stem cells.* J Biosci Bioeng, 2007. 103(5): p. 389-98.

23. Wiese, C., G. Kania, A. Rolletschek, P. Blyszczuk, and A.M. Wobus, *Pluripotency: Capacity for in vitro differentiation of undifferentiated embryonic stem cells.* Methods Mol Biol, 2006. 325: p. 181-205.

24. Yoon, B.S., S.J. Yoo, J.E. Lee, S. You, H.T. Lee, and H.S. Yoon, *Enhanced differentiation of human embryonic stem cells into cardiomyocytes by combining hanging drop culture and 5-azacytidine treatment.* Differentiation, 2006. 74(4): p. 149-59.

25. Sargent, C.Y., G.Y. Berguig, and T.C. McDevitt, *Cardiomyogenic differentiation of embryoid bodies is promoted by rotary orbital suspension culture.* Tissue Eng Part A, 2009. 15(2): p. 331-342.

26. Sargent, C.Y., G.Y. Berguig, M.A. Kinney, L.A. Hiatt, R.L. Carpenedo, R.E. Berson, and T.C. McDevitt, *Hydrodynamic modulation of embryonic stem cell differentiation by rotary orbital suspension culture.* Biotechnol Bioeng, 2010. 105(3): p. 611-26.

27. Chilton, J.M. and J.M. Le Doux, *Quantitative analysis of retroviral and lentiviral gene transfer to murine embryonic stem cells.* J Biotechnol, 2008. 138(1-2): p. 42-51.

28. Ma, Y., A. Ramezani, R. Lewis, R.G. Hawley, and J.A. Thomson, *High-level sustained transgene expression in human embryonic stem cells using lentiviral vectors.* Stem Cells, 2003. 21(1): p. 111-7.

29. van Noort, M., J. Meeldijk, R. van der Zee, O. Destree, and H. Clevers, *Wnt signaling controls the phosphorylation status of beta-catenin.* J Biol Chem, 2002. 277(20): p. 17901-5.

30. David, R., C. Brenner, J. Stieber, F. Schwarz, S. Brunner, M. Vollmer, E. Mentele, J. Muller-Hocker, S. Kitajima, H. Lickert, R. Rupp, and W.M. Franz, *Mesp1 drives vertebrate cardiovascular differentiation through dkk-1-mediated blockade of wnt-signalling.* Nat Cell Biol, 2008. 10(3): p. 338-45.

31. Lindsley, R.C., J.G. Gill, T.L. Murphy, E.M. Langer, M. Cai, M. Mashayekhi, W. Wang, N. Niwa, J.M. Nerbonne, M. Kyba, and K.M. Murphy, *Mesp1 coordinately regulates cardiovascular fate restriction and epithelial-mesenchymal transition in differentiating escs.* Cell Stem Cell, 2008. 3(1): p. 55-68.

32. Klaus, A., Y. Saga, M.M. Taketo, E. Tzahor, and W. Birchmeier, *Distinct roles of wnt/beta-catenin and bmp signaling during early cardiogenesis.* Proc Natl Acad Sci U S A, 2007. 104(47): p. 18531-6.

33. Riazi, A.M., J.K. Takeuchi, L.K. Hornberger, S.H. Zaidi, F. Amini, J. Coles, B.G. Bruneau, and G.S. Van Arsdell, *Nkx2-5 regulates the expression of beta-catenin and gata4 in ventricular myocytes.* PLoS One, 2009. 4(5): p. e5698.

34. Carpenedo, R.L., C.Y. Sargent, and T.C. McDevitt, *Rotary suspension culture enhances the efficiency, yield, and homogeneity of embryoid body differentiation.* Stem Cells, 2007. 25(9): p. 2224-34.

35. Dang, S.M., S. Gerecht-Nir, J. Chen, J. Itskovitz-Eldor, and P.W. Zandstra, *Controlled, scalable embryonic stem cell differentiation culture.* Stem Cells, 2004. 22(3): p. 275-82.

36. Fok, E.Y. and P.W. Zandstra, *Shear-controlled single-step mouse embryonic stem cell expansion and embryoid body-based differentiation.* Stem Cells, 2005. 23(9): p. 1333-42.

37. Dasgupta, A., R. Hughey, P. Lancin, L. Larue, and P.V. Moghe, *E-cadherin synergistically induces hepatospecific phenotype and maturation of embryonic stem cells in conjunction with hepatotrophic factors.* Biotechnol Bioeng, 2005. 92(3): p. 257-66.

38. Larue, L., C. Antos, S. Butz, O. Huber, V. Delmas, M. Dominis, and R. Kemler, *A role for cadherins in tissue formation.* Development, 1996. 122(10): p. 3185-94.

39. Kam, Y. and V. Quaranta, *Cadherin-bound beta-catenin feeds into the wnt pathway upon adherens junctions dissociation: Evidence for an intersection between beta-catenin pools.* PLoS One, 2009. 4(2): p. e4580.

40. Nelson, W.J. and R. Nusse, *Convergence of wnt, beta-catenin, and cadherin pathways.* Science, 2004. 303(5663): p. 1483-7.

41. Bryant, D.M. and J.L. Stow, *The ins and outs of e-cadherin trafficking.* Trends Cell Biol, 2004. 14(8): p. 427-34.

CHAPTER 6

FUTURE CONSIDERATIONS

This project in its entirety illustrates how hydrodynamics can regulate spheroid formation and size, resulting in the modulation of signaling pathways and ultimately affecting cardiomyocyte differentiation. The sum of the results clearly demonstrates the importance of defining the effects of hydrodynamic environments on stem cell differentiation and conceptually proves the potential for utilizing these parameters for the design of specific bioreactors for the directed differentiation of desired cell types. However, the results also suggest several avenues for further investigation: the relationship between spheroid size, hydrodynamics and differentiation, the contribution of transport properties to stem cell spheroid differentiation, and the manipulation of other differentiation pathways.

Hydrodynamic culture of mESCs and hESCs can be used to efficiently generate large yields of homogeneous EBs [1-6]. In addition to improving the formation kinetics of spheroids, hydrodynamic culture can also modulate spheroid size dependent on the mixing speed utilized [2, 5-9]. Whereas the results from this project have correlated EB differentiation modulation with formation kinetics, other studies have linked ESC colony and EB spheroid size to alterations of stem cell differentiation without the presence of hydrodynamics [10-15]; however, besides a noticeable correlation between size and differentiation, few studies have reported on the mechanism involved in differentiation regulation due to spheroid size. Similar to results presented here, other laboratories have reported that cardiomyogenic differentiation appears to be enhanced within larger EBs

[10, 12, 14]; therefore, it will be important to separate the effects of hydrodynamics from EB size on ESC differentiation. On-going studies combining ultra-high throughput technology to generate large numbers of equally sized EBs and rotary orbital culture to expose the EBs to different hydrodynamic conditions have illustrated that the subtle differences in ESC differentiation due to rotary speed are reduced by removing the size component. Thus, suggesting that spheroid size may be more important than hydrodynamic conditions for modulating differentiation. However, forming EBs in ultra-high throughput microwells also negates the differences in EB formation kinetics observed within rotary orbital culture, possibly accounting for the reduction of differentiation control observed instead of EB size.

Transport properties are also determined by hydrodynamic conditions and could account for some of the differences observed in ESC differentiation. Additionally, as cell aggregates grow in size, gradients develop within the three-dimensional structure, ultimately affecting the availability of oxygen and nutrients within spheroids, impacting the cell expansion and doubling time of stem and progenitor cells. Human ESCs grown in several mixed culture formats, including rotary, roller ball and spinner flask, exhibit increased expansion compared to static culture [16-17]. Oxygen transport has been modeled under convective flow conditions to explain the increased cell expansion due to mixing [18], and the partial oxygen pressure within the interior of the EB decreases depending on the size of the EB, with larger EBs having a reduced internal pO2 [19]. Interestingly, in addition to larger-sized spheroids increasing cardiomyocyte differentiation, hypoxic conditions have also been shown to enhance cardiogenesis within EBs [16, 20-21]. However, the early differences (days 2 and 4 of differentiation) in

cardiogenic gene expression observed in this project may not be explained by transport limitations, as EBs are still relatively small at these time points. Additionally, differentiating EBs construct an outer shell-like structure which may limit transport across all rotary orbital condition regardless of speed [22-23]. Still, convective transport should be modeled within the rotary orbital system to determine how nutrient delivery is altered by rotary orbital speed, and depending on the findingss, rotary orbital culture could be used to deliver soluble biomolecules more efficiently than with static culture techniques. Current studies are being conducted that examine perfusion through EBs as a method to interrogate the importance of transport in EB differentiation and also to potentially deliver biomolecules to differentiating EBs.

The rotary orbital suspension culture system (as well as other hydrodynamic systems involving mixing conditions) allows for unique examination of cell aggregate formation kinetics without completely changing the culture technique used. It is accepted within the stem community that EB formation methods can affect ESC differentiation, as hanging drop culture is known to enhance mesoderm and cardiogenic differentiation compared to static cultre [4, 24-26], but this project is the first to identify a developmentally-relevant pathway potentially modulated by hydrodynamic conditions and EB formation kinetics. The Wnt/β-catenin pathway is a highly conserved signaling pathway involved in many aspects of development. Most notably at the early time points recapitulated by EB differentiation, β-catenin signaling activation is responsible for axis patterning and is required for early mesoderm development [27-31]. Beta-catenin is also an important component of cell-cell contacts, as it associates with E-cadherin at the cell membrane and mediates connections with the actin cytoskeleton. Although the

possibility of cross-over between E-cadherin bound β-catenin and signaling active β-catenin is a point of debate, several studies have illustrated that the availability of β-catenin for nuclear transcription events can be modulated by the dynamic regulation of E-cadherin [32-36].

The data presented in this study suggest that β-catenin location and phosphorylation state are modulated by rotary orbital culture compared to static culture and are affected by rotary orbital speed (Figures 5.3-5.6). These alterations of β-catenin occur at early time points of differentiation (differences in location noted by day 1, and differences in transcription observed by day 2), during which time transport can be assumed not to be limited by EB size. The major difference in EB culture conditions examined at such early time points is formation kinetics, as slower rotary speeds are shown to enhance EB formation and primitive EBs are observed as early as 12 hours of culture (Figure 3.5). The increased efficiency of EB formation may augment the pool of β-catenin bound to E-cadherin at cell-cell junctions, which could be made available for nuclear translocation upon tyrosine kinase phosphorylation of E-cadherin, E-cadherin endocytosis, or Wnt binding to the frizzled receptor [32]. Interestingly, when the formation kinetics are held constant by pre-forming EBs in ultra-high throughput microwells prior to rotary orbital culture at different speeds, differences in EB differentiation are less apparent. However, to conclusively determine if EB formation kinetics are responsible for the modulation of β-catenin signaling, further studies should be conducted. These studies may include two approaches to modulate E-cadherin bound β-catenin. First, E-cadherin could be stabilized at the cell membrane, preventing the dissociation of the adheren junction or endocytosis of E-cadherin. Additionally, the E-

cadherin/β-catenin complex should be stabilized so that β-catenin is permanently sequestered by E-cadherin and not available for nuclear transcription. Examining the location of β-catenin and subsequent changes in gene expression under these conditions will elucidate whether the pool of β-catenin from E-cadherin is released and responsible for the modulation of gene expression seen in hydrodynamic culture of EBs.

In addition to being necessary for early mesoderm and cardiac progenitor differentiation, β-catenin signaling is also implicated in regulating endodermal gene expression. Hydrodynamic conditions from rotary orbital culture also modulated *AFP* gene expression, an early endoderm marker (Figures 4.2 and 4.7) [2, 5], and PCR array analysis indicated that endoderm related genes, *Sox17* and *Fox2a*, were upregulated compared to static conditions (Figure 3.10, Nair and Ngangan 2010, *in prep*). Beta-catenin, cooperatively with Sox17, has been shown to target *Foxa1* and *Foxa2* transcription [37]. Therefore, hydrodynamic conditions imparted by rotary orbital culture may also regulate endoderm differentiation. In fact, early developing endoderm secretes factors from both the visceral and parietal lineages [38-41] that modulate cardiomyocyte differentiation, including Insulin growth factor-2 (Igf-2) from the primitive and parietal endoderm and Bone morphogenetic protein-2 (BMP-2) from the visceral endoderm [41]. Secreted frizzled-related proteins (Sfrp) 1 and 5 are also secreted by the anterior visceral endoderm (AVE) [42-43] and can inhibit β-catenin signaling by binding Wnt; thus expression of Sfrps may also contribute to the modulation of cardiomyocyte differentiation [44]. Therefore, rotary orbital suspension culture may enhance cardiomyocyte differentiation through early activation of β-catenin signaling, the promotion of endoderm formation, and the subsequent endogenously regulated inhibition

of β-catenin signaling by Mesp-1 directed Dkk-1 transcription and Sfrp secretion by the early endoderm.

The fact that rotary orbital culture conditions modulate stem cell differentiation has implications on bioprocessing and bioreactor design for the future application of stem cell therapies. This platform technology can be combined with other directed differentiation methods to increase efficiency and yield of differentiating stem cells, such as combinations with biomolecule delivery. In addition to potentially increasing the delivery of soluble biomolecules, rotary orbital culture can be used to incorporate microspheres within EBs to deliver morphogens more homogeneously throughout the EB interior, resulting in directed and homogeneous differentiation [23, 45]. One could foresee utilizing hydrodynamic conditions and microsphere delivery to synergistically direct differentiation. Besides the addition of bio-signaling molecules to hydrodynamic culture, mixing conditions could also be combined with other external factors, such as culture under hypoxic conditions. As previously discussed, oxygen gradients within cell spheroids may affect differentiation, but it has also been illustrated that culture under hypoxic conditions can regulate differentiation. Another avenue which has been preliminarily explored is the application of hydrodynamic regimens (Appendix A). By forming spheroids under one mixing condition and then switching to a different hydrodynamic environment, it may be possible to impart increased control over differentiation. In fact alpha-fetoprotein (AFP) expression was modulated to a larger extent when EBs formed at slower conditions were switched to faster rotary culture speeds (Figure A.1)

As several hydrodynamic systems have been used to form EBs in addition to rotary orbital suspension culture, the principles of hydrodynamic differentiation regulation may be applied on larger-scales (10^2-10^3 mL), allowing for the increased production of differentiating cells required for large-scale drug screening or the potential therapeutic application of stem-cell derived products (whether secreted regenerative molecules or terminally differentiated cells). Defining the governing properties within hydrodynamic culture systems that regulate differentiation will aid in the development of efficient bioprocessing protocols and bioreactor design. Primary and other progenitor cell types can also be cultured as spheroids, including primary rat embryonic brain cells, chondrocytes, and neural stem cells [7, 46-47]; therefore hydrodynamic culture could be applied to regulate the phenotype and function of cell types other than embryonic stem cells. Additionally, rotary orbital culture has recently been used to generate spheroids from mesenchymal stem cells and baby hamster kidney cells, which typically do not spontaneously aggregate, suggesting that this type of gentle mixing may support cellular aggregation when other methods (such centrifugation) do not.

Overall, the project presented demonstrates the intertwining complexities between hydrodynamic culture, spheroid formation and size, and differentiation. In order to realize the potential application of stem cells, three key achievements must be made.

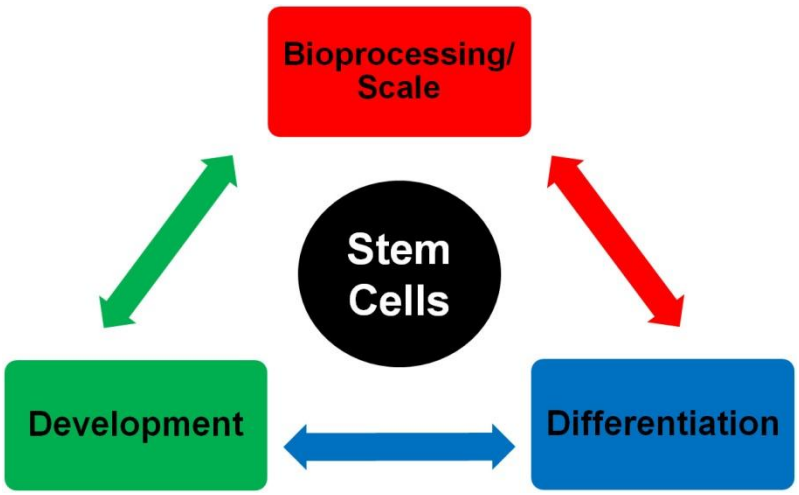

Figure 6.1: The stem cell potential. The components required to realize the potential of stem cells are highly related and impact one another. To efficiently direct stem cell differentiation, biological development and large-scale culture methods must be examined in parallel.

1. The endogenous regulatory mechanisms for development must be understood. 2. Stem cells must be reproducibly directed to differentiate into desired cell types. And 3. Stem cell culture and differentiation must be carried out in a large-scale manner to address bioprocessing requirements for clinical applications (Figure 6.1). These three elements are intimately connected, and they should be examined in conjunction with one another to eventually realize the promise of stem cell therapy. This project illustrates how examining these three components simultaneously can yield insights into directed differentiation methods that utilize natural biological paradigms to manipulate large-scale production of desired cell types.

References

1. Cameron, C.M., W.S. Hu, and D.S. Kaufman, *Improved development of human embryonic stem cell-derived embryoid bodies by stirred vessel cultivation.* Biotechnol Bioeng, 2006. 94(5): p. 938-48.

2. Carpenedo, R.L., C.Y. Sargent, and T.C. McDevitt, *Rotary suspension culture enhances the efficiency, yield, and homogeneity of embryoid body differentiation.* Stem Cells, 2007. 25(9): p. 2224-34.

3. Gerecht-Nir, S., S. Cohen, and J. Itskovitz-Eldor, *Bioreactor cultivation enhances the efficiency of human embryoid body (heb) formation and differentiation.* Biotechnol Bioeng, 2004. 86(5): p. 493-502.

4. Kurosawa, H., *Methods for inducing embryoid body formation: In vitro differentiation system of embryonic stem cells.* J Biosci Bioeng, 2007. 103(5): p. 389-98.

5. Sargent, C.Y., G.Y. Berguig, M.A. Kinney, L.A. Hiatt, R.L. Carpenedo, R.E. Berson, and T.C. McDevitt, *Hydrodynamic modulation of embryonic stem cell differentiation by rotary orbital suspension culture.* Biotechnol Bioeng, 2010. 105(3): p. 611-26.

6. Schroeder, M., S. Niebruegge, A. Werner, E. Willbold, M. Burg, M. Ruediger, L.J. Field, J. Lehmann, and R. Zweigerdt, *Differentiation and lineage selection of mouse embryonic stem cells in a stirred bench scale bioreactor with automated process control.* Biotechnol Bioeng, 2005. 92(7): p. 920-33.

7. Baghbaderani, B.A., L.A. Behie, A. Sen, K. Mukhida, M. Hong, and I. Mendez, *Expansion of human neural precursor cells in large-scale bioreactors for the treatment of neurodegenerative disorders.* Biotechnology Progress, 2008. 24(4): p. 859-70.

8. Fok, E.Y. and P.W. Zandstra, *Shear-controlled single-step mouse embryonic stem cell expansion and embryoid body-based differentiation.* Stem Cells, 2005. 23(9): p. 1333-42.

9. Santos, S.S., S.B. Leite, U. Sonnewald, M.J. Carrondo, and P.M. Alves, *Stirred vessel cultures of rat brain cells aggregates: Characterization of major metabolic pathways and cell population dynamics.* J Neurosci Res, 2007. 85(15): p. 3386-97.

10. Bauwens, C.L., R. Peerani, S. Niebruegge, K.A. Woodhouse, E. Kumacheva, M. Husain, and P.W. Zandstra, *Control of human embryonic stem cell colony and aggregate size heterogeneity influences differentiation trajectories.* Stem Cells, 2008. 26(9): p. 2300-10.

11. Hwang, Y.S., B.G. Chung, D. Ortmann, N. Hattori, H.C. Moeller, and A. Khademhosseini, *Microwell-mediated control of embryoid body size regulates embryonic stem cell fate via differential expression of wnt5a and wnt11.* Proc Natl Acad Sci U S A, 2009. 106(40): p. 16978-83.

12. Lee, L.H., R. Peerani, M. Ungrin, C. Joshi, E. Kumacheva, and P. Zandstra, *Micropatterning of human embryonic stem cells dissects the mesoderm and endoderm lineages.* Stem Cell Res, 2009. 2(2): p. 155-62.

13. Messana, J.M., N.S. Hwang, J. Coburn, J.H. Elisseeff, and Z. Zhang, *Size of the embryoid body influences chondrogenesis of mouse embryonic stem cells.* J Tissue Eng Regen Med, 2008. 2(8): p. 499-506.

14. Niebruegge, S., C.L. Bauwens, R. Peerani, N. Thavandiran, S. Masse, E. Sevaptisidis, K. Nanthakumar, K. Woodhouse, M. Husain, E. Kumacheva, and P.W. Zandstra, *Generation of human embryonic stem cell-derived mesoderm and cardiac cells using size-specified aggregates in an oxygen-controlled bioreactor.* Biotechnol Bioeng, 2009. 102(2): p. 493-507.

15. Xu, C., S. Police, N. Rao, and M.K. Carpenter, *Characterization and enrichment of cardiomyocytes derived from human embryonic stem cells.* Circ Res, 2002. 91(6): p. 501-8.

16. Niebruegge, S., A. Nehring, H. Bar, M. Schroeder, R. Zweigerdt, and J. Lehmann, *Cardiomyocyte production in mass suspension culture: Embryonic stem cells as a source for great amounts of functional cardiomyocytes.* Tissue Eng Part A, 2008.

17. Yirme, G., M. Amit, I. Laevsky, S. Osenberg, and J. Itskovitz-Eldor, *Establishing a dynamic process for the formation, propagation, and differentiation of human embryoid bodies.* Stem Cells Dev, 2008. 17(6): p. 1227-41.

18. Pathi, P., T. Ma, and B.R. Locke, *Role of nutrient supply on cell growth in bioreactor design for tissue engineering of hematopoietic cells.* Biotechnology and Bioengineering, 2005. 89(7): p. 743-58.

19. Gassmann, M., J. Fandrey, S. Bichet, M. Wartenberg, H.H. Marti, C. Bauer, R.H. Wenger, and H. Acker, *Oxygen supply and oxygen-dependent gene expression in differentiating embryonic stem cells.* Proc Natl Acad Sci U S A, 1996. 93(7): p. 2867-72.

20. Bauwens, C., T. Yin, S. Dang, R. Peerani, and P.W. Zandstra, *Development of a perfusion fed bioreactor for embryonic stem cell-derived cardiomyocyte generation: Oxygen-mediated enhancement of cardiomyocyte output.* Biotechnol Bioeng, 2005. 90(4): p. 452-61.

21. Li, J., M. Stouffs, L. Serrander, B. Banfi, E. Bettiol, Y. Charnay, K. Steger, K.H. Krause, and M.E. Jaconi, *The nadph oxidase nox4 drives cardiac differentiation: Role in regulating cardiac transcription factors and map kinase activation.* Mol Biol Cell, 2006. 17(9): p. 3978-88.

22. Sachlos, E. and D.T. Auguste, *Embryoid body morphology influences diffusive transport of inductive biochemicals: A strategy for stem cell differentiation.* Biomaterials, 2008. 29(34): p. 4471-80.

23. Carpenedo, R.L., A.M. Bratt-Leal, R.A. Marklein, S.A. Seaman, N.J. Bowen, J.F. McDonald, and T.C. McDevitt, *Homogeneous and organized differentiation within embryoid bodies induced by microsphere-mediated delivery of small molecules.* Biomaterials, 2009. 30(13): p. 2507-15.

24. Boheler, K.R., J. Czyz, D. Tweedie, H.T. Yang, S.V. Anisimov, and A.M. Wobus, *Differentiation of pluripotent embryonic stem cells into cardiomyocytes.* Circ Res, 2002. 91(3): p. 189-201.

25. Sargent, C.Y., G.Y. Berguig, and T.C. McDevitt, *Cardiomyogenic differentiation of embryoid bodies is promoted by rotary orbital suspension culture.* Tissue Eng Part A, 2009. 15(2): p. 331-342.

26. Yoon, B.S., S.J. Yoo, J.E. Lee, S. You, H.T. Lee, and H.S. Yoon, *Enhanced differentiation of human embryonic stem cells into cardiomyocytes by combining hanging drop culture and 5-azacytidine treatment.* Differentiation, 2006. 74(4): p. 149-59.

27. Kwon, C., J. Arnold, E.C. Hsiao, M.M. Taketo, B.R. Conklin, and D. Srivastava, *Canonical wnt signaling is a positive regulator of mammalian cardiac progenitors.* Proc Natl Acad Sci U S A, 2007. 104(26): p. 10894-9.

28. Kwon, C., L. Qian, P. Cheng, V. Nigam, J. Arnold, and D. Srivastava, *A regulatory pathway involving notch1/beta-catenin/isl1 determines cardiac progenitor cell fate.* Nat Cell Biol, 2009. 11(8): p. 951-7.

29. Lindsley, R.C., J.G. Gill, M. Kyba, T.L. Murphy, and K.M. Murphy, *Canonical wnt signaling is required for development of embryonic stem cell-derived mesoderm.* Development, 2006. 133(19): p. 3787-96.

30. Naito, A.T., I. Shiojima, H. Akazawa, K. Hidaka, T. Morisaki, A. Kikuchi, and I. Komuro, *Developmental stage-specific biphasic roles of wnt/beta-catenin signaling in cardiomyogenesis and hematopoiesis.* Proc Natl Acad Sci U S A, 2006. 103(52): p. 19812-7.

31. Ueno, S., G. Weidinger, T. Osugi, A.D. Kohn, J.L. Golob, L. Pabon, H. Reinecke, R.T. Moon, and C.E. Murry, *Biphasic role for wnt/beta-catenin signaling in*

cardiac specification in zebrafish and embryonic stem cells. Proc Natl Acad Sci U S A, 2007. 104(23): p. 9685-90.

32. Bryant, D.M. and J.L. Stow, *The ins and outs of e-cadherin trafficking.* Trends Cell Biol, 2004. 14(8): p. 427-34.

33. Gavard, J. and R.M. Mege, *Once upon a time there was beta-catenin in cadherin-mediated signalling.* Biol Cell, 2005. 97(12): p. 921-6.

34. Gottardi, C.J. and B.M. Gumbiner, *Distinct molecular forms of beta-catenin are targeted to adhesive or transcriptional complexes.* J Cell Biol, 2004. 167(2): p. 339-49.

35. Nelson, W.J. and R. Nusse, *Convergence of wnt, beta-catenin, and cadherin pathways.* Science, 2004. 303(5663): p. 1483-7.

36. Noles, S.R. and A. Chenn, *Cadherin inhibition of beta-catenin signaling regulates the proliferation and differentiation of neural precursor cells.* Mol Cell Neurosci, 2007. 35(4): p. 549-58.

37. Sinner, D., S. Rankin, M. Lee, and A.M. Zorn, *Sox17 and beta-catenin cooperate to regulate the transcription of endodermal genes.* Development, 2004. 131(13): p. 3069-80.

38. Bin, Z., L.G. Sheng, Z.C. Gang, J. Hong, C. Jun, Y. Bo, and S. Hui, *Efficient cardiomyocyte differentiation of embryonic stem cells by bone morphogenetic protein-2 combined with visceral endoderm-like cells.* Cell Biol Int, 2006. 30(10): p. 769-76.

39. Mummery, C., D. Ward-van Oostwaard, P. Doevendans, R. Spijker, S. van den Brink, R. Hassink, M. van der Heyden, T. Opthof, M. Pera, A.B. de la Riviere, R. Passier, and L. Tertoolen, *Differentiation of human embryonic stem cells to cardiomyocytes: Role of coculture with visceral endoderm-like cells.* Circulation, 2003. 107(21): p. 2733-40.

40. Rudy-Reil, D. and J. Lough, *Avian precardiac endoderm/mesoderm induces cardiac myocyte differentiation in murine embryonic stem cells.* Circ Res, 2004. 94(12): p. e107-16.

41. Stary, M., W. Pasteiner, A. Summer, A. Hrdina, A. Eger, and G. Weitzer, *Parietal endoderm secreted sparc promotes early cardiomyogenesis in vitro.* Exp Cell Res, 2005. 310(2): p. 331-43.

42. Finley, K.R., J. Tennessen, and W. Shawlot, *The mouse secreted frizzled-related protein 5 gene is expressed in the anterior visceral endoderm and foregut*

endoderm during early post-implantation development. Gene Expr Patterns, 2003. 3(5): p. 681-4.

43. Kemp, C., E. Willems, S. Abdo, L. Lambiv, and L. Leyns, *Expression of all wnt genes and their secreted antagonists during mouse blastocyst and postimplantation development.* Dev Dyn, 2005. 233(3): p. 1064-75.

44. Deb, A., B.H. Davis, J. Guo, A. Ni, J. Huang, Z. Zhang, H. Mu, and V.J. Dzau, *Sfrp2 regulates cardiomyogenic differentiation by inhibiting a positive transcriptional autofeedback loop of wnt3a.* Stem Cells, 2008. 26(1): p. 35-44.

45. Carpenedo, R.L., S.A. Seaman, and T.C. McDevitt, *Microsphere size effects on embryoid body incorporation and embryonic stem cell differentiation.* J Biomed Mater Res A, 2010.

46. Bueno, E.M., B. Bilgen, R.L. Carrier, and G.A. Barabino, *Increased rate of chondrocyte aggregation in a wavy-walled bioreactor.* Biotechnology and Bioengineering, 2004. 88(6): p. 767-77.

47. Sen, A., M. Kallos, and L. Behie, *Effects of hydrodynamics on cultures of mammalian neural stem cell aggregates in suspension bioreactors.* Ind. Eng. Chem. Res, 2001. 40(23): p. 5350-5357.

APPENDIX A

COMBINATORIAL ROTARY ORBITAL SUSPENSION CULTURE ALTERS EB MORPHOLOGY AND ALPHA-FETOPROTEIN EXPRESSION

Based on the aforementioned differences in size, yield, morphology, and differentiation between EBs cultured at different singular rotary speeds (Chapters 3 and 4), an additional series of combinatorial rotary experiments was conducted. EBs were exposed to different rotary speeds during initial formation (up to 2 days) and later stages of suspension culture to examine whether the previously observed differences in EBs were primarily due to the initial effects of different rotary speeds or were impacted by continuous exposure to rotary motion. EBs were initially formed at one rotary speed (25, 40, or 55 rpm) for 2 days, upon which EBs were switched to a secondary rotary speed for an additional 5 days of culture (Figure A.1 A). EBs exposed to 25 rpm initial or secondary rotary speeds were consistently larger than EBs exposed to combinations of 40 and 55 rpm (Figure A.1 B). EBs maintained at consistent speeds as those in the originally examined are highlighted in green (25rpm), red (40 rpm), and blue (55 rpm).

Upon histological examination, EBs continuously exposed to 25 rpm largely contained an enucleated central core and evidence of cavitation (consistent with original constant speed studies, Figure 3.8), but EBs formed at 25 rpm and switched to faster rotary speeds exhibited an increased nuclear density and less of an enucleated center. In contrast, EBs initially formed at 40 and 55 rpm and switched to 25 rpm exhibited a more

cystic appearance and a less dense arrangement of cells than EBs cultured at combinations of only 40 and 55 rpm (Figure A.1 C). The histological analysis of EB cross-sections revealed that both primary and secondary speeds modulated the cellular morphology and spatial organization within EBs, indicating that EBs differentially responded to changes in rotary speeds during the entire course of suspension culture.

EBs initially exposed to 25 rpm and switched to 55 rpm expressed higher levels of AFP than EBs maintained at 25 rpm or switched to 40 rpm (Figure A.1 D). EBs initially exposed to 40 rpm and switched to 25 rpm expressed levels of AFP comparable to that of EBs only exposed to 25 rpm and relatively higher than EBs maintained at 40 rpm or switched to 55 rpm, though not statistically significant ($p=0.072$ and $p=0.067$, respectively). On the other hand, EBs initially formed at 55 rpm and switched to slower rotary speeds exhibited no significant change in levels of AFP expression compared to EBs maintained at 55 rpm. Overall, these results suggest that differentiation pathways established by initial rotary speeds can be further modulated by changes in rotary speeds during the course of suspension culture.

In an attempt to confirm the gene expression results, immunohistochemical staining was performed to detect AFP expression within EBs at day 7 of differentiation. EBs exposed to either initial or secondary 25 rpm rotary speeds exhibited more pronounced AFP expression than EBs exposed to combinations of 40 and 55 rpm speeds (Figure A.1 E). In general, AFP expression was largely sequestered to the outer edges of EBs, however EBs initially formed at 25 rpm and switched to 55 rpm exhibited slightly more AFP expression within the interior of EBs as well. The combined gene and protein analysis results indicate that combinational rotary speed regimens may offer more control

of ESC differentiation compared to a singular rotary speed and that both the formation rotary speed and maintenance rotary speed during EB culture can affect differentiation.

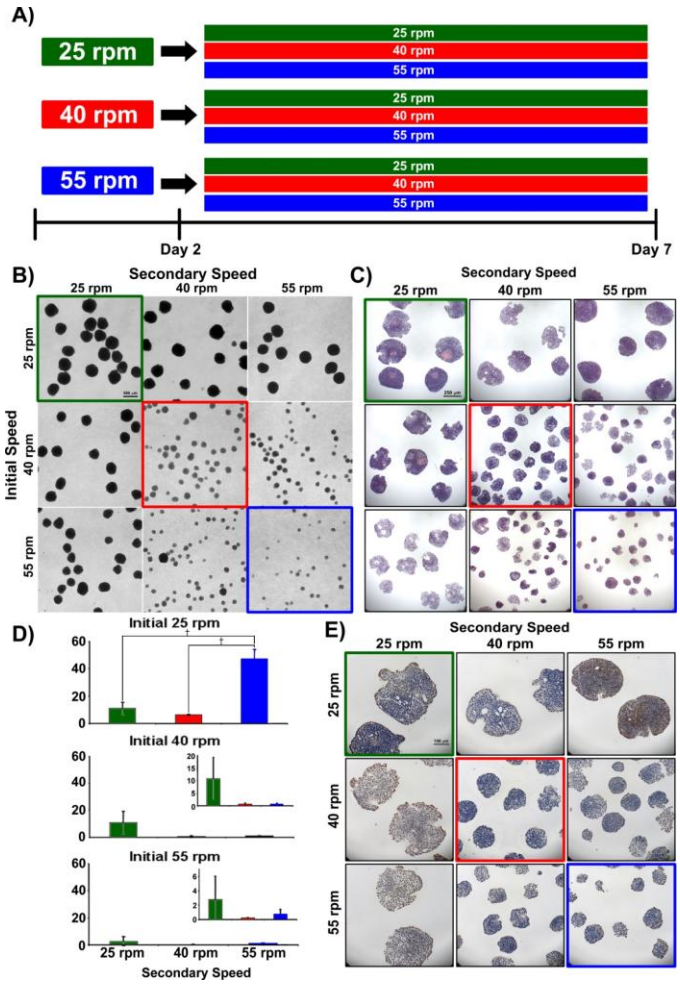

Figure A.1: Combinatorial rotary orbital speed culture. EBs were formed for 2 days at a consistent, initial rotary speed, then switched to secondary rotary speed for 5 additional days (A). At day 7, EBs exposed to any combination of 25 rpm were larger than EBs exposed to only combinations of 40 and 55 rpm (B). EBs initially formed at 25 rpm and switched to higher rotary speeds had increased nuclear density with increased speed, and EBs initially formed at 40 or 55 rpm then switched to 25 rpm had increased enucleated areas and a more cystic appearance than EBs remaining at faster speeds (C). AFP expression levels were also modulated by combinatorial rotary speed exposure (D). EBs formed at 25, 40, and 55 rpm exhibited similar AFP expression at day 7 of differentiation to initial studies, with 25 rpm having the highest expression levels. EBs formed at 25 rpm and switched to 55 rpm had the most AFP expression. EBs initially at 25 rpm also exhibited positive (brown) staining for AFP around the outer edge of EBs, with EB switched from 25 to 55 rpm appearing to exhibit more AFP+ areas than other secondary rotary speeds (E). EBs switched to a secondary speed of 25 rpm also had increased AFP+ staining as compared to counterpart EBs maintained at combinations of 40 and 55 rpm. Images of EBs maintained at constant, original rotary speeds are outlined in green, red, and blue (25, 40, and 55 rpm respectively). Black arrows indicate positive staining. († = $p \leq 0.01$).